

He Cooled Granular Target Analytical Results and CFD Analysis

Jozsef Szabo

Thesis for the Degree of Master of Science

Division of Fluid Mechanics
Department of Energy Sciences
Faculty of Engineering
Lund University



Abstract

A multidisciplinary scientific research center harnessing the world's most powerful neutron source is going to be built in Lund: ESS, The European Spallation Source. Researchers will be able to study the materials of everyday life in all their rich diversity – from plastics and proteins to medicines and molecules – in order to understand how they are built up and how they work. ESS will become a hub in Europe's research infrastructure

ESS consists of an accelerator and a target station. A first step is to accelerate protons close to the speed of light. This is achieved using front edge technology in a 600 m long linear accelerator. The protons are impinging materials such as lead, tungsten or mercury. When protons interact with heavy nuclei, neutrons are released from those nuclei: this reaction is called spallation. A large amount of energy is deposited by the proton beam into the target. This causes a temperature rise in the material and requires efficient cooling.

There are many different concepts for the target, one of them is a stationary target consisting of granular tungsten spheres and another one is a rotating target consisting of densely packed tungsten cylinders. This thesis will be about simulating the cooling of these target concepts. The cooling is achieved by helium flowing through the granular target.

As a first step analytical calculations are performed on a global level on the bed of tungsten spheres. This is done to study and get an understanding of how the essential parameters affect the cooling. The results are presented as graphs with the essential parameters and contour plots of the outlet helium temperature and pressure. The next step is to perform CFD calculations with ANSYS CFX, also on a global level with a porous domain acting as the tungsten spheres. The analytic calculations are used as a guideline to determine the properties of the boundary conditions. Finally CFD calculations are performed on the rotating target with the densely packed cylinders. These are performed on both larger and smaller scale.

The different analyses give an understanding of how the essential parameters affect the results of the granular targets. Requirements are set up and have to be fulfilled by the design. Unfortunately the results show that the stationary target with the tungsten spheres does not fulfill some important requirements. Conclusions were drawn that the rotating target is more viable than the stationary. The reasons for this can be read in the thesis.

Preface

It has been an honor performing my master thesis work for the European Spallation Source. It has been inspiring and very interesting. With such an interesting subject, I was always in the mood to work on the thesis. I have expanded my knowledge within CFD significantly. I have also learned new ways to tackle and solve problems which will be useful for me in the future. Last but not least, with the thesis written in English, I have improved my English significantly.

I want to thank my supervisors: Johan Revstedt at LTH and Cyril Kharoua at ESS for spending their valuable time with me. They have been very helpful and cooperative. Whenever I had questions they were answered on a short notice. It has been inspiring getting comments and suggestions from them; it clearly shows that they enjoy their work. I am glad that I had the chance getting to know them.

I would also like to thank Pascal Sabbagh for helping me with troubleshooting in ANSYS CFX. Finally I want to thank François Plewinski for giving me his opinions on my thesis during the project time.

I hereby acknowledge the financial support of the European Spallation Source who financially supported my master thesis.

Jozsef Szabo

Table of Contents

Abstract.....	II
Preface.....	III
Table of Contents.....	IV
Table of Figures.....	VI
1. Introduction.....	1
1.1 Project background.....	1
1.2 Project Goals	1
1.3 Problem Description	2
1.4 Requirements	3
2. Helium cooled stationary granular target.....	4
2.1 Analytic calculations.....	4
2.1.1 Material Properties	4
2.1.2 Equations.....	4
2.1.3 “backwards” iterative method	8
2.1.3.1 Iteration	9
2.1.3.2 For-loop.....	10
2.1.4 Straight forward method	10
2.1.5 Graphs.....	11
2.1.5.1 Input Variables	11
2.1.5.2 Results.....	12
2.1.6 Contour Plots.....	15
2.1.6.1 Zone Inlet Parameters.....	16
2.1.6.2 Results.....	16
2.1.7 Flow from the top	21
2.1.7.1 Graphs	21
2.1.7.2 Contour Plots	24
2.1.7.3 Difficulties.....	30
2.1.8 Conclusions	32
2.2 Global analyses with ANSYS CFX.....	33
2.2.1 Theory	33
2.2.1.1 Resistance Coefficients.....	33
2.2.2 Methodology	34
2.2.2.1 Modeling.....	34
2.2.2.2 Meshing	35
2.2.2.3 Pre-Processing	35
2.2.2.4 Simulation.....	36
2.2.2.5 Post-Processing.....	36
2.2.3 Results	37
2.2.3.1 Comparison for Zone 1	39
2.2.3.2 Investigating the cause of different results.....	40
2.2.4 Conclusions	45
3. Helium cooled rotating granular target.....	46
3.1 Methodology	46
3.2 Resistance coefficients.....	47
3.3 Analysis of 1 “tube”	47

3.3.1 Modeling.....	47
3.3.2 Meshing.....	48
3.3.3 Pre processing.....	49
3.3.4 Simulation.....	50
3.3.5 Post-Processing.....	50
3.3.6 Results	51
3.3.7 Resistance coefficients	53
3.4 Test with porous domain	55
3.4.1 Modeling & Meshing	55
3.4.2 Pre Processing.....	56
3.4.4 Simulation.....	57
3.4.5 Post Processing.....	57
3.4.6 Results	58
3.5 1cm of the rotating target	59
3.5.1 Modeling.....	59
3.5.2 Meshing.....	60
3.5.3 Pre Processing.....	61
3.5.4 Simulation.....	62
3.5.5 Post Processing.....	62
3.5.6 Results	62
3.6 Conclusions.....	71
4. References	72
5. Appendix.....	73
5.1 ANSYS CFX Theory.....	73
5.1.1 Governing Equations.....	73
5.1.2 Full Porous Model.....	74
5.1.3 Loss models.....	75
5.2 Mat lab code: “backwards” iterative method	77
5.3 Mat lab code: handling the FLUKA file	79
5.4 Mat lab code: straight forward method.....	80

Table of Figures

Figure 1. Problem Description. The bed of spheres is split into three zones. Each zone contains three domains; an inlet, a porous volume and an outlet. The porous domains have the dimensions: 22 x 20 x 8 cm. The inlet and outlet domain lengths are not yet defined..... 2

Figure 2. Power Density. The power densities in each zone of the target are shown in the picture. This is the amount of power that the helium has to evacuate. Zone 1 contains about 70% of the total power in the sphere bed. Therefore it is convenient to split the target into three zones. 3

Figure 3. Backwards iterative method. The inlet temperature and the outlet pressure are known. The pumping power is given. An inlet velocity is guessed and with help of an iteration process the unknown variables can be calculated..... 8

Figure 4. Cell wise calculations. A zone is split up into columns and then the columns are split up into cells. The columns are isolated from each other, which means that the calculations are unidirectional along the column. The mass flow rate is conserved along a column. Calculations are done cell wise. The outlet parameters from the first cell become the inlet parameters for the next one, and so on..... 11

Figure 5. Graph, Zone 1. The graph shows the results for sphere diameters 6,8,10 and 12 mm when the static pressure is 10 bar. The left y-axis shows the maximum sphere temperature and the average helium outlet temperature. The right y-axis shows the maximum pressure in the system. The x axis shows the pumping power..... 13

Figure 6 Graph, Zone 2. The graph shows the results for sphere diameters 6,8,10 and 12 mm when the static pressure is 10 bar. The left y-axis shows the maximum sphere temperature and the average helium outlet temperature. The right y-axis shows the maximum pressure in the system. The x axis shows the pumping power..... 14

Figure 7 Graph, Zone 3. The graph shows the results for sphere diameters 6,8,10 and 12 mm when the static pressure is 10 bar. The left y-axis shows the maximum sphere temperature and the average helium outlet temperature. The right y-axis shows the maximum pressure in the system. The x axis shows the pumping power..... 15

Figure 8. Plot surfaces. Contour plots are made for the outlet surfaces of the three zones according to the figure. The proton beam hits the target along the z-axis. 15

Figure 9. Helium outlet temperature, Zone 1. X- and y-axes show the target length and height in [cm] of a zone. Helium is flowing perpendicular, outwards of the plot surface. The contour plot shows the helium outlet temperature at the outlet surface of zone 1, in [C]. 17

Figure 10. Outlet pressure, Zone 1. X- and y-axes show the target length and height in [cm] of a zone. Helium is flowing perpendicular, outwards of the plot surface. The contour plot shows the pressure at the outlet surface of zone 1, in [bar]. Table 4 shows the inlet parameters, with help of this the pressure drop can be calculated..... 17

Figure 11. Helium outlet temperature, Zone 2. X- and y-axes show the target length and height in [cm] of a zone. Helium is flowing perpendicular, outwards of the plot surface. The contour plot shows the helium outlet temperature at the outlet surface of zone 2, in [C]..... 18

Figure 12. Outlet pressure, Zone 2. X- and y-axes show the target length and height in [cm] of a zone. Helium is flowing perpendicular, outwards of the plot surface. The contour plot shows the pressure at the outlet surface of zone 2, in [bar]. Table 4 shows the inlet parameters, with help of this the pressure drop can be calculated..... 19

Figure 13. Helium outlet temperature, Zone 3. X- and y-axes show the target length and height in [cm] of a zone. Helium is flowing perpendicular, outwards of the plot surface. The contour plot shows the helium outlet temperature at the outlet surface of zone 3, in [C]..... 20

Figure 14. Outlet pressure, Zone 3. X- and y-axes show the target length and height in [cm] of a zone. Helium is flowing perpendicular, outwards of the plot surface. The contour plot shows the pressure at the outlet surface of zone 3, in [bar]. Table 4 shows the inlet parameters, with help of this the pressure drop can be calculated.....	20
Figure 15. Plot Surfaces, flow from top. Contour plots are made for the outlet surfaces of the three zones according to the figure.....	21
Figure 16. Graph Zone 1, flow from top. The graph shows the results for sphere diameters 6,8,10 and 12 mm when the static pressure is 10 bar. The left y-axis shows the maximum sphere temperature and the average helium outlet temperature. The right y-axis shows the maximum pressure in the system. The x axis shows the pumping power.....	22
Figure 17. Graph Zone 2, flow from top. The graph shows the results for sphere diameters 6,8,10 and 12 mm when the static pressure is 10 bar. The left y-axis shows the maximum sphere temperature and the average helium outlet temperature. The right y-axis shows the maximum pressure in the system. The x axis shows the pumping power.....	23
Figure 18. Graph Zone 3, flow from top. The graph shows the results for sphere diameters 6,8,10 and 12 mm when the static pressure is 10 bar. The left y-axis shows the maximum sphere temperature and the average helium outlet temperature. The right y-axis shows the maximum pressure in the system. The x axis shows the pumping power.....	24
Figure 19. Helium outlet temperature, Zone 1, flow from top. X- and y-axes show the target length and width in [cm] of a zone. Helium is flowing perpendicular, outwards of the plot surface. The contour plot shows the helium outlet temperature at the outlet surface of zone 1, in [C].	25
Figure 20. Outlet pressure, Zone 1, flow from top. X- and y-axes show the target length and width in [cm] of a zone. Helium is flowing perpendicular, outwards of the plot surface. The contour plot shows the pressure at the outlet surface of zone 1, in [bar]. Table 8 shows the inlet parameters, with help of this the pressure drop can be calculated.....	26
Figure 21. Helium outlet temperature, Zone 2, flow from top. X- and y-axes show the target length and width in [cm] of a zone. Helium is flowing perpendicular, outwards of the plot surface. The contour plot shows the helium outlet temperature at the outlet surface of zone 2, in [C].	27
Figure 22. Outlet pressure, Zone 2, flow from top. X- and y-axes show the target length and width in [cm] of a zone. Helium is flowing perpendicular, outwards of the plot surface. The contour plot shows the pressure at the outlet surface of zone 2, in [bar]. Table 8 shows the inlet parameters, with help of this the pressure drop can be calculated.....	27
Figure 23. Helium outlet temperature, Zone 3, flow from top. X- and y-axes show the target length and width in [cm] of a zone. Helium is flowing perpendicular, outwards of the plot surface. The contour plot shows the helium outlet temperature at the outlet surface of zone 3, in [C].	28
Figure 24. Outlet pressure, Zone 3, flow from top. X- and y-axes show the target length and width in [cm] of a zone. Helium is flowing perpendicular, outwards of the plot surface. The contour plot shows the pressure at the outlet surface of zone 3, in [bar]. Table 8 shows the inlet parameters, with help of this the pressure drop can be calculated.....	29
Figure 25. Contour plot of the velocity vectors on a plane in the middle of the geometry. The plot is coming from a ANSYS CFX CFD calculation. A design of the inlet and outlet pipes when the helium is entering at the top. There are three inlet pipes and three porous zones. The outlet pipe is common for all three. The height of both the inlet pipes and outlet pipes is 15 cm. The rounded edges in the front of the each pipe are problematic. Recirculation zones are created according to the red marked shapes in the figure.	30
Figure 26. Contour plot of the velocity vectors on a plane in the middle of the geometry. The plot is coming from a ANSYS CFX CFD calculation. A design of the inlet and outlet pipes when the	

helium is entering at the top. There are three inlet pipes and three porous zones. The outlet pipe is common for all three. The height of both the inlet pipes and outlet pipes is 15 cm. 31

Figure 27. Contour plot of the velocity vectors on a plane in the middle of the geometry. The plot is coming from a ANSYS CFX CFD calculation. A design of the inlet and outlet pipes when the helium is entering at the top. There are three inlet pipes and three porous zones. The outlet pipe is common for all three. The height of both the inlet pipes and outlet pipes is 8 cm. 31

Figure 28. ANSYS Workbench simulation process. 34

Figure 29. Model made with ANSYS DesignModeler. The porous domain has the dimensions 22 x 20 x 8 cm, according to the first analytical case. The inlet domain is 10 cm long and the outlet domain is 30 cm long. 34

Figure 30. Mesh made with ANSYS Meshing. A uniform 5 mm mesh is made over the whole model. Such a simple mesh is made because it allows fast simulations. 35

Figure 31. Pre-Processing with ANSYS CFX-Pre. The model consists of the domains, an inlet, a porous and an outlet. Boundary surfaces are green in the figure. Different preferences can also be seen as text in the figure. 36

Figure 32. Planes used for plots in ANSYS CFX-Post. Plots are made on the described surfaces in the figure. 37

Figure 33. Contour plot, Absolute Pressure. 38

Figure 34. Contour plot, Temperature. 38

Figure 35. Contour plot, Velocity. 38

Figure 36. Mass flow contour plot of the 20 bar case. In this case the porous domain has an isotropic loss model. 41

Figure 37. Mass flow contour plot of the 40 bar case. In this case the porous domain has an isotropic loss model. 41

Figure 38. Mass flow contour plot of the 60 bar case. In this case the porous domain has an isotropic loss model. 41

Figure 39. Mass flow contour plot of the 20 bar case. In this case the porous domain has directional loss. 42

Figure 40. Mass flow contour plot of the 40 bar case. In this case the porous domain has directional loss. 42

Figure 41. Mass flow contour plot of the 60 bar case. In this case the porous domain has directional loss. 42

Figure 42. 9 columns of the hottest part of the target are cut out. This is located 4 cm into the target along the z-axis. The columns are isolated from each other by "imaginary" walls. This is equivalent to the analytic calculation where there is no transverse loss. There is heat transfer between the columns. 2 x 2 elements per column cross section. 43

Figure 43. Temperature plot of 0.5 cm columns. 44

Figure 44. Mass flow plot of 0.5 cm columns. The mass flow is constant through the porous domain. 44

Figure 45. Temperature plot of 1 cm columns. 44

Figure 46. Mass flow contour plots of 1 cm column. The mass flow is constant through the porous domain. 45

Figure 47. Problem description. A rotating target with 8 cm high cylinders with 2 cm diameter is densely packed in a circle with the outer diameter 150 cm and inner diameter 50 cm. The target rotates of 30 rpm. The beam hits the target along the z-axis (blue). 46

Figure 48. ANSYS Workbench simulation process. 46

Figure 49. Model of the part cut out. 48

Figure 50. Mesh of the tube model. Coarse mesh on the cylinders, Medium mesh on the inlet and outlet domains, fine mesh on the helium in the middle.	48
Figure 51. Mesh Zoom & cut. The helium in the middle has 1 mm long elements.	49
Figure 52. Boundary conditions for “1 tube”	50
Figure 53. The contour plot plane.	51
Figure 54. Line where data is collected for the resistance coefficients.....	51
Figure 55. Contour plot of the pressure on a middle plane. A comparison between the 8m/s case and the 10m/s case.....	52
Figure 56. Contour plot of the velocity on a middle plane. A comparison between the 8m/s case and the 10m/s case.....	52
Figure 57. Contour plot of the temperature on a middle plane. A comparison between the 8m/s case and the 10m/s case.	53
Figure 58. The linear resistance coefficients for the cylinders vs. the cylinder length. the target height, (from -4 to 4 cm).	54
Figure 59. The quadratic resistance coefficient for the cylinders vs. the cylinder length, (the target height, from -4 to 4 cm). The y-axis is the quadratic resistance coefficient.	54
Figure 60. The quadratic resistance coefficient for the cylinders vs. the cylinder length, (the target height, from -4 to 4 cm). The y-axis is the quadratic resistance coefficient. The first points are removed to see the rest of the graph in a decent way.....	55
Figure 61. Model of porous domain with a part cut out of the circular rotating target. It is composed of an inlet domain, a porous domain and an outlet domain. It is 50 cm long and 22 cm wide. It has been simplified to a perfect rectangle.....	56
Figure 62. Meshed model of the cut out part. Very simple mesh, 5 mm body sizing on all domains.	56
Figure 63. Boundary conditions for cut out part from the rotating target.	57
Figure 64. Planes for the contour plots. Five planes with the first 4 cm in z-axis and the last 4 cm in the z-axis. The three planes between them are equally distributed.....	57
Figure 65. Contour plots of the pressure on 5 planes equally distributed along the z-axis.....	58
Figure 66. Contour plots of the temperature on 5 planes equally distributed along the z-axis.	58
Figure 67. Contour plot of the pressure drop, only the porous domain.. This is the first contour plane located 4 cm in z-axis.	59
Figure 68. Iso view of the 1 cm part cut out of the rotating target. It has inlet and outlet pipe height of 2.5 cm each.....	59
Figure 69. Iso view of the model with the outlet domain invisible and the reduction shape of the helium on top of the cylinders.....	60
Figure 70. Meshed model from the side of the 1 cm part cut out from the rotating target.....	60
Figure 71. A zoomed iso view of the meshed 1 cm part cut out from the rotating target.....	61
Figure 72. Mesh from top of the cylinders and helium between the cylinders.	61
Figure 73. Illustration of the pre-processing for the 1 cm cut out case	61
Figure 74. The contour plots are of a plane in the middle of the model.	62
Figure 75. Contour plot on the middle plane, of the temperature in both the helium and cylinders of the 160 m/s inlet case.	64
Figure 76. Contour plot on the middle plane, of the temperature in both the helium and cylinders of the 100 m/s inlet case.	64
Figure 77. Contour plot on the middle plane, of the temperature in both the helium and cylinders of the 40 m/s inlet case.	64
Figure 78. Contour plot on the middle plane, of the helium velocity of the 160 m/s inlet case.	66

Figure 79. Contour plot on the middle plane, of the helium velocity of the 100 m/s inlet case. 66

Figure 80. Contour plot on the middle plane, of the helium velocity of the 40 m/s inlet case. 66

Figure 81. Contour plot on the middle plane, of the helium velocity in vertical direction, of the 160 m/s inlet case. 68

Figure 82. Contour plot on the middle plane, of the helium velocity in vertical direction, of the 100 m/s inlet case. 68

Figure 83. Contour plot on the middle plane, of the helium velocity in vertical direction, of the 40 m/s inlet case. 68

Figure 84. Contour plot on the middle plane, of the pressure, of the 160 m/s inlet case. 70

Figure 85. Contour plot on the middle plane, of the pressure, of the 100 m/s inlet case. 70

Figure 86. Contour plot on the middle plane, of the pressure, of the 40 m/s inlet case..... 70

1. Introduction

1.1 Project background

The European Spallation Source (ESS) will be a multidisciplinary scientific research center harnessing the world's most powerful neutron source. Researchers will be able to study the materials of everyday life in all their rich diversity – from plastics and proteins to medicines and molecules – in order to understand how they are built up and how they work. ESS will become a hub in Europe's research infrastructure

Broadly, it consists of an accelerator and a target station. A first step is to accelerate protons up to the speed of light. This is achieved using front edge technology in a long linear accelerator. The protons are impinging materials such as lead, tungsten or mercury. When protons interact with heavy nuclei, neutrons are released from those nuclei's: this reaction is called spallation. More than 30 neutrons are produced per incident proton. The neutrons are then cooled by a moderator placed close to the target.

There are many different concepts for the target: one of them consists of granular tungsten spheres. A large amount of energy is deposited by the proton beam into the tungsten spheres. This causes a temperature rise in the material and requires cooling. This can be achieved by helium flowing through the bed of spheres.

1.2 Project Goals

This thesis is about simulating the cooling of the tungsten target. It is divided into three phases; the goal of the first phase is to determine the range of the essential parameters on a global level. Because of safety concern and mechanical reasons, one does not want to reach too high temperatures in either the helium or the tungsten spheres. High pressure in the system represents also a safety risk. Therefore analytical calculations have been made on a global level to determine some important parameters. Special attention has been paid to create graphs and contour plots with the important parameters in order to have a good overview and to easily choose appropriate parameters.

The 2nd phase will consist of modeling a porous domain with ANSYS CFD tool, ANSYS CFX, which will represent the bed of tungsten spheres. A porous domain is used because the whole bed can be modeled with a coarse mesh and does not need much CPU-power. Only 5-6 spheres can be modeled per analysis with the computers available. Analyses will be done on a global level just like in the first phase. With the help of the analytic studies it is easier to choose appropriate parameters to begin with.

The 3rd phase was first supposed to consist of local analysis of the tungsten sphere bed. Spheres are modeled at the hottest and most stressed part of the target where the essential parameters are studied as well as the flow pattern. Because of the complex geometry this analysis would require a lot of CPU-power and solving time, which on my own and with I did not have. Instead of the tungsten spheres, another concept of the target was considered for the local analysis. The local analysis will be done on a rotating target with tungsten cylinders. In this case the geometry is less complex and the flow is forced to be one directional between the cylinders.

1.3 Problem Description

The target consists of a bed of tungsten spheres. The bed is 60 cm long, 22 cm wide and 8 cm high. A 5 MW proton beam hits the target, entering first in zone 1, which is the front part of the target. The zones are at this time only imaginarily separated, a solution for the walls between them will be developed at a later stage. The beam deposits heat into the spheres. This is cooled by a helium flow which enters at one side and exits at the opposite. The reason to split the target into three zones is to adapt the cooling adequately. Each zone has a cross flow section of 0.016m^2 and a length of 0.22m according to *Figure 1*. There are three inlet flows and three outlet flows as a start, one to each zone. The helium enters straight from the side and exits straight out at the other side. At a later stage bent pipes have to be modeled at the inlet and outlet. The outlet will be common for the three zones, for the moment they are split because analyses will be done zone wise.

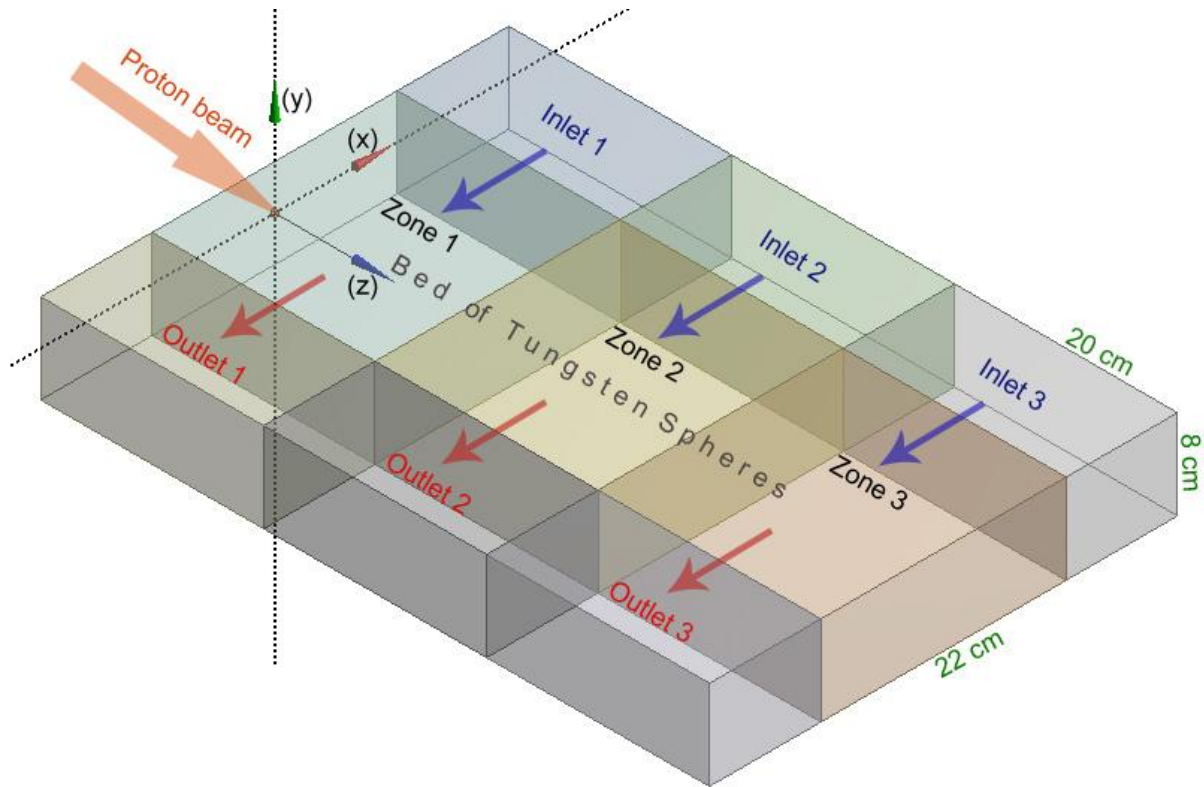


Figure 1. Problem Description. The bed of spheres is split into three zones. Each zone contains three domains; an inlet, a porous volume and an outlet. The porous domains have the dimensions: $22 \times 20 \times 8$ cm. The inlet and outlet domain lengths are not yet defined.

The proton beam hits zone 1, where the power density is highest. Then the hadronic cascade resulting from the protons interaction creates a fast decrease of the power density. *Figure 2* shows the power densities in the zones. It is convenient to consider them separately because they have different power densities and require different cooling. This means that lower inlet pressures and velocities can be used in the two other zones. The chosen geometry is not a constraint, i.e. if the analytical calculations or analyses in Workbench, CFX shows that the results are not satisfying, the geometry can be adjusted.

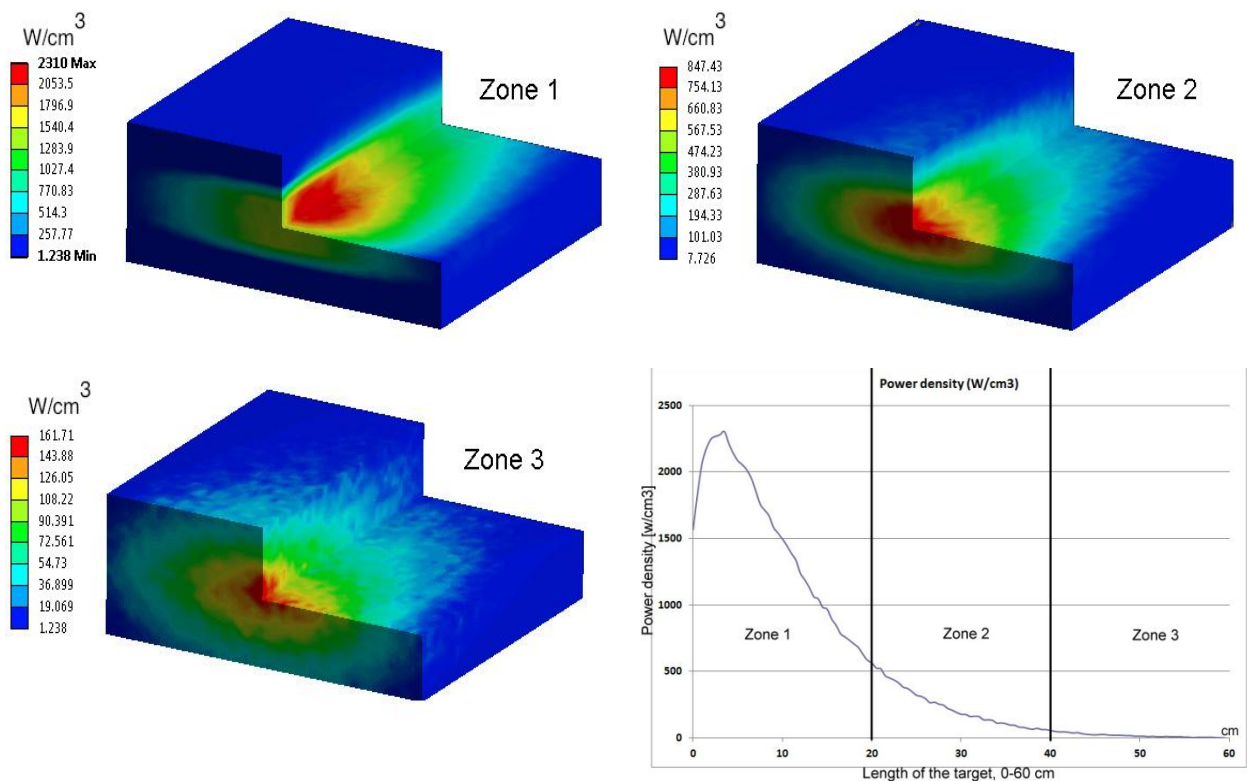


Figure 2. Power Density. The power densities in each zone of the target are shown in the picture. This is the amount of power that the helium has to evacuate. Zone 1 contains about 70% of the total power in the sphere bed. Therefore it is convenient to split the target into three zones.

1.4 Requirements

In the analyses there are requirements that have to be respected, for example:

- The maximum allowed pressure in the system is 20 bar.
- The maximum allowed sphere temperature is 800 °C.
- The average helium outlet temperature should be below 400 °C.
- The total pumping power should be below 500 kW.

The maximum pressure is an important safety requirement and must be followed, while the maximum sphere temperature could be allowed to be a little higher. Also the requirements for the average helium outlet temperature and the total pumping power could be slightly adjusted.

2. Helium cooled stationary granular target

2.1 Analytic calculations

The first task in the thesis is to perform analytic calculations on a global level to determine some major parameters as mentioned earlier. Two different ways were considered with the same equations. One of them is used for generating graphs with the important parameters as variables. The other one is used to generate contour plots of different surfaces in the sphere bed. To generate the graphs, a “backwards” iterative method is used. To generate the contour plots a straight forward method is used. These will be explained later.

2.1.1 Material Properties

In the analytic calculations the following properties are used for the tungsten and the helium:

	<u>Helium</u>	<u>Tungsten</u>
Density:	Temperature and pressure dependent	Density: 18500 kg/m ³
Dynamic viscosity:	18.6 · 10 ⁻⁶ Ns/m ²	Specific heat: 135 J/kg · K
Specific heat:	5193.2 J/kg · K	
Molar mass:	4.0026 · 10 ⁻³ g/mol	
Gas constant:	8.314 J/mol · K	
Thermal conductivity:	0.144 W/m · K	

Table 1. Properties of materials used.

2.1.2 Equations

There are three “sets” of equations used in the calculations and a few auxiliary are applied to solve the problem:

- Equations to calculate the pressure drop when taking both the inlet pressure and temperature in to account.
- Equations to calculate the heat transfer coefficient between the solid and fluid.
- Equations to estimate the maximum sphere temperature.
- Auxiliary equations such as the ideal gas law and calorimetry equation.

The equations for calculating the pressure drop including the temperature raise in the Helium are taken from Handbook of hydraulic Resistance [1]. For a volume of loose bodies of spherical shape the resistance coefficient can be calculated with a precision of ±20-35% according to the following equations.

$$\zeta = \frac{2 \cdot \Delta p}{\rho_{in} \cdot w_1^2} = \left[\frac{360(1 - \epsilon)^2}{\epsilon^3 \cdot Re_1} + \frac{B(1 - \epsilon)}{\epsilon^3} \right] \cdot \frac{l_0}{d_{el}} \quad (1)$$

$$Re_1 = \frac{w_1 \cdot d_{el}}{\nu} \quad (2)$$

$$d_{el} = \varphi \cdot d_{gr} \quad (3)$$

$$\zeta_t = \frac{2 \cdot \Delta p}{\rho_m \cdot w_{1m}^2} = \zeta + \Delta\zeta_t \quad (4)$$

$$\Delta\zeta_t = 2 \frac{T_{ex} - T_{in}}{T_m} \quad (5)$$

$$T_m = \frac{T_{in} + T_{ex}}{2} \quad (6)$$

$$w_{1m} = w_1 \frac{T_m}{T_{in}} \quad (7)$$

$$\rho_m = \rho_{in} \frac{273}{T_m} \quad (8)$$

- ζ Resistance coefficient
- ζ_t Resistance coefficient with temperature taken in account
- Δp Pressure drop
- ρ_{in} Helium density
- w_1 Inlet flow velocity
- ϵ Porosity
- B 1.8 for smooth surfaces
- l_0 Length
- ν Kinematic viscosity =Dynamic viscosity/Density
- φ Shape coefficient
- d_{gr} Sphere diameter
- T_{in} Inlet He temperature
- T_{ex} Outlet He temperature

The heat transfer coefficient is not constant and was calculated according to VDI-Wärmeatlas [2], with the following equations:

$$Nu = f_a \cdot Nu_{One\ Sphere} = \frac{\alpha \cdot d_{gr}}{k} \quad (9)$$

$$f_a = 1 + 1.5(1 - \epsilon) \quad (10)$$

$$Nu_{One\ Sphere} = 2 + \sqrt{Nu_{lam}^2 + Nu_{turb}^2} \quad (11)$$

$$Nu_{lam} = 0.644 \cdot \sqrt{Re_\psi} \cdot \sqrt[3]{Pr} \quad (12)$$

$$Nu_{turb} = \frac{0.037 \cdot Re_{\psi}^{0.8} \cdot Pr}{1 + 2.443 \cdot Re_{\psi}^{-0.1} \cdot (Pr^{2/3} - 1)} \quad (13)$$

$$Re_{\psi} = \frac{w_1 \cdot d_{gr}}{\nu \cdot \psi} \quad (14)$$

$$Pr = \frac{\nu}{a} \quad (15)$$

$$a = \frac{k}{\rho \cdot c_p} \quad (16)$$

$$\alpha = \frac{f_a \cdot Nu_{one\ sphere} \cdot k}{d_{gr}} \quad (17)$$

The estimation of the temperature of the hottest sphere was done according to the Champion report on Helium Cooled Granular Target [3]. The following equations are used:

$$T_0 = 20^{\circ}\text{C} + 0.5T_2 + T_1 + \Delta T \quad (18)$$

T_1 Is the temperature above that of the He at the location of the hottest sphere, just before a proton pulse.

T_2 Is the temperature rise in the cooling fluid between the inlet and outlet at the location of the hottest part of the target, assuming a lateral flow.

ΔT Is the temperature rise due to one pulse.

$$\Delta T = \frac{Q_m}{c_{p,w}} \quad (19)$$

$$t_0 = \frac{m \cdot c_{p,w}}{\alpha \cdot S} \quad (20)$$

α is the heat transfer coefficient.

$$m = \rho_w \cdot \frac{4\pi r^3}{3} \quad (21)$$

$$S = 4\pi r^2 \quad (22)$$

$$T_1 = \frac{\Delta T \cdot e^{-\frac{t_p}{t_0}}}{1 - e^{-\frac{t_p}{t_0}}} \quad (23)$$

$$t_p = 50 \text{ms}$$

$$T_2 = T_{ex} - T_{in} \quad (24)$$

The following auxiliary equations are applied to solve the problem. The calorimetry equation is given as:

$$P = \rho \cdot A \cdot w_1 \cdot C_p \cdot (T_{ex} - T_{in}) \quad (25)$$

The inlet density of helium depends on the inlet pressure and temperature. The following equation is derived from the ideal gas law:

$$\rho_{in} = \frac{M \cdot p_{in}}{R \cdot T_{in}} \quad (26)$$

where:

M Molar mass

R Gas constant

The outlet velocity can be calculated since the mass flow rate into the system should be equal to the mass flow rate out of the system according to the following:

$$\rho_{in} \cdot w_1 \cdot A = \rho_{ex} \cdot w_2 \cdot A \Rightarrow w_2 = \frac{\rho_{in}}{\rho_{ex}} w_1 \quad (27)$$

By combining equation (26) and (27) the following equation is derived:

$$w_2 = \frac{p_{in} T_{ex}}{p_{ex} T_{in}} w_1 \quad (28)$$

The inlet pressure p_{in} in the system is given by:

$$p_{in} = p_{ex} + \Delta p \quad (29)$$

When calculating the pumping power, an incompressible fluid is assumed:

$$P_{pump} = \Delta p \cdot w_1 \cdot A \quad (30)$$

The tightest way to pack spheres is called close packing. The average density is then defined as $\pi/\sqrt{18}$ which yields a porosity ϵ of:

$$\epsilon = 1 - \frac{\pi}{\sqrt{18}} = 0.2595 \quad (31)$$

2.1.3 “backwards” iterative method

The calculations were made zone wise in Mat lab on an iterative “backwards” way. In order to use this method the inlet temperature and the outlet pressure has to be known. Also a pumping power over the zone must be given. The calculations then give the inlet flow velocity, the outlet flow velocity, the outlet temperature and the inlet pressure. Initially the inlet velocity is guessed. Then with help of the iterations the correct inlet velocity is calculated for the given pumping power. *Figure 3* below illustrates the problem setup for this method.

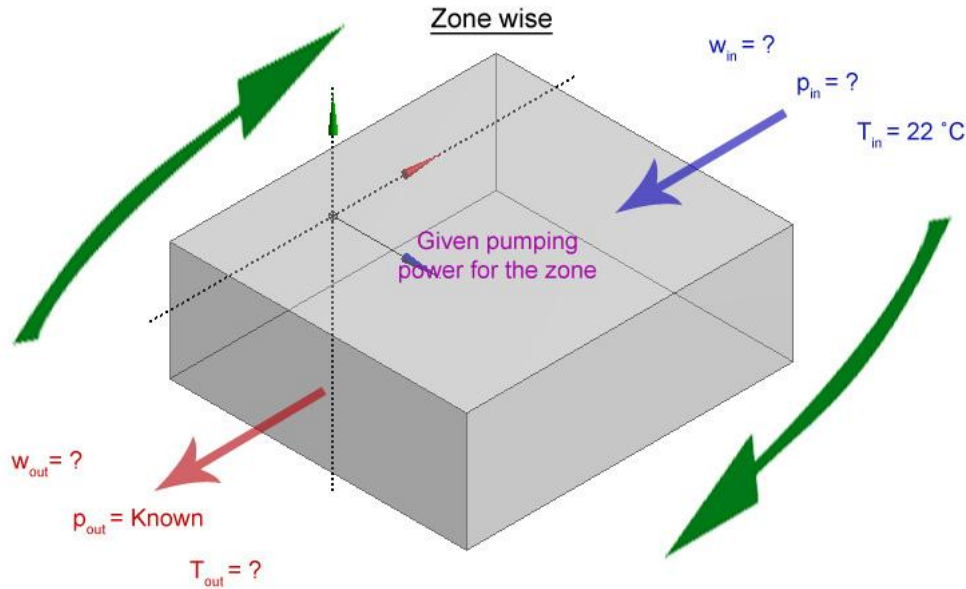


Figure 3. Backwards iterative method. The inlet temperature and the outlet pressure are known. The pumping power is given. An inlet velocity is guessed and with help of an iteration process the unknown variables can be calculated.

Equation (4) gives the pressure drop over the zone:

$$\Delta p = \frac{\rho_m \cdot w_{1m}^2}{2} (\zeta + \Delta\zeta_t) \quad (32)$$

Inserting (5), (6), (7), and (8) into (32) gives:

$$\Delta p = \frac{273 \cdot \rho_{in}}{T_{in} + T_{ex}} \cdot w_1^2 \left(\frac{T_{in} + T_{ex}}{2 \cdot T_{in}} \right)^2 \left(\zeta + 4 \frac{T_{ex} - T_{in}}{T_{in} + T_{ex}} \right) \quad (33)$$

By rearranging equation (25) the inlet velocity is derived:

$$w_1 = \frac{P}{\rho_{in} \cdot A \cdot c_p \cdot (T_{ex} - T_{in})} \quad (34)$$

Inserting equation (34) into (33) and adding and then subtracting T_{in} in some places gives:

$$\Delta p = \frac{273 \cdot \rho_{in}}{T_{in} + T_{ex}} \cdot \left(\frac{P}{\rho \cdot A \cdot c_p} \right)^2 \cdot \frac{1}{(T_{ex} - T_{in} + T_{in} - T_{in})^2} \cdot \left(\frac{T_{in} + T_{ex}}{2 \cdot T_{in}} \right)^2 \cdot \left(\zeta + 4 \frac{T_{ex} - T_{in} + T_{in} - T_{in}}{T_{in} + T_{ex}} \right) \quad (35)$$

Making a variable change $J = T_{in} + T_{ex}$ and renaming some parts gives:

$$\Delta p = \frac{1}{J} C \cdot D \cdot \frac{1}{(J - 2T_{in})^2} \cdot \left(\frac{J}{1}\right)^2 \cdot \left(\zeta + 4 \frac{J - 2T_{in}}{J}\right) \quad (36)$$

$$C = \frac{273 \cdot \rho_{in}}{4 \cdot T_{in}^2}$$

$$D = \left(\frac{P}{\rho_{in} \cdot A \cdot c_p}\right)^2$$

By developing (36) and simplifying for J:

$$J^2 - J \left(4T_{in} + \frac{\zeta \cdot C \cdot D}{\Delta p} + \frac{4 \cdot C \cdot D}{\Delta p}\right) + 4T_{in}^2 + \frac{8T_{in} \cdot C \cdot D}{\Delta p} = 0 \quad (37)$$

This is a quadratic equation and can be written on the form: $J = \frac{a}{2} \pm \sqrt{\left(\frac{b}{2}\right)^2 - q}$

Where $a = 4T_{in} + \frac{\zeta \cdot C \cdot D}{\Delta p} + \frac{4 \cdot C \cdot D}{\Delta p}$ and $b = 4T_{in}^2 + \frac{8T_{in} \cdot C \cdot D}{\Delta p}$

Changing back the variable and solving for T_{ex} gives:

$$T_{ex} = J - T_{in} \quad (38)$$

This way of calculating the outlet temperature is the “backwards” way. The inlet pressure and velocity are not known and iterations have to be done to get the correct outlet temperature.

2.1.3.1 Iteration

The inlet temperature is known, an outlet pressure is chosen for the calculations and initially the inlet velocity is guessed. This is introduced into the for-loop where the pumping power varies from 1W to 900kW.

Relating the pumping power to the pressure drop using equation (30) gives:

$$\Delta p = \frac{P_{pump}}{w_1 \cdot A} \quad (39)$$

Inserting equation (39) into (29) gives the inlet pressure:

$$p_{in} = p_{ex} + \frac{P_{pump}}{w_1 \cdot A} \quad (40)$$

The pressure at the inlet has to be calculated at the beginning of the iteration so that the density can be calculated by inserting equation (40) into (26). This has to be done because the density is needed when calculating the outlet temperature.

The next step is to replace the pressure drops in the quadratic equation (37) with (39). This step is required to relate the outlet temperature directly by the pumping power. It results:

$$J^2 - J \left(4T_{in} + \frac{\zeta \cdot C \cdot D}{\frac{P_{pump}}{w_1 \cdot A}} + \frac{4 \cdot C \cdot D}{\frac{P_{pump}}{w_1 \cdot A}} \right) + 4T_{in}^2 + \frac{8T_{in} \cdot C \cdot D}{\frac{P_{pump}}{w_1 \cdot A}} = 0 \quad (41)$$

Now the quadratic equation (41) has to be solved. Then T_{ex} can be calculated with help of equation (38), by simply changing back the variables.

A new inlet velocity is now calculated with help of equation (34).

The new inlet velocity is inserted into equation (40) at the beginning of the iteration process. This is done to be able to calculate the new inlet pressure, p_{in} which gives the new density.

This is done 20 times to assure convergence, i.e. the unknown inlet and outlet variables for the given pumping power are correct.

2.1.3.2 For-loop

The for-loop contains all of the equations including the iteration process. The for-loop varies with the pumping power from 1-900 kW. Important data are saved in a matrix for every given pumping power by the for-loop. This matrix is then copied to excel where the graphs are generated.

2.1.4 Straight forward method

The straight forward method is used to generate contour plots of different surfaces in the sphere bed. It is also more accurate because the calculations are done cell wise instead of zone wise. If the inlet parameters are known, then the outlet parameters can easily be calculated by making direct use of eq. (1)-(31).

A zone is split up into columns; the columns are then split up into cells according to *Figure 4*. The columns are isolated from each other, i.e. heat transfer and pressure, etc only varies along a column. The mass flow rate is conserved along the column. This simplification is done because the equations are one dimensional. In the real case there would be flow and heat transfer sidewise as well. If the inlet pressure, the inlet temperature and the inlet velocity are known one, gets the wanted outlet parameters, without iteration needed. With help of the FLUKA [4] file, which contains data about the energy deposition in (x,y,z) Cartesian coordinates, the beam intensity and the time distribution, the power density in every cell can be calculated. The outlet parameters of the first cell become the inlet parameters for the next one and so on, according to *Figure 4*. This means that the helium temperature at the outlet or inlet of each cube in a column can be calculated. Also the outlet and inlet velocity, and pressure of each cube can be calculated. In Mat lab the value of each variable in each cell is stored in matrixes or cells, with help of this, it is easy to generate contour plots of different surfaces.

Because of that both the inlet and outlet temperature of a cell can be calculated, the equation to estimate the maximum sphere temperature is now:

$$T_0 = \frac{T_{in,i} + T_{ex,i}}{2} + T_1 + \Delta T \quad (42)$$

A zone is split up into columns and then cells

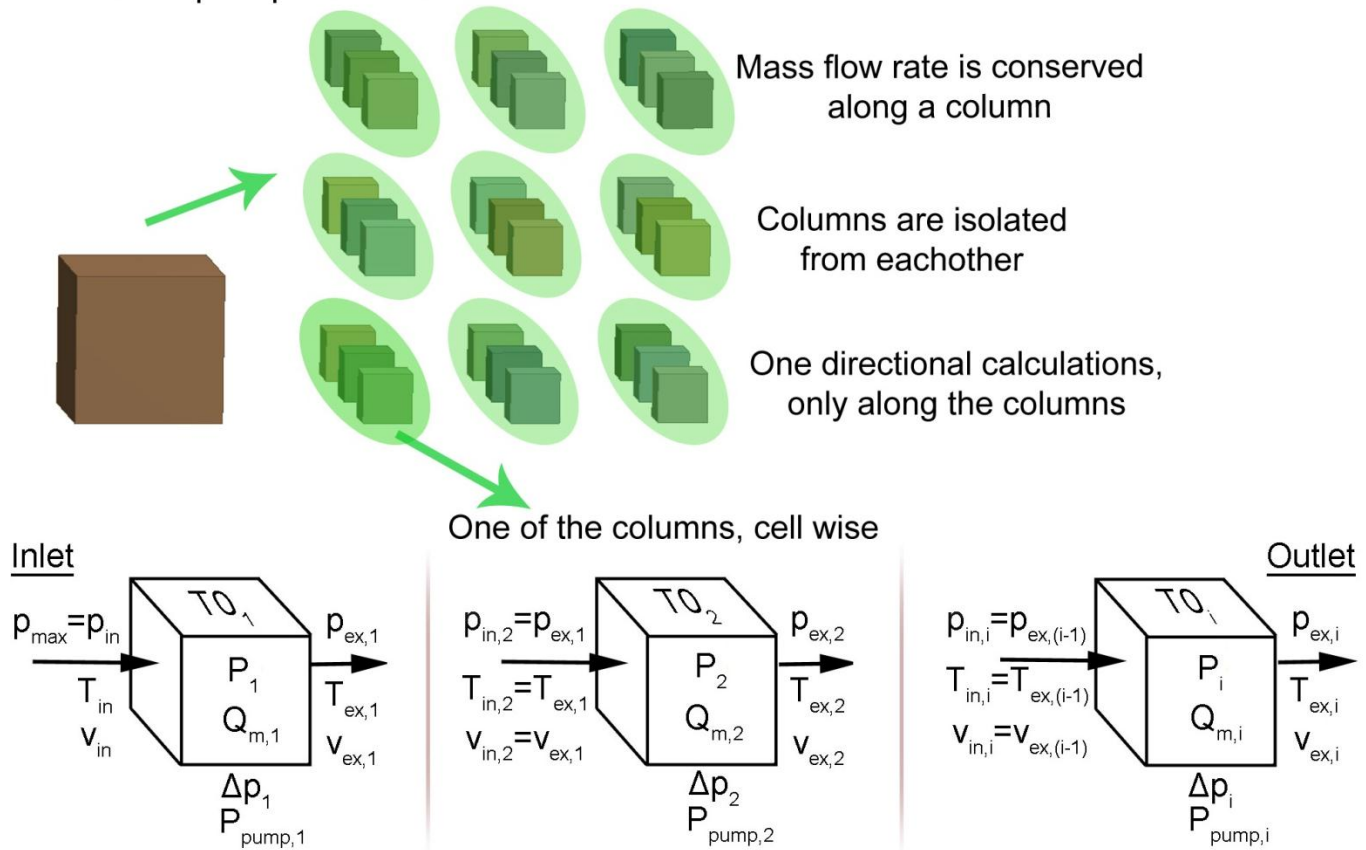


Figure 4. Cell wise calculations. A zone is split up into columns and then the columns are split up into cells. The columns are isolated from each other, which means that the calculations are unidirectional along the column. The mass flow rate is conserved along a column. Calculations are done cell wise. The outlet parameters from the first cell become the inlet parameters for the next one, and so on.

2.1.5 Graphs

The “backwards” iterative method is used for generating graphs with the essential parameters. Calculations are done for when the static pressure is 10 bar and with sphere diameters of 6, 8, 10 and 12mm. The pumping power ranges from 1W to 900kW with an interval of 5kW.

2.1.5.1 Input Variables

There are some variables that are held constant all the time according to *Table 2*:

$$T_{in} = 22 \text{ } ^\circ\text{C} \quad l_0 = 0.22 \text{ m} \quad \epsilon = 0.2595$$

$$A = 0.016 \text{ m}^2 \quad B = 1.8 \quad \varphi = 1$$

Table 2. Constant variables for graph generation

The initially guessed inlet velocity is $w_1 = 15 \text{ m/s}$. The value 1.8 of the constant B is for when the spheres have smooth surface. φ is the shape coefficient, its value is 1 for a perfectly round sphere.

In the three zones the following values are used according to *Table 3*. The values given are the power within a zone and the maximum energy per gram and pulse to calculate the hottest sphere temperature. These are derived from the FLUKA file [4].

	<u>Zone 1</u>	<u>Zone 2</u>	<u>zone 3</u>
Power P [MW] :	1.684	0.5315	0.1057
Q_m [J/g/pulse] :	5.98	2.13	0.403

Table 3. Power and energy values for the graph generation

2.1.5.2 Results

The results are presented as graphs for the three different zones. These contain the maximum sphere temperature and the average helium outlet temperature on the left y-axis. The pumping power is on the x-axis and the maximum pressure in the system on the right y-axis.

Graphs are generated for the three different zones. Zone 1 is the most interesting one to investigate because about 70% of the total power is located here. The goal is to have an efficient cooling with the lowest pumping power achievable. However the maximum allowed pumping power for cooling the three zones shall not exceed 500kW. At the same time the maximum pressure in the system should be lower than 20 bar. The average outlet helium temperature should be below 400 °C and the maximum sphere temperature should be below 800 °C. All of this according to the requirements mentioned earlier.

Figure 5 below shows the graph for zone 1. The temperatures and the pumping power should be within the green box. For example if the variables are studied for the maximum pressure of 20 bar and a sphere diameter of 10 mm, in this case the blue lines in the graph. Follow the yellow line from the right y-axis at 20 bar until it reaches the blue dotted line, which represents the maximum pressure in the system. Now follow the yellow line vertically upwards, here the pumping power can be seen on the x-axis. It is approximately 250 kW which is well below the requirement. Continue following the yellow line upwards until it reaches the blue line. This line represents the maximum sphere temperature. In this case it is slightly below 600 °C which also fulfills the requirement. Finally follow the yellow line downwards until it reaches the other blue line. This line represents the average helium outlet temperature. In this case it is slightly below 400 °C which does not fulfill the requirement. However this can be accepted.

Notice, if the maximum pressure would be lowered by only 2-3 bar, the average helium outlet temperature would rise to an unaccepted level. By having a low maximum pressure in the system, the pumping power needed is lower, while the temperatures rise in both the helium and the spheres. It can also be seen that 12mm spheres get hotter than the 6 mm spheres. For the helium it is the other way around, the average helium outlet temperature is hotter for 6 mm spheres than for 12 mm spheres.

Zone 1

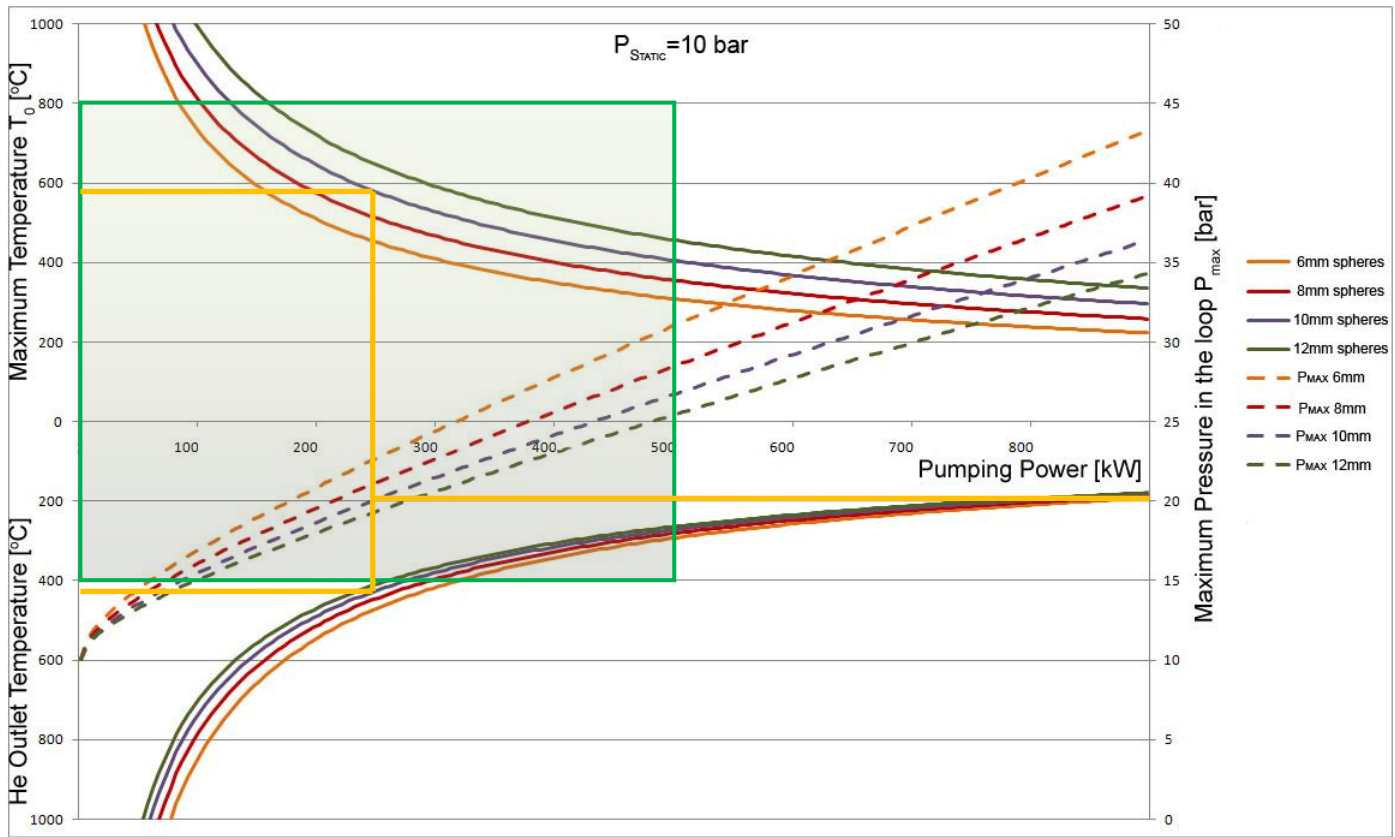


Figure 5. Graph, Zone 1. The graph shows the results for sphere diameters 6,8,10 and 12 mm when the static pressure is 10 bar. The left y-axis shows the maximum sphere temperature and the average helium outlet temperature. The right y-axis shows the maximum pressure in the system. The x axis shows the pumping power.

Figure 6 and Figure 7 below show the same type of graph but for zone 2 and 3. The green box and the yellow lines are drawn in these graphs as well; the difference is that the maximum pressure can be lowered. For zone 2 the yellow line represents maximum pressure of 15 bar and for zone 3, 12.5 bar. The pumping power needed for zone 2 is slightly above 100 kW. The temperatures are well below the maximum allowed. For zone 3, the pumping power needed is approximately 50kW, the temperatures fulfill the requirements here as well. The sum of the pumping power from the three zones is approximately 400 kW which is below the maximum allowed.

According to the equations used to generate the graphs it is possible to cool the target and fulfill the requirements. These results should only be used as guide lines. It is a global analysis which is done zone wise, more accurate results will be derived with the cell wise calculation.

Zone 2

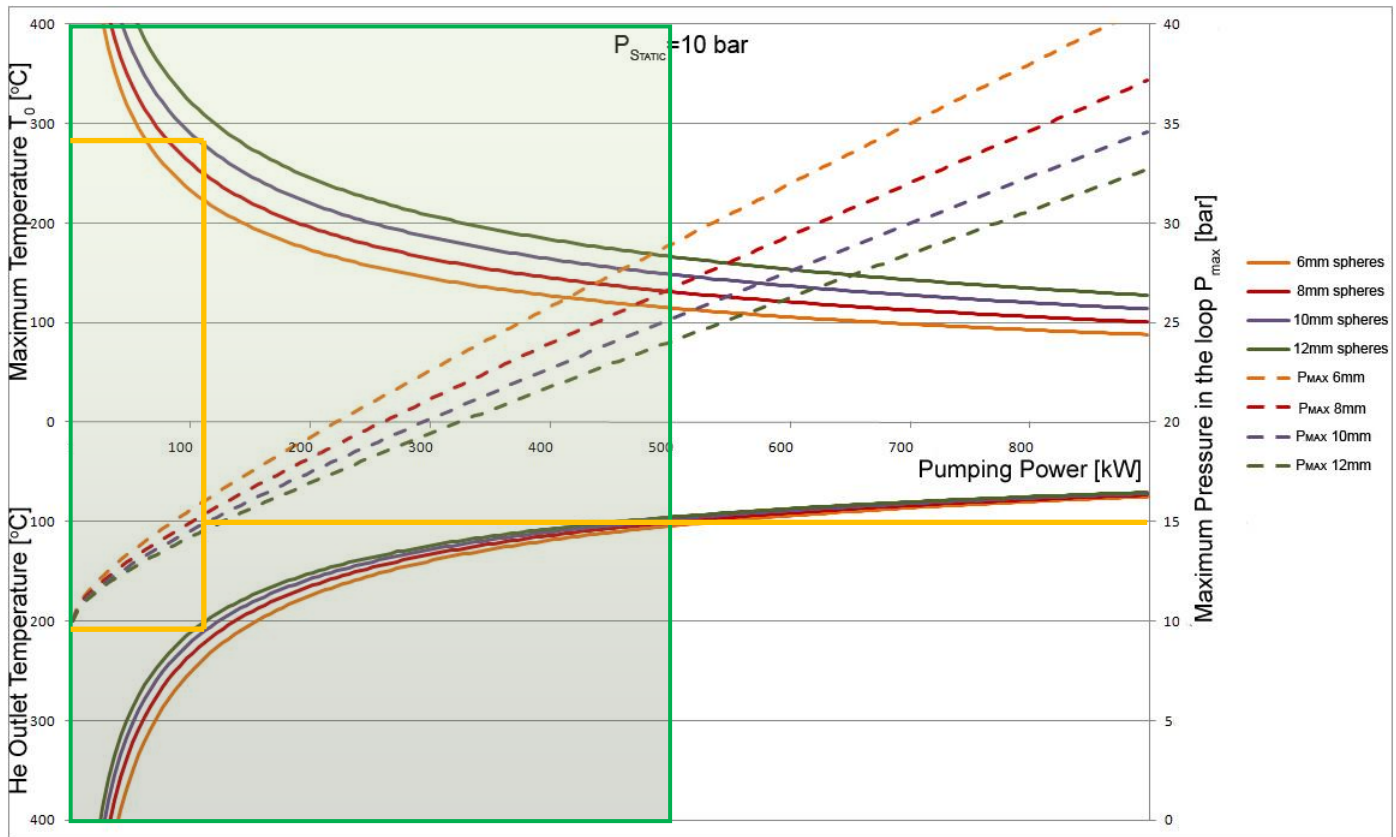


Figure 6 Graph, Zone 2. The graph shows the results for sphere diameters 6,8,10 and 12 mm when the static pressure is 10 bar. The left y-axis shows the maximum sphere temperature and the average helium outlet temperature. The right y-axis shows the maximum pressure in the system. The x axis shows the pumping power.

Zone 3

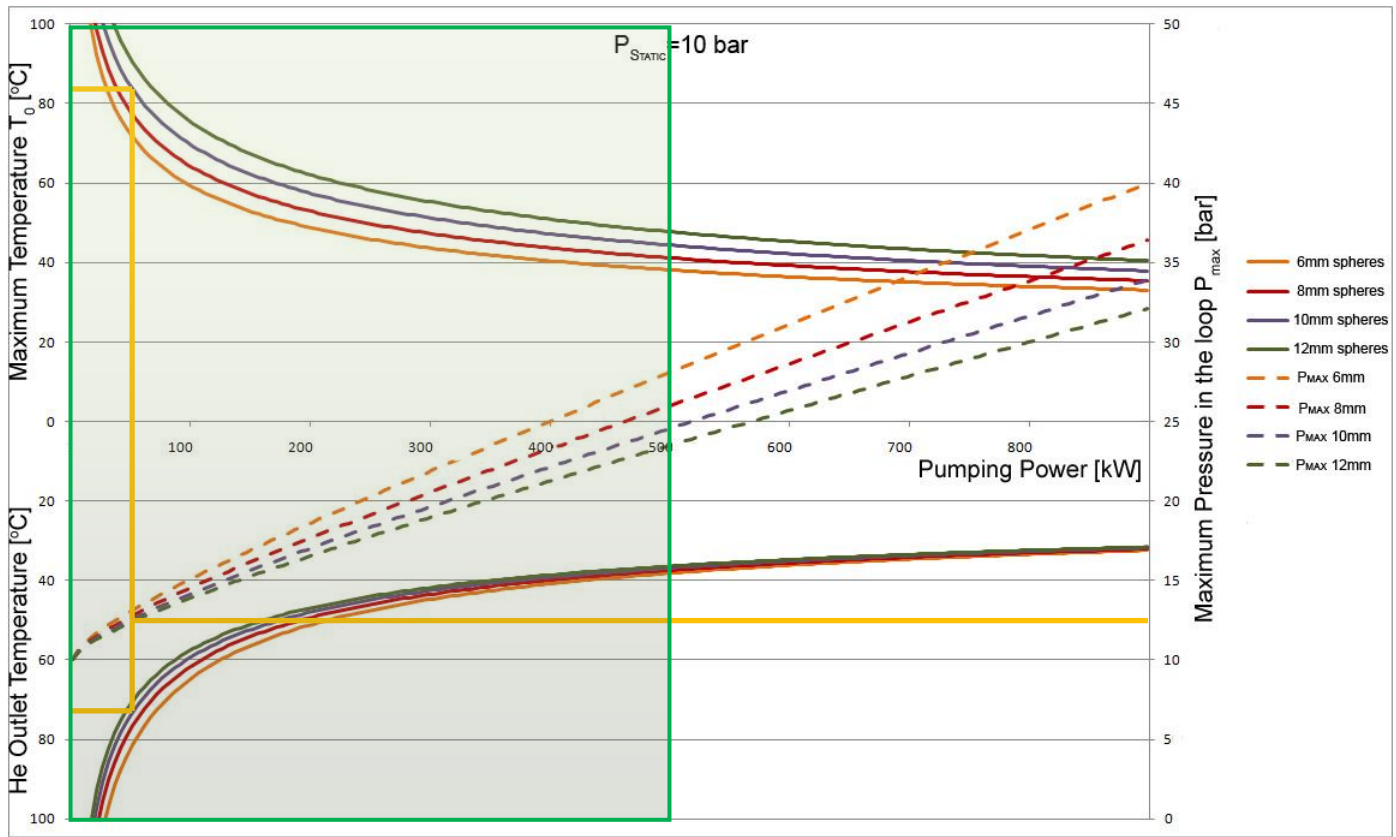


Figure 7 Graph, Zone 3. The graph shows the results for sphere diameters 6,8,10 and 12 mm when the static pressure is 10 bar. The left y-axis shows the maximum sphere temperature and the average helium outlet temperature. The right y-axis shows the maximum pressure in the system. The x axis shows the pumping power.

2.1.6 Contour Plots

To generate contour plots the straight forward method is used with cell wise calculations. Plots are made for the three different zones on their outlet surfaces, as shown in Figure 8 below. Contour plots are made for the helium outlet temperature and the outlet pressure of each zone.

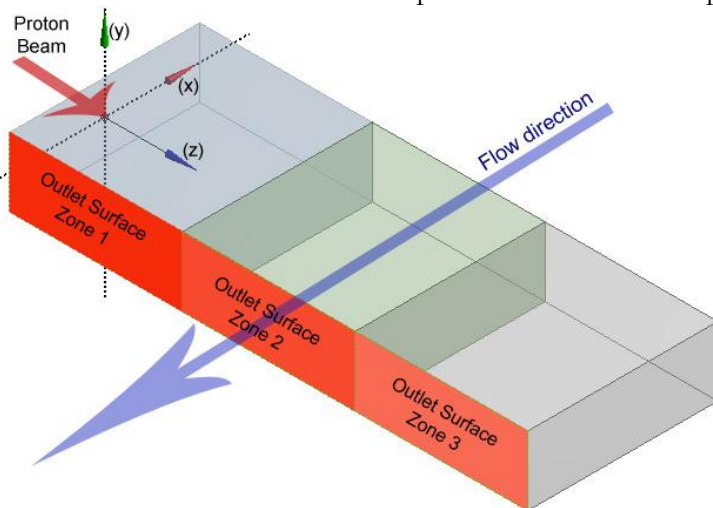


Figure 8. Plot surfaces. Contour plots are made for the outlet surfaces of the three zones according to the figure. The proton beam hits the target along the z-axis.

2.1.6.1 Zone Inlet Parameters

All zones have a sphere diameter of 10mm and an inlet temperature of 22°C is assumed. *Table 4* below shows the used inlet parameters for the columns in the different zones.

<u>Zone</u>	<u>p_{in} [bar]</u>	<u>V_{in} [m/s]</u>
1	20	15
2	14.5	8.5
3	13.2	3.0

Table 4. Inlet parameters, Contour plots

2.1.6.2 Results

Beside the contour plots there is a table for each zone that shows the average helium outlet temperature, the maximum sphere temperature and the pumping power for each zone. The flow direction is perpendicular to the contour plots. The plots show contour on the outlet surfaces as shown in *Figure 8*.

According to the inlet parameters the maximum allowed pressure is used for zone 1. Even with this high pressure the temperatures are too high. The average helium outlet temperature is 436 °C according to *Table 5* below, this is slightly above the maximum allowed temperature. The maximum sphere temperature is far above the allowed 800 °C and this is not acceptable. The tungsten will not sustain such high temperatures in these conditions. The pumping power needed for zone 1 is 370 kW and fulfill the requirements. *Figure 9* below shows the helium outlet temperature at the outlet surface of zone 1. The flow direction is perpendicular and outwards from the figure. The hottest part of the sphere bed is located approximately 4 cm into zone 1 in the z direction. As mentioned earlier, about 70% of the total power deposition is located in zone 1; this explains the high temperatures. The temperatures are relatively low at the top and bottom of the target. *Figure 10* is a similar contour plot but of the helium outlet pressure. It shows that the pressure drop is higher at high temperatures.

Zone 1

Average Helium Outlet Temperature :	436 °C
Maximum Sphere Temperature:	1179 °C
Pumping Power:	370 kW

Table 5. Zone 1 results

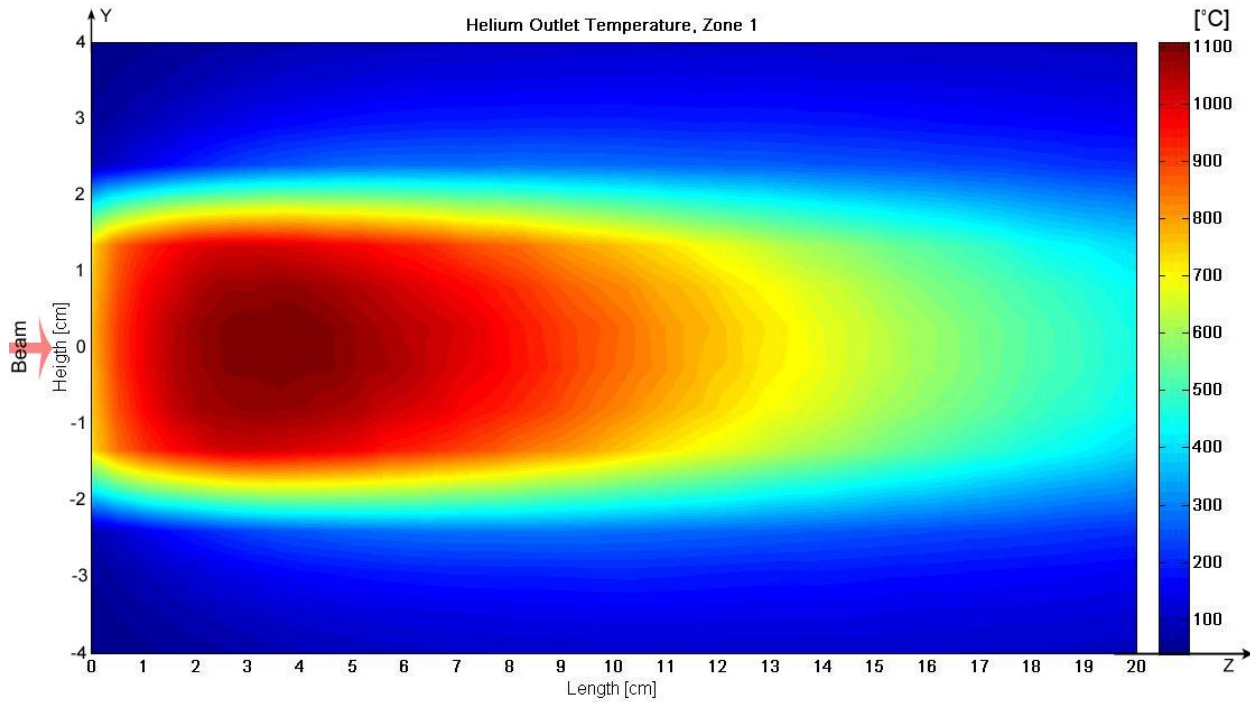


Figure 9. Helium outlet temperature, Zone 1. X- and y-axes show the target length and height in [cm] of a zone. Helium is flowing perpendicular, outwards of the plot surface. The contour plot shows the helium outlet temperature at the outlet surface of zone 1, in [C].

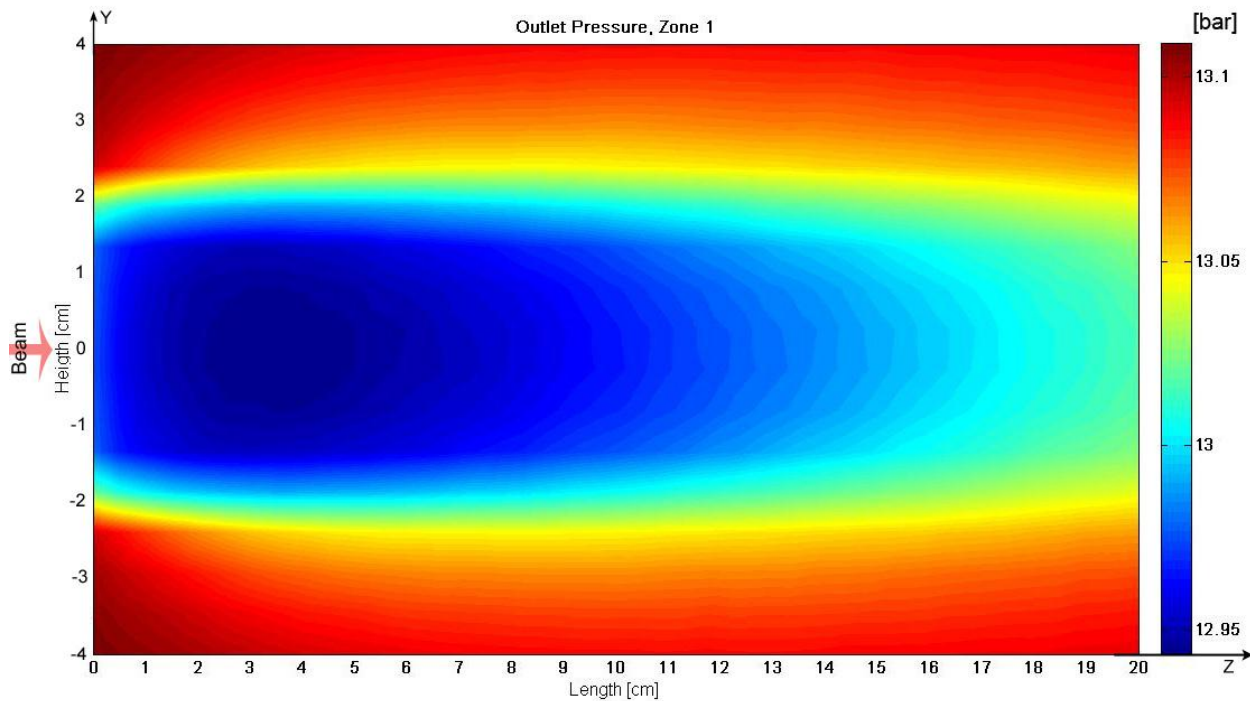


Figure 10. Outlet pressure, Zone 1. X- and y-axes show the target length and height in [cm] of a zone. Helium is flowing perpendicular, outwards of the plot surface. The contour plot shows the pressure at the outlet surface of zone 1, in [bar]. Table 4 shows the inlet parameters, with help of this the pressure drop can be calculated.

The inlet pressure for zone 2 is 14.5 bar and the inlet velocity is 8.5 m/s. Lower inlet pressure and velocity can be used compared to zone 1. This is because the significantly lower power deposition in the zone. In zone 2 the maximum sphere temperature is still too high according to *Table 6*. The other variables fulfill the requirements. The inlet variables could be adjusted to be higher and faster, in that case lower temperatures could be achieved. This change will contribute to increase the pumping power.

Figure 11 and *Figure 12* show contour plots of the average helium outlet temperature and the outlet pressure. These plots are the same type of contour plots as the ones for zone 1.

Zone 2

Average Helium Outlet Temperature : 340 °C

Maximum Sphere Temperature: 1078 °C

Pumping Power: 31.5 kW

Table 6. Zone 2 results

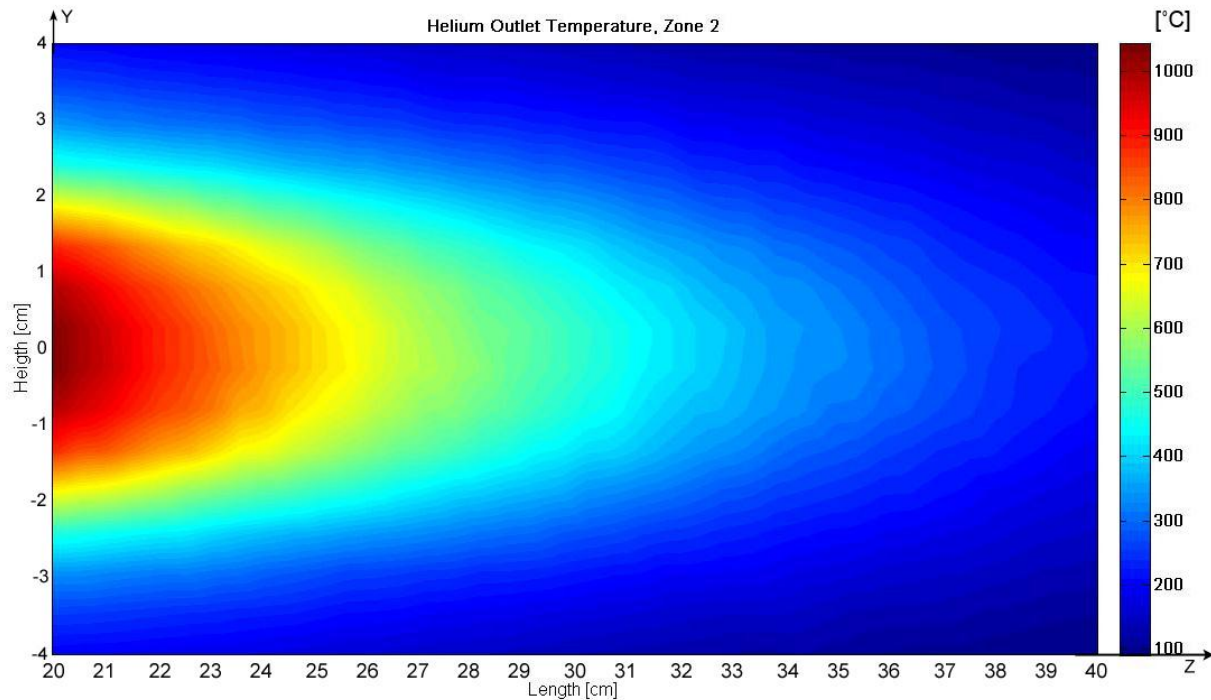


Figure 11. Helium outlet temperature, Zone 2. X- and y-axes show the target length and height in [cm] of a zone. Helium is flowing perpendicular, outwards of the plot surface. The contour plot shows the helium outlet temperature at the outlet surface of zone 2, in [C].

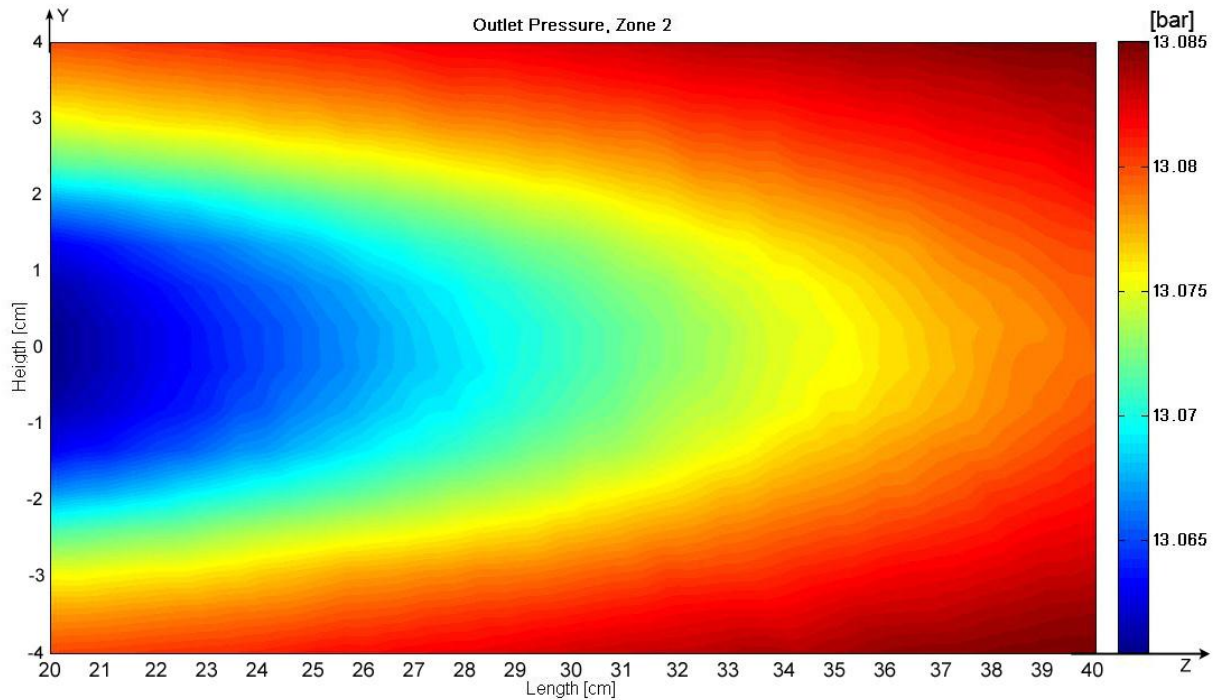


Figure 12. Outlet pressure, Zone 2. X- and y-axes show the target length and height in [cm] of a zone. Helium is flowing perpendicular, outwards of the plot surface. The contour plot shows the pressure at the outlet surface of zone 2, in [bar]. Table 4 shows the inlet parameters, with help of this the pressure drop can be calculated.

The temperatures and pumping power for zone 3 are well below the requirements, according to Table 7. Figure 13 and Figure 14 shows the average helium outlet temperature and the outlet pressure in the same way as the 2 other zones.

The sum of the pumping power for the three zones is approximately 400 kW, the requirement is fulfilled. Zone 1 and 2 has too hot sphere temperatures which cannot be accepted. Another solution to cool the target has to be thought of.

Zone 3

Average Helium Outlet Temperature : 219 °C

Maximum Sphere Temperature: 630 °C

Pumping Power: 1.0 kW

Table 7. Zone 3 results

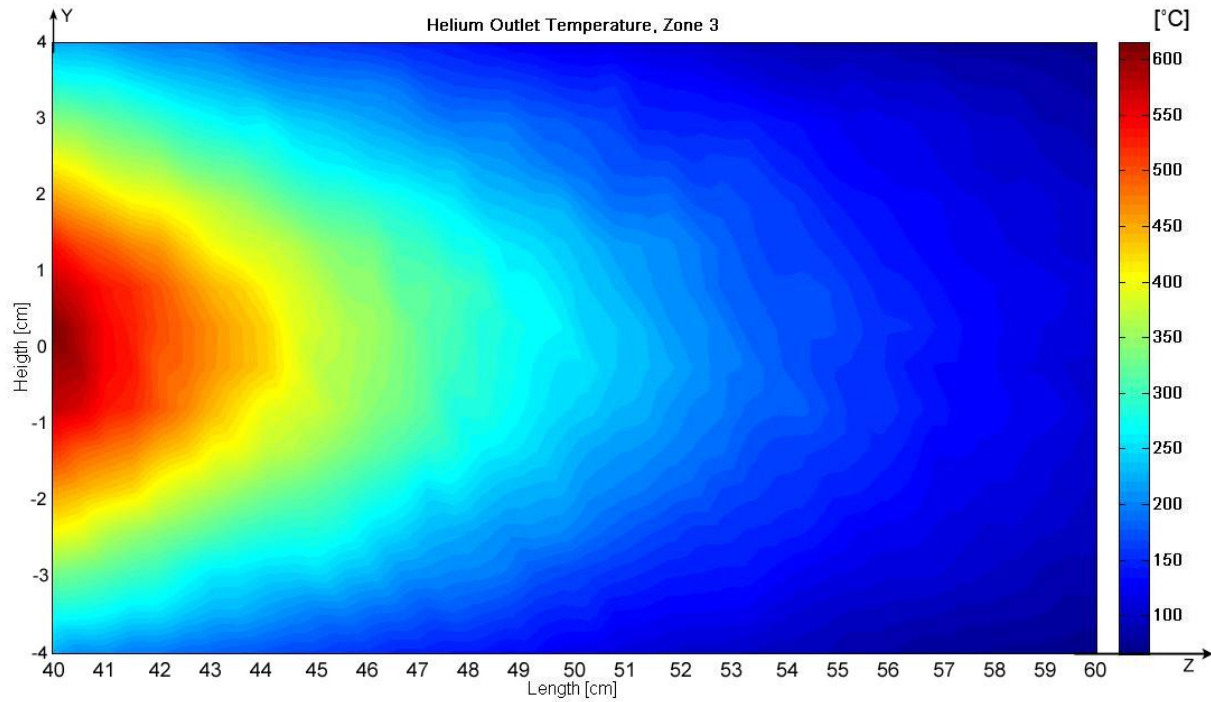


Figure 13. Helium outlet temperature, Zone 3. X- and y-axes show the target length and height in [cm] of a zone. Helium is flowing perpendicular, outwards of the plot surface. The contour plot shows the helium outlet temperature at the outlet surface of zone 3, in [C].

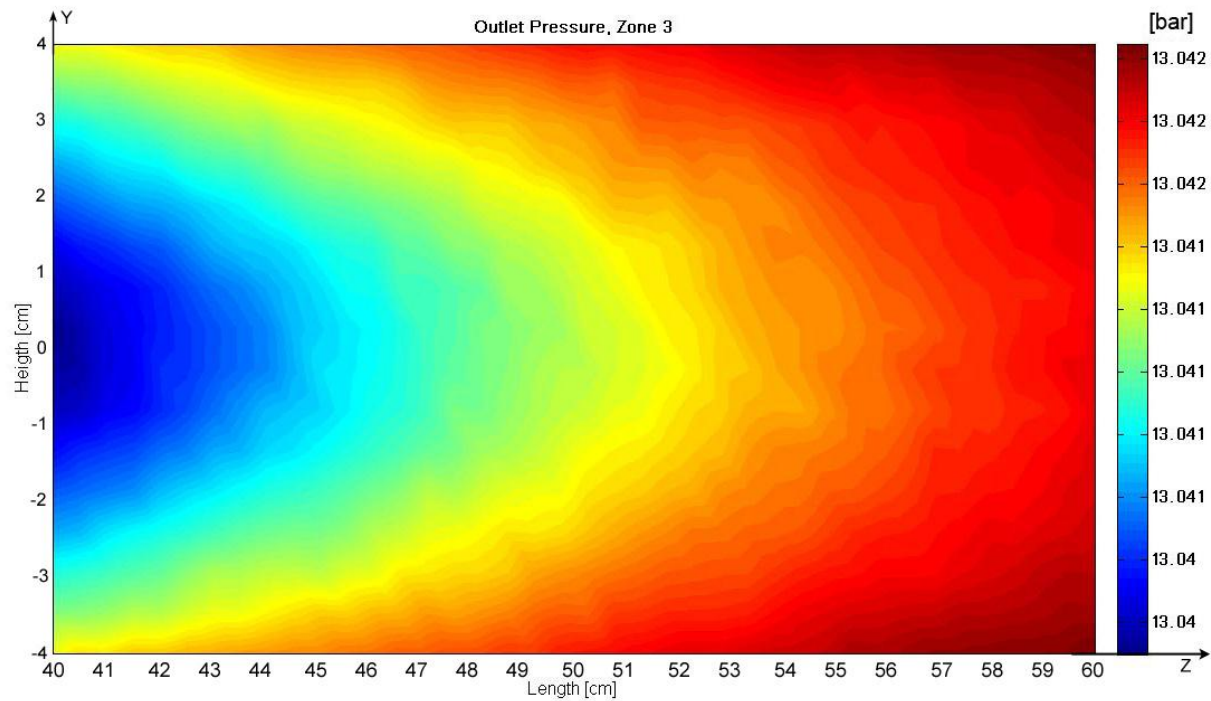


Figure 14. Outlet pressure, Zone 3. X- and y-axes show the target length and height in [cm] of a zone. Helium is flowing perpendicular, outwards of the plot surface. The contour plot shows the pressure at the outlet surface of zone 3, in [bar]. Table 4 shows the inlet parameters, with help of this the pressure drop can be calculated.

2.1.7 Flow from the top

Because the maximum sphere temperature is too high in the previous case it was decided that it had to be improved. Adjusting the dimensions should be enough to lower the temperature. The length that the helium has to flow through in the sphere bed should be shortened. This will lower the pressure drop significantly, which means that a lower pressure in the system could be used. Instead of adjusting the dimensions, the flow can enter from the top instead. *Figure 15* shows the new plot surfaces and flow direction. The flow-through length is now only 8 cm compared to 22 cm in the previous case. The graphs and contour plots are generated in the same way as before.

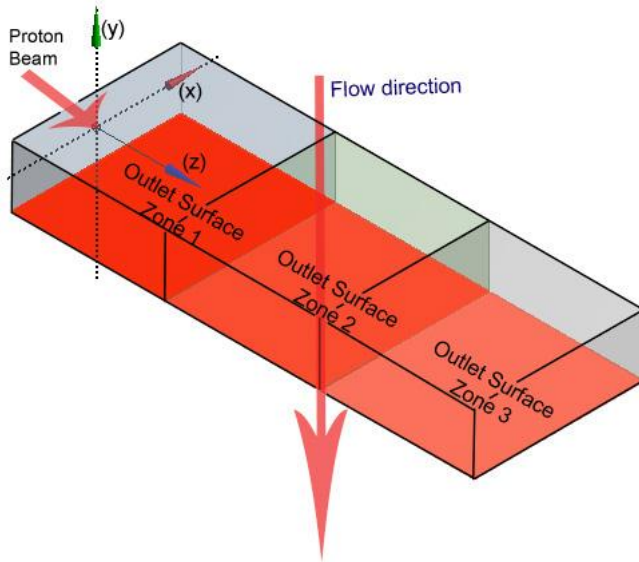


Figure 15. Plot Surfaces, flow from top. Contour plots are made for the outlet surfaces of the three zones according to the figure.

2.1.7.1 Graphs

The inlet parameters are the same as in the previous case according to *Table 2* and *Table 3*, except for the changes of the dimensions. The length is now, $l_0 = 0.08 \text{ m}$ and the inlet area of a zone is, $A = 0.044 \text{ m}^2$

Because of the short length the helium has to flow through the sphere bed, the pressure drop decreases. Due to this lower inlet pressure can be used. The yellow line shows an example if the maximum pressure is 12 bar and the sphere diameter is 10 mm for zone 1. In this case the maximum sphere temperature is slightly above 600 °C, the average helium outlet temperature is about 250 °C and the pumping power needed is approximately 150 kW. The other two zones easily fulfill the requirements.

Zone 1

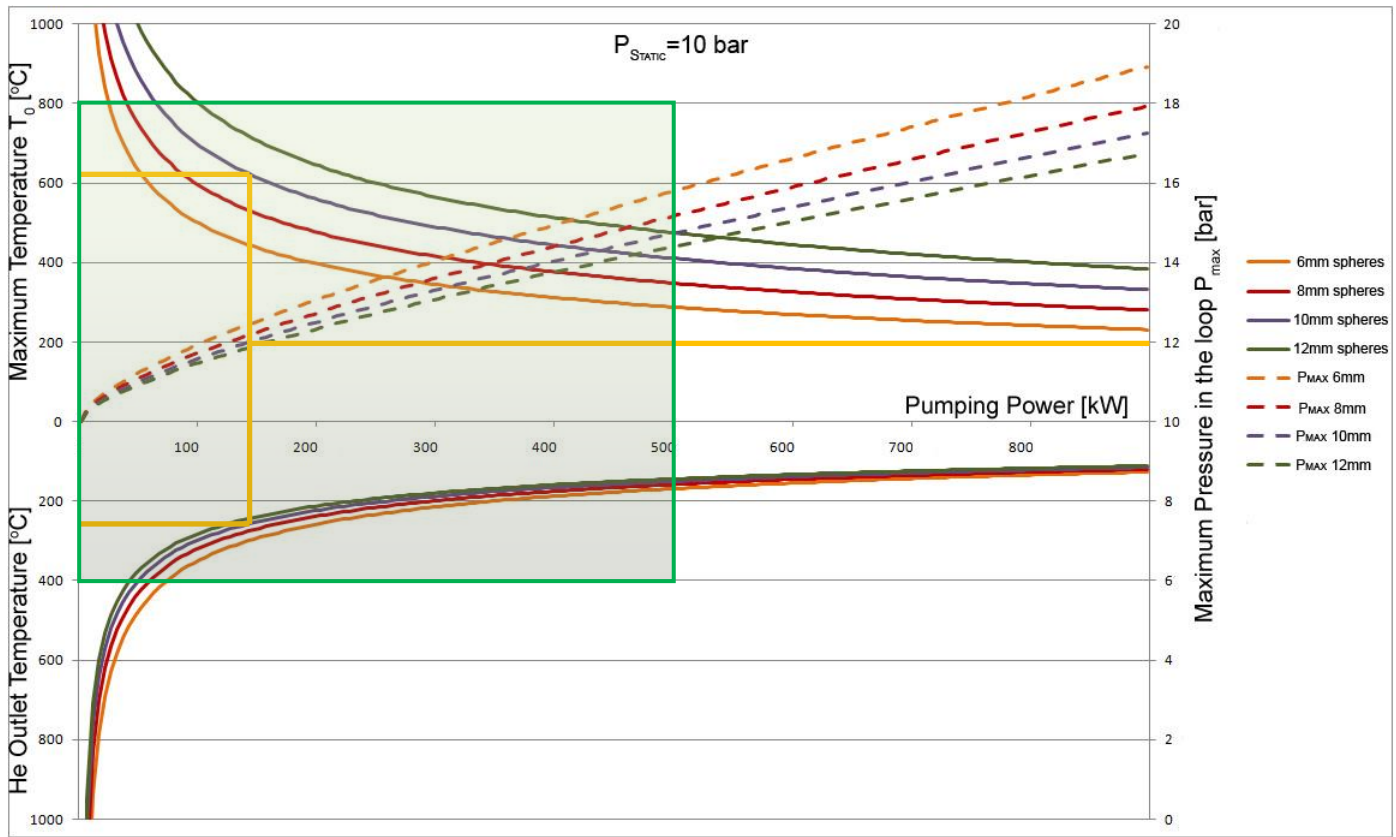


Figure 16. Graph Zone 1, flow from top. The graph shows the results for sphere diameters 6,8,10 and 12 mm when the static pressure is 10 bar. The left y-axis shows the maximum sphere temperature and the average helium outlet temperature. The right y-axis shows the maximum pressure in the system. The x axis shows the pumping power.

Zone 2

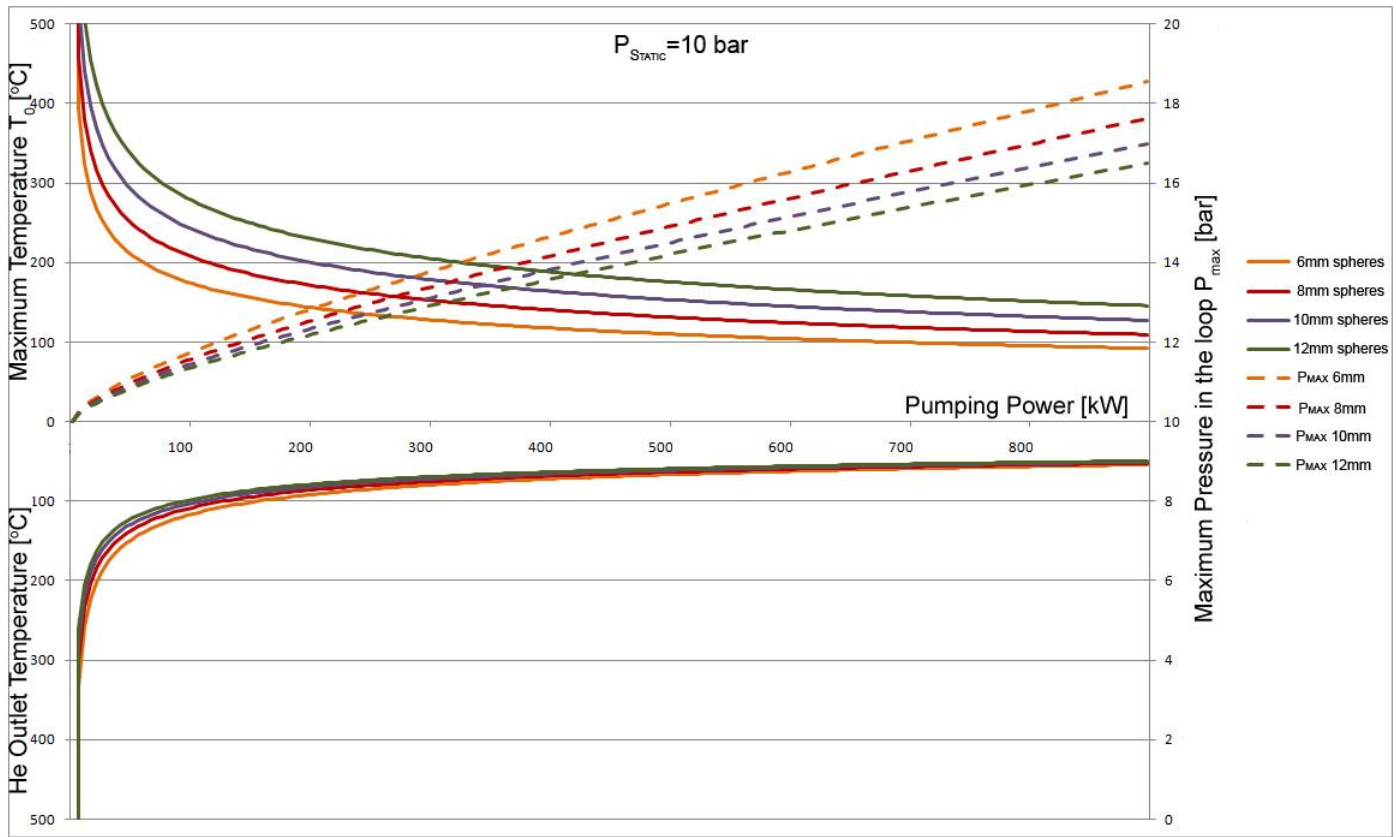


Figure 17. Graph Zone 2, flow from top. The graph shows the results for sphere diameters 6,8,10 and 12 mm when the static pressure is 10 bar. The left y-axis shows the maximum sphere temperature and the average helium outlet temperature. The right y-axis shows the maximum pressure in the system. The x axis shows the pumping power.

Zone 3

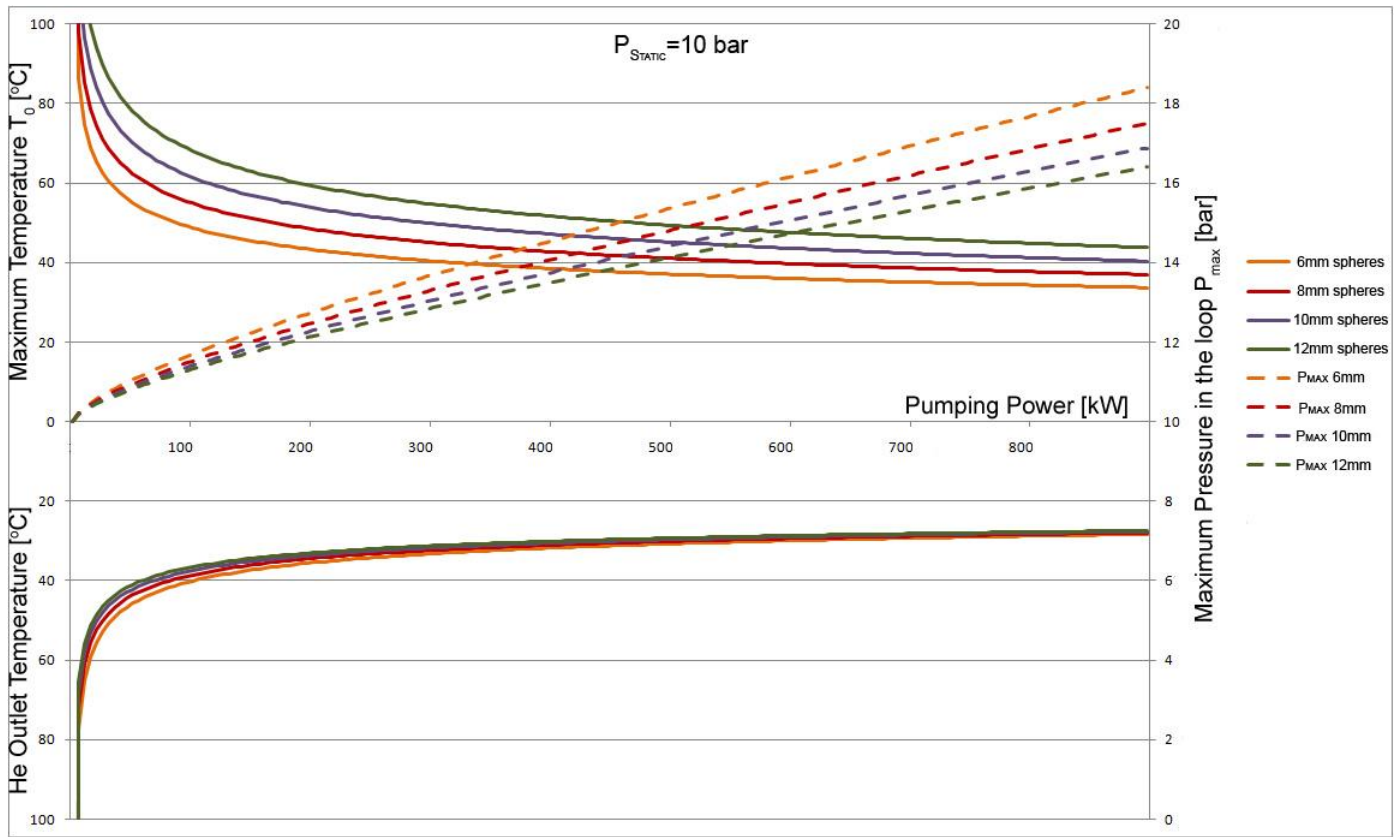


Figure 18. Graph Zone 3, flow from top. The graph shows the results for sphere diameters 6,8,10 and 12 mm when the static pressure is 10 bar. The left y-axis shows the maximum sphere temperature and the average helium outlet temperature. The right y-axis shows the maximum pressure in the system. The x axis shows the pumping power.

2.1.7.2 Contour Plots

Contour plots are made for the outlet surfaces according to Figure 15. The flow direction is perpendicular to the contour plot surfaces. They are of the helium outlet temperatures and the outlet pressures. The sphere diameter and inlet temperature is the same as in the previous case, 10 mm and 22 °C. Inlet parameters used for the zones are shown in Table 8 below.

Zone	p_{in} [bar]	V_{in} [m/s]
1	15	15
2	13.7	8
3	13.4	4.0

Table 8. Inlet parameters, Contour plots, flow from top

Table 9 below shows the results for zone 1, when the helium enters from the top. Compared to the previous case both temperatures are significantly lower. With the shorter flow-through length it is possible to decrease the temperatures to too acceptable ones. All the requirements are fulfilled with this solution according to the cell wise analytic calculations.

Zone 1

Average Helium Outlet Temperature : 223 °C

Maximum Sphere Temperature: 741 °C

Pumping Power: 156 kW

Table 9. Zone 1 results, flow from top

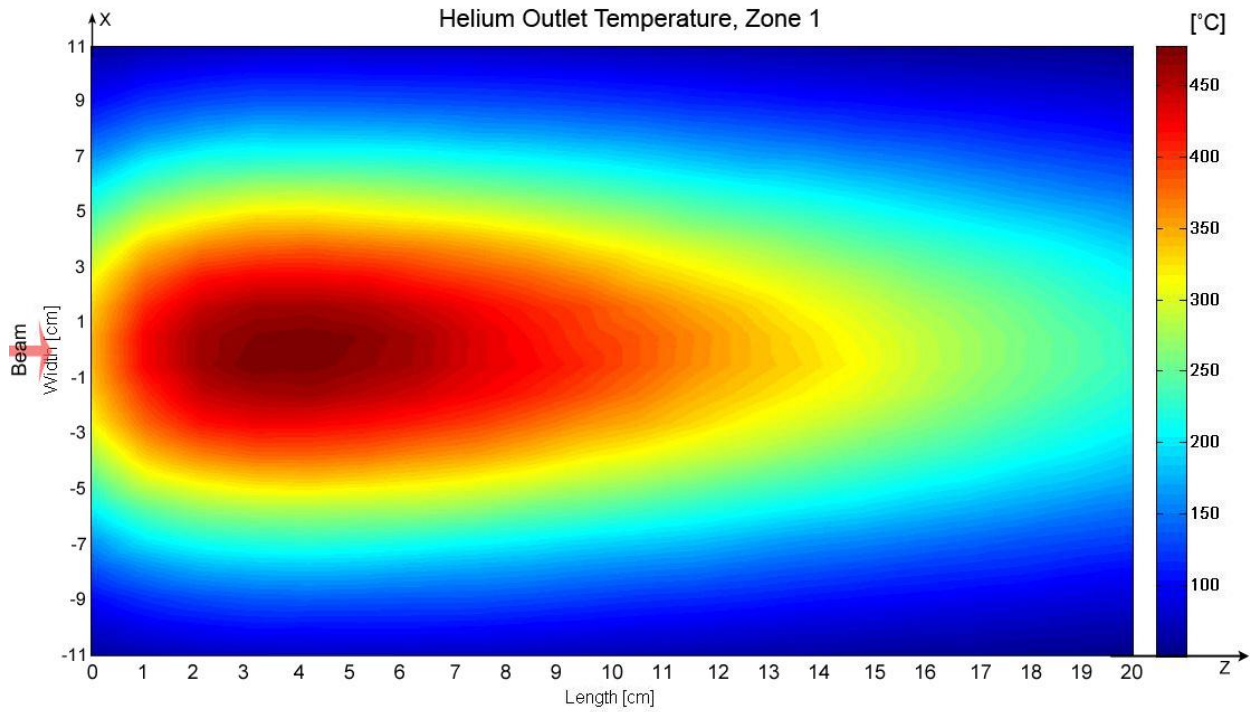


Figure 19. Helium outlet temperature, Zone 1, flow from top. X- and y-axes show the target length and width in [cm] of a zone. Helium is flowing perpendicular, outwards of the plot surface. The contour plot shows the helium outlet temperature at the outlet surface of zone 1, in [C].

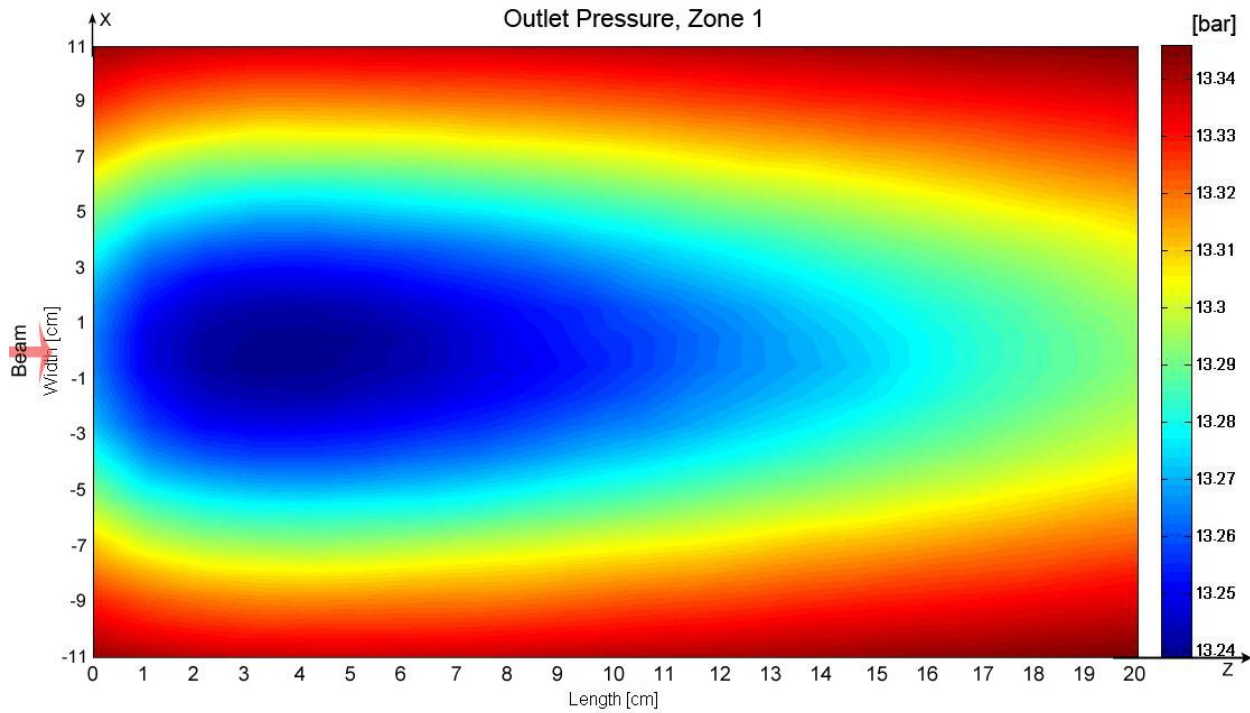


Figure 20. Outlet pressure, Zone 1, flow from top. X- and y-axes show the target length and width in [cm] of a zone. Helium is flowing perpendicular, outwards of the plot surface. The contour plot shows the pressure at the outlet surface of zone 1, in [bar]. Table 8 shows the inlet parameters, with help of this the pressure drop can be calculated.

Zone 2

Average Helium Outlet Temperature : 152 °C

Maximum Sphere Temperature: 525 °C

Pumping Power: 18.2 kW

Table 10. Zone 2 results, flow from top

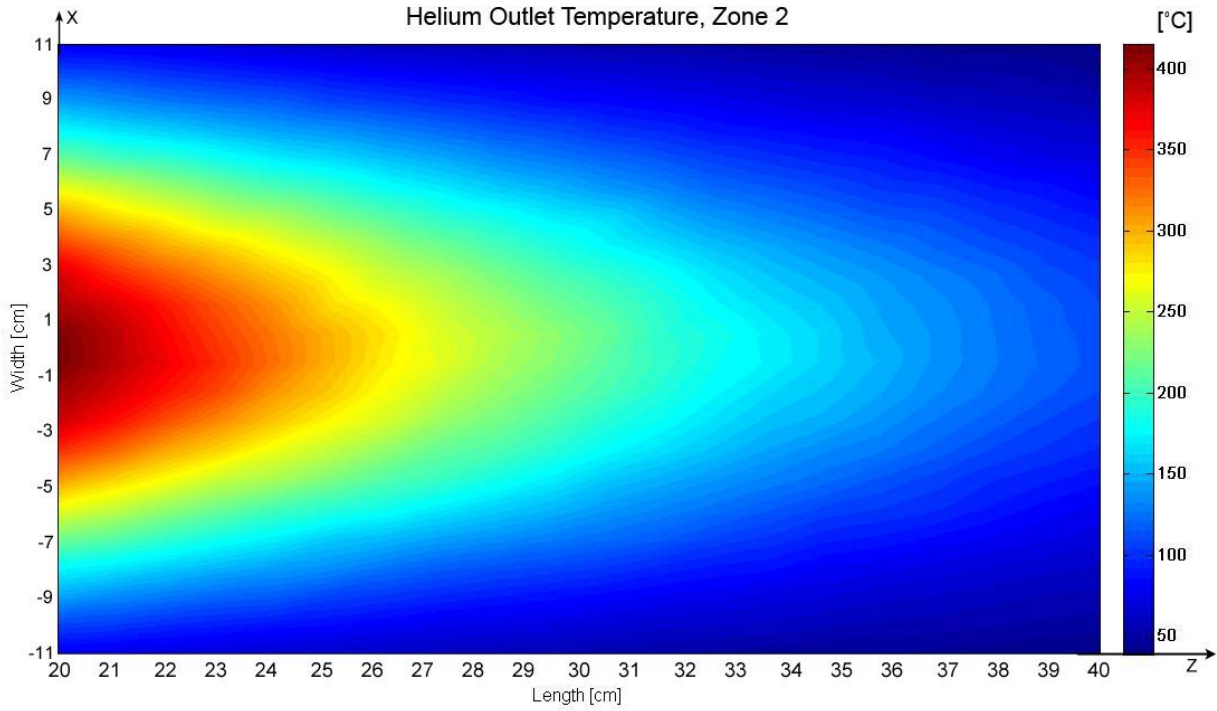


Figure 21. Helium outlet temperature, Zone 2, flow from top. X- and y-axes show the target length and width in [cm] of a zone. Helium is flowing perpendicular, outwards of the plot surface. The contour plot shows the helium outlet temperature at the outlet surface of zone 2, in [C].

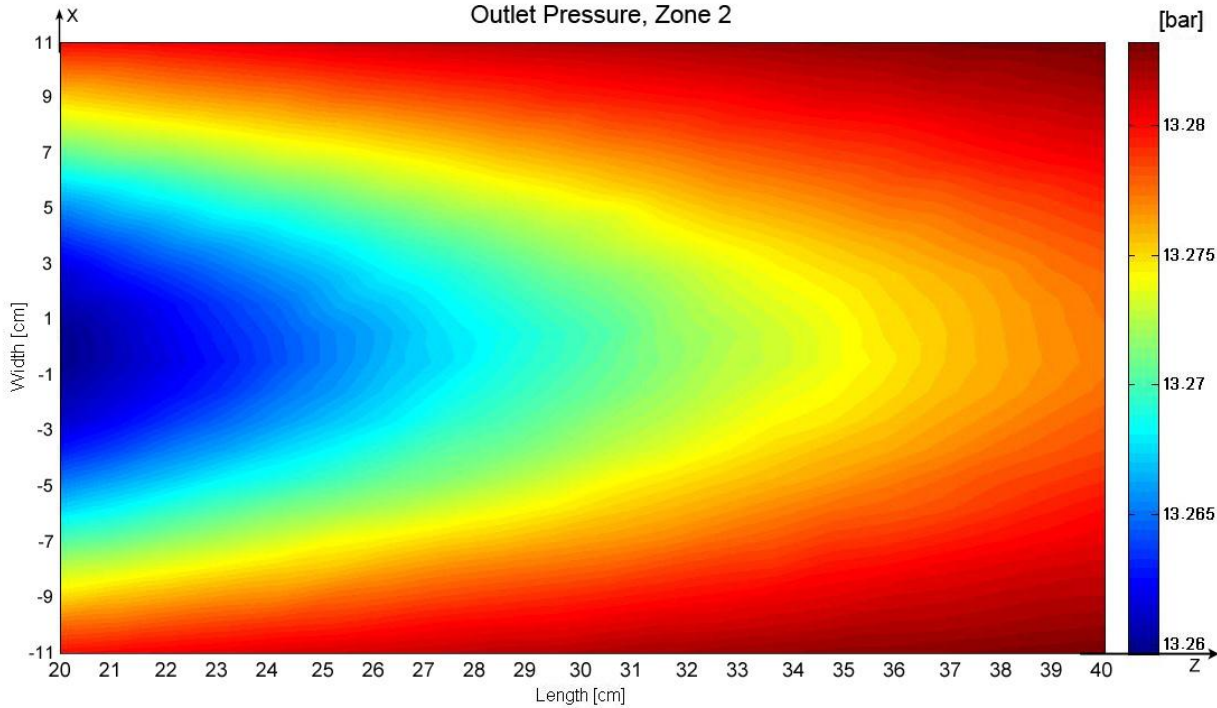


Figure 22. Outlet pressure, Zone 2, flow from top. X- and y-axes show the target length and width in [cm] of a zone. Helium is flowing perpendicular, outwards of the plot surface. The contour plot shows the pressure at the outlet surface of zone 2, in [bar]. Table 8 shows the inlet parameters, with help of this the pressure drop can be calculated.

Zone 3

Average Helium Outlet Temperature : 75 °C

Maximum Sphere Temperature: 217 °C

Pumping Power: 2 kW

Table 11. Zone 3 results, flow from top

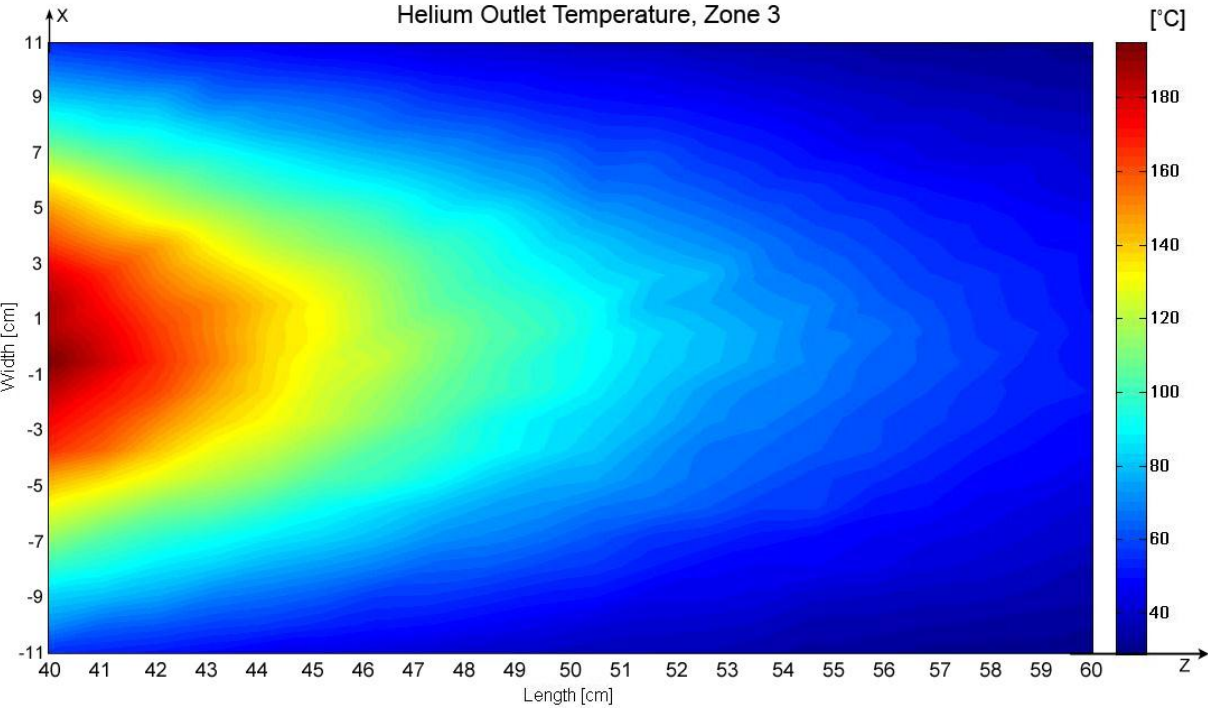


Figure 23. Helium outlet temperature, Zone 3, flow from top. X- and y-axes show the target length and width in [cm] of a zone. Helium is flowing perpendicular, outwards of the plot surface. The contour plot shows the helium outlet temperature at the outlet surface of zone 3, in [C].

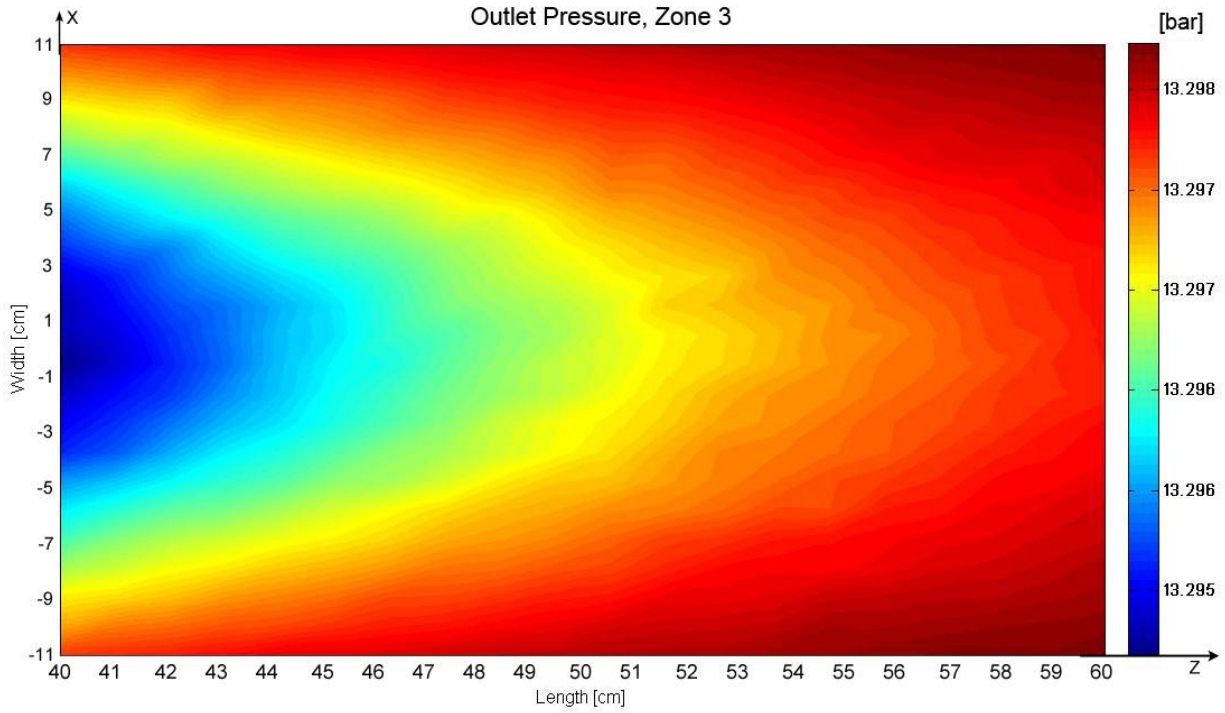


Figure 24. Outlet pressure, Zone 3, flow from top. X- and y-axes show the target length and width in [cm] of a zone. Helium is flowing perpendicular, outwards of the plot surface. The contour plot shows the pressure at the outlet surface of zone 3, in [bar]. Table 8 shows the inlet parameters, with help of this the pressure drop can be calculated.

2.1.7.3 Difficulties

The space around the target is limited in the vertical direction because the moderator needs to be placed very close to the target. Therefore the height of the inlet and outlet pipes has to be minimized. For such big inlet areas, it is hard to construct efficient inlet and outlet pipes with very low height. *Figure 25* shows a design with rounded edges and a height of 15 cm for both the inlet and outlet pipes. There are three inlet zones and three porous domains separated by a thin wall. The outlet is common for all. This design has a round edge which causes problems (marked red): recirculation zones. This is due to the will of the fluid wanting to take the easiest path through the porous domain, and to the too fast increase of the hydraulic diameter.

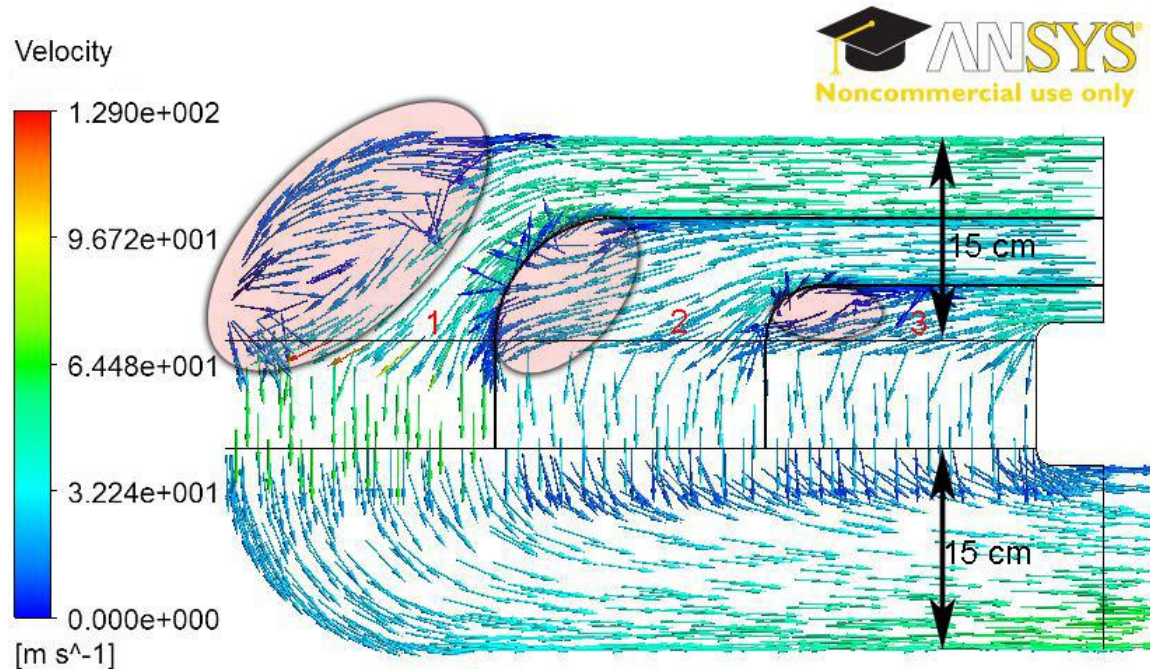


Figure 25. Contour plot of the velocity vectors on a plane in the middle of the geometry. The plot is coming from a ANSYS CFX CFD calculation. A design of the inlet and outlet pipes when the helium is entering at the top. There are three inlet pipes and three porous zones. The outlet pipe is common for all three. The height of both the inlet pipes and outlet pipes is 15 cm. The rounded edges in the front of the each pipe are problematic. Recirculation zones are created according to the red marked shapes in the figure.

Figure 26 has the same dimensions except that the shapes of the pipes have been changed. The flow has a very low velocity at the red marked parts and a very high velocity at the yellow marked parts. This also shows that the fluid is “lazy” and takes the easiest path. It is important to have the flow velocity more evenly distributed on the inlet surface of the porous domain. This is to have an adequate cooling of the whole zone and not only in the rear part.

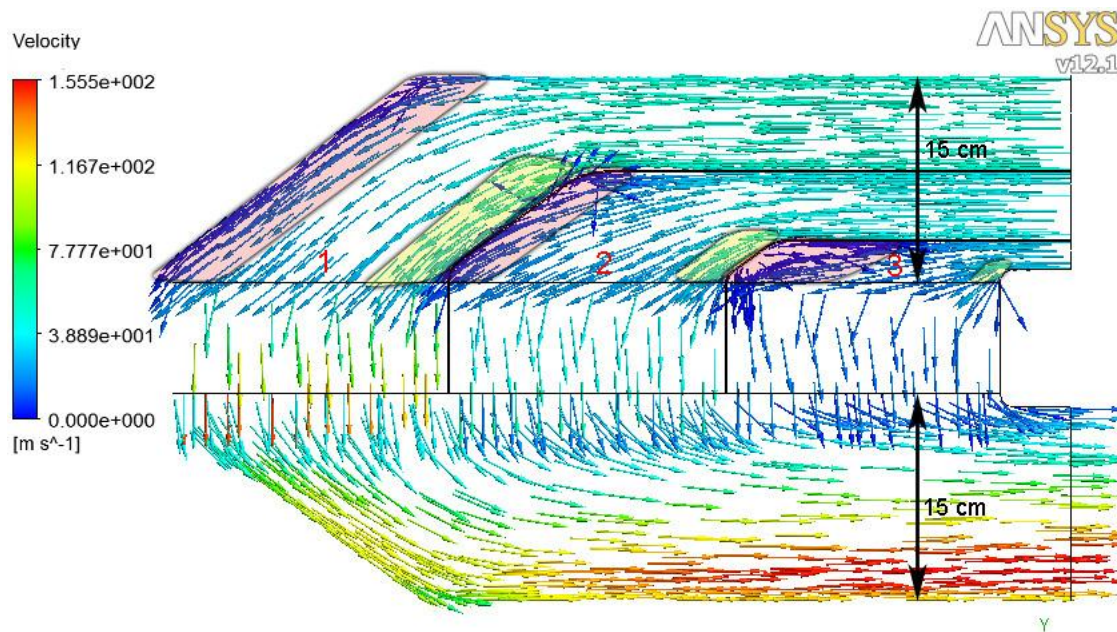


Figure 26. Contour plot of the velocity vectors on a plane in the middle of the geometry. The plot is coming from a ANSYS CFX CFD calculation. A design of the inlet and outlet pipes when the helium is entering at the top. There are three inlet pipes and three porous zones. The outlet pipe is common for all three. The height of both the inlet pipes and outlet pipes is 15 cm.

Figure 27 shows another design with smaller height on the inlet and outlet pipes, 8 cm each. This height is still too much, 5-6 cm is allowed at most. In the figure it is shown that most of the fluid enters the porous domain at the rear part of each zone, to the right of every red line. This is because of the big difference between the small inlet area and the big inlet area of the porous domain. The described problem occurs because of the quick change increasing hydraulic diameter.

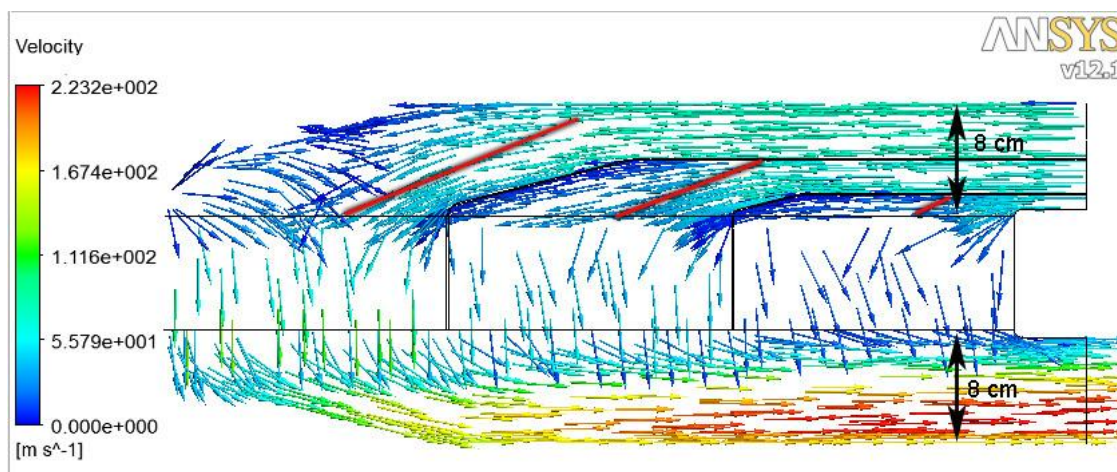


Figure 27. Contour plot of the velocity vectors on a plane in the middle of the geometry. The plot is coming from a ANSYS CFX CFD calculation. A design of the inlet and outlet pipes when the helium is entering at the top. There are three inlet pipes and three porous zones. The outlet pipe is common for all three. The height of both the inlet pipes and outlet pipes is 8 cm.

2.1.8 Conclusions

In the first case, when the flow enters from the side the analytic calculations show that the temperatures are too high. First the graphs showed that they were slightly too high, then more accurate calculations were done. These were presented as contour plots, according to these the solution is not acceptable.

According to the graphs and contour plots, the solution with the flow entering at the top is feasible. This case fulfills the requirements but has limited space in vertical direction for the inlet and outlet pipes which makes it less desirable. There will not be much cooling in the front part of each zone where the hottest parts are located according to *Figure 27*. The described problem occurs because of the quick change in increasing hydraulic diameter. This is the reason why it is complicated to construct pipes with minimizes height. A solution could be to have the pipes coming from the other side of the target, then the cooling would be directed to the front part of the zones. Another solution could be to guide the helium with vanes to get it evenly distributed.

The analytic calculations are made for one direction, that is, heat, velocity etc. are transmitted only in x-direction. The mass flow is conserved along a column. In reality, it would not be like this, then the helium would flow sidewise as well. The heating will cause expansion of the gas, this makes the helium flow sidewise. Therefore the analytic calculations should not be fully trusted. They should only be used as guidelines; this is only an approximation of the real case.

By varying the inlet pressure, temperature and velocity the results can be affected negatively and positively. Increasing the inlet pressure leads to lower temperatures in the spheres and helium, while the pumping power increases. By choosing spheres with small or big diameter the results are affected as well. A sphere with a small diameter leads to a higher pressure drop, higher helium outlet temperature and lower maximum sphere temperature. Studying the graphs easily gives understanding of how changes in different parameters affect the results.

2.2 Global analyses with ANSYS CFX

Analyses are done with ANSYS CFX. They are done on a global level, with a porous domain representing the spheres. The porous domain can be set with isotropic or directional loss. This is useful when comparing with the analytical calculations which are done along a column. Analyses with different input variables were performed to compare with the analytic calculations in a proper way. The results are not expected to be exactly the same but they should have the same tendencies.

2.2.1 Theory

The equations used by ANSYS CFX for calculating this type of problem are shown in the appendix: 5.1 ANSYS CFX Theory. They are taken from ANSYS CFX-Solver Theory Guide. The resistance coefficients are derived from the equations in the first phase of the thesis.

2.2.1.1 Resistance Coefficients

The porous domain needs to have information about its resistance. This is done by entering resistance coefficients, a linear and a quadratic. These have to be calculated so the pressure drop will be similar to the real case.

Equation (1)-(3) and (31) give the equations below by some rearrangement:

$$\Delta p = \frac{\rho_{in} \cdot w_1^2}{2} \left[\frac{360(1-\epsilon)^2}{\epsilon^3 \cdot Re_1} + \frac{B(1-\epsilon)}{\epsilon^3} \right] \cdot \frac{l_0}{d_{el}} \quad (43)$$

$$\frac{\Delta p}{l_0} = \frac{180(1-\epsilon)^2 \cdot \rho_{in} \cdot \nu}{\epsilon^3 \cdot d_{el}^2} \cdot w_1 + \frac{B(1-\epsilon) \cdot \rho_{in}}{2 \cdot \epsilon^3 \cdot d_{el}} \cdot w_1^2 \quad (44)$$

The isotropic loss can be written as:

$$\frac{\Delta p}{\Delta x} = C^{R1} \cdot U + C^{R2} \cdot |U|U \quad (45)$$

which gives the linear and quadratic resistance coefficients below:

$$C^{R1} = \frac{180(1-\epsilon)^2 \cdot \mu}{\epsilon^3 \cdot d_{el}^2} \quad (46)$$

$$C^{R2} = \frac{B(1-\epsilon) \cdot \rho_{in}}{2 \cdot \epsilon^3 \cdot d_{el}} \quad (47)$$

These equations provide understandable results when incompressible fluid is used. When the gas is ideal and while the heat is added, these equations no longer give understandable results. In this case, only the quadratic resistance coefficient is used by the following equation:

$$C^{R2} = \frac{\Delta p}{w_1^2} \quad (48)$$

Unfortunately it shows that neither this equation give understandable results. Further work has to be done on how to determine the resistance coefficients for when ideal gas is used and heat is added.

2.2.2 Methodology

When running CFD analyses with ANSYS Workbench tools, the simulation process can be divided into the following steps:



Figure 28. ANSYS Workbench simulation process.

2.2.2.1 Modeling

As a start a simple model is made with ANSYS DesignModeler. Such a simple model allows to run different analyses relatively fast. It contains only the front part of the target, which is made of an inlet, a porous and an outlet domain. The dimensions for the porous zone are the same as in the first case, *Figure 1*, of the analytic calculations, 22 x 8 x 20 cm, where 22cm is the length that the fluid has to flow through the porous domain. The inlet domain is 10 cm long and the outlet domain is 30 cm long. The model can be seen in *Figure 29* below. If the results of the analyses with the simple model are good, later all three zones will be added. A further step is to model the inlet and outlet pipes. These are bent 90° in the real case and it has to be modeled according to that.

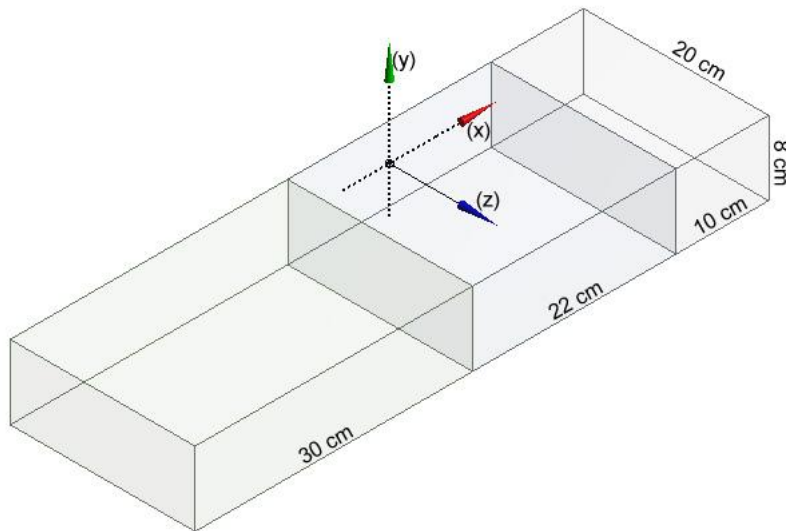


Figure 29. Model made with ANSYS DesignModeler. The porous domain has the dimensions 22 x 20 x 8 cm, according to the first analytical case. The inlet domain is 10 cm long and the outlet domain is 30 cm long.

2.2.2.2 Meshing

The meshing is done with ANSYS Meshing. A very simple mesh is made as a first step with relatively few elements, in order to have a model which is solved relatively fast. Body sizing and mapped face meshing are added to the model. Body sizing lets one set the element size within the whole model, in this case 5 mm elements are chosen. Mapped face meshing ensures that the elements are aligned properly and evenly on all surfaces. If the results are heading towards the right direction, the mesh will be improved. Smaller elements will be used as well as inflation at the inlet- and outlet- domains surrounding walls. The simple mesh can be seen in *Figure 30* below.

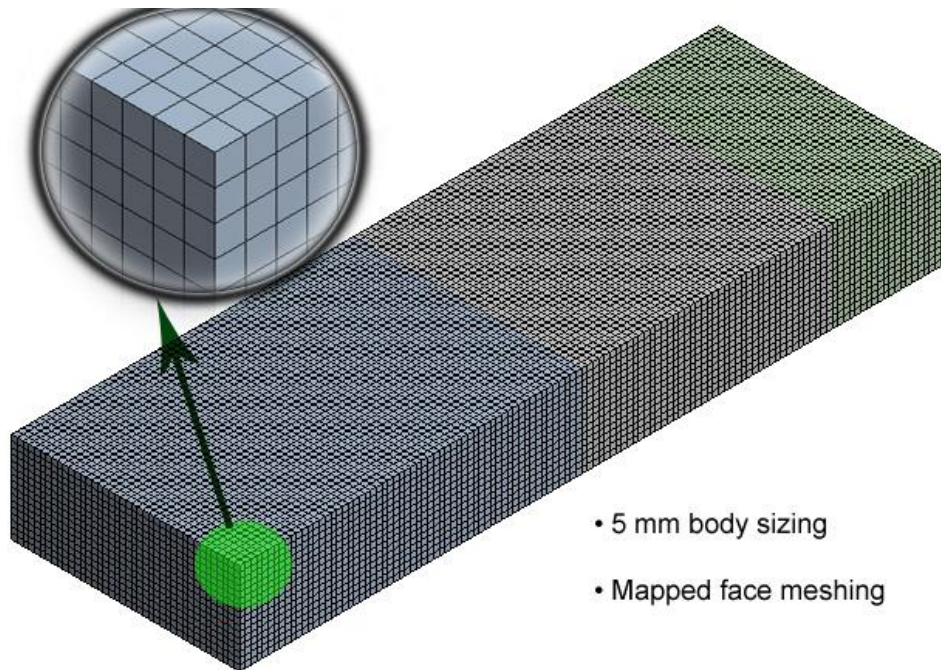


Figure 30. Mesh made with ANSYS Meshing. A uniform 5 mm mesh is made over the whole model. Such a simple mesh is made because it allows fast simulations.

2.2.2.3 Pre-Processing

In the pre-processor the problem is set up according to the constraints and requirements. The boundary conditions are chosen to be similar to the ones in the analytic calculations. The inlet pressure is known and the mass flow rate also. Therefore the inlet BC is set to total pressure, which means that the pressure at the inlet can be specified. In order to obtain this pressure the reference pressure of the system must be set to 0 atm. The outlet BC is set to mass flow rate which is known. The amount of mass that enters at the inlet must be the same as the amount that flows out from the outlet. Therefore the same value is used at the outlet. The energy deposition is interpolated into the volume of the porous domain. The energy deposition is implemented by the interpolation of the data given by the FLUKA [4] file. To specify the resistance within the porous domain, resistance coefficients are defined. The resistance coefficients are easily calculated as long as helium is considered incompressible. But while considering helium as an ideal gas another equation is used, equation (48), see the theory part. The volume porosity of the porous domain is 0.2595, the same as in the analytical calculations. The turbulence model, shear stress transport is used. As heat transfer method, total energy is used, this is described in the theory part. The outer walls of the three domains are set to be free slip walls. An illustration of the domains and some boundary conditions can be seen in *Figure 31* below.

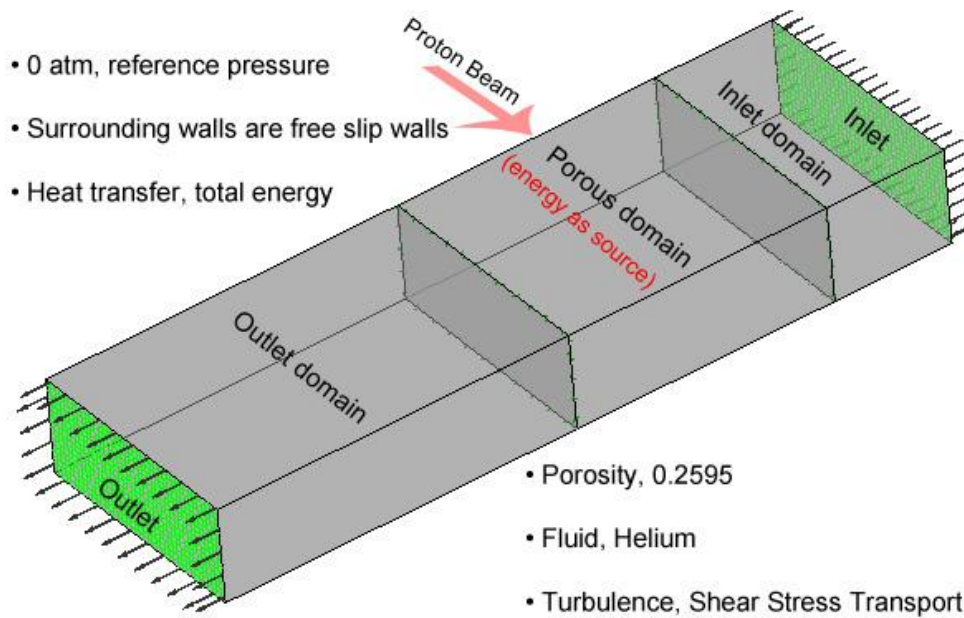


Figure 31. Pre-Processing with ANSYS CFX-Pre. The model consists of the domains, an inlet, a porous and an outlet. Boundary surfaces are green in the figure. Different preferences can also be seen as text in the figure.

2.2.2.4 Simulation

The convergence criterion for the simulations is set at $1e-04$ for the RMS residuals. This should be accurate enough and it will allow fast convergence. While the solver is running the momentum, mass, heat transfer and turbulence residuals are monitored. Besides these a couple of other monitors are added. One for the pressure drop over the porous domain, one for the maximum temperature of the outlet of the porous domain, one for the energy and one for the average helium outlet temperature from the porous domain. It is important that also these parameters converge. The imbalances of the three domains are also monitored.

2.2.2.5 Post-Processing

The post-processing tool, CFX-Post is used to view the results of the simulation. Planes can be created in any place within the geometry. On these planes all used variables can be plotted either by contour plots, vector plots, streamlines, etc. Streamlines and vector plots can also be plotted in the volume. This is very useful to investigate the results, to find any errors.

To illustrate the results of these simulations three planes are created according to Figure 32:

- A plane at the inlet of the porous domain.
- A plane at the outlet of the porous domain.
- A plane in the middle of all three domains.

On these planes several variables will be plotted with contour plots. This should be enough to illustrate the results in a sufficient way.

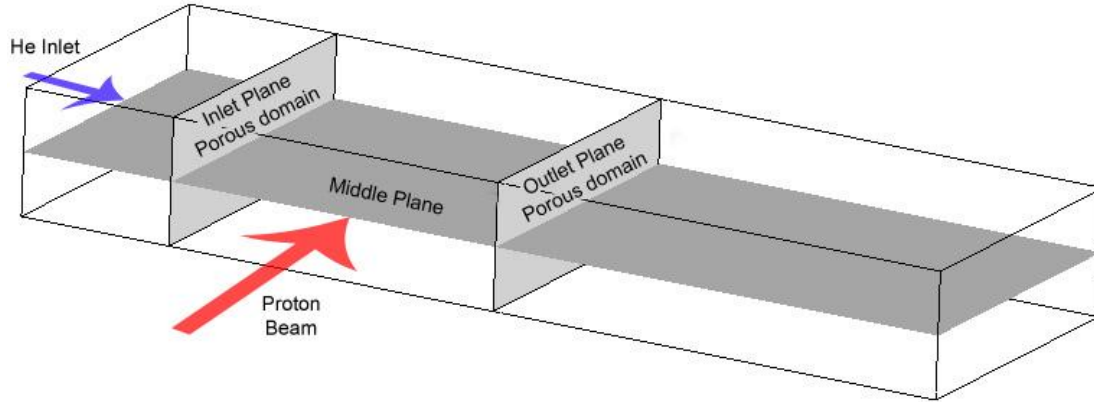


Figure 32. Planes used for plots in ANSYS CFX-Post. Plots are made on the described surfaces in the figure.

2.2.3 Results

To start and debug the model a simple analysis is done without the energy source and using helium as an incompressible gas. Secondly, an analysis is performed also with incompressible gas but with the energy source added. During these simulations the linear and quadratic resistance coefficients are used, according to equations (46) and (47). The boundary conditions of the inlet and outlet are according to the analytic calculations. It shows that results of the second analysis are very similar to the one in the analytic calculation, this can be seen in *Table 13*. It was not expected to obtain similar results as incompressible gas in CFX and ideal gas in the analytical calculations. The reason for the similarity is due to the mass flow conservation within and along a column in the analytic calculations.

Next, helium as ideal gas is used in CFX. The results of this are very different from the ones in the analytical calculations, see *Table 13* to compare. Also the previous resistance coefficients do not work with heat added and ideal gas. Therefore another resistance coefficient is used according to equation (48).

Because of these concerns, like the large differences in pressure drop and temperature, several analyses were carried with different total pressures. The objective was to get an understanding on how the resistance coefficients and different inlet pressures affect the results. The results of these analyses are shown in *Table 13* and *Table 14*. It is a comparison between all analysis. *Table 12* shows the values of some variables used in the different analyses.

Three figures below show the results of one of the analyses. It is the one that has an inlet pressure of 20 bar and an inlet velocity of 15 m/s. Ideal gas is used in this analysis and heat is added. The porous domain is set to have isotropic loss in this case. *Figure 33* show contour plots of the absolute pressure of the three planes described previously. *Figure 34* shows the temperature and *Figure 35* shows the velocity of the outlet domain.

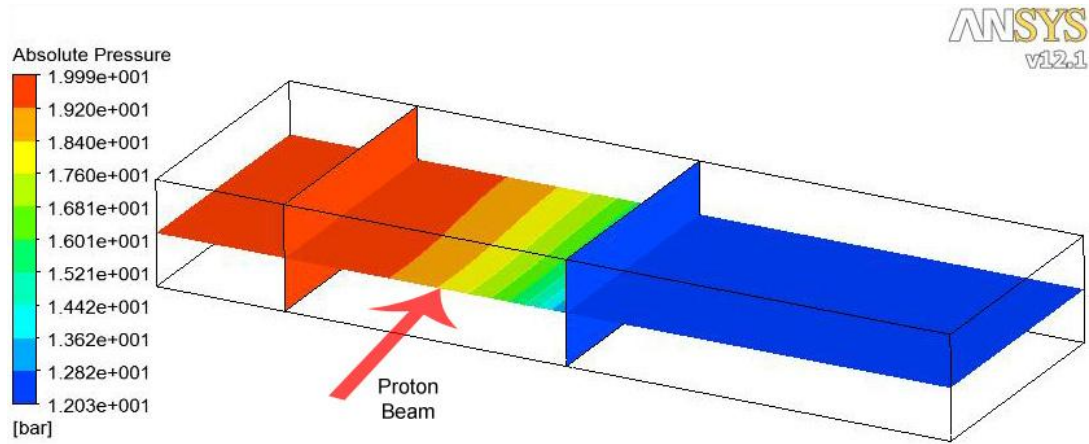


Figure 33. Contour plot, Absolute Pressure

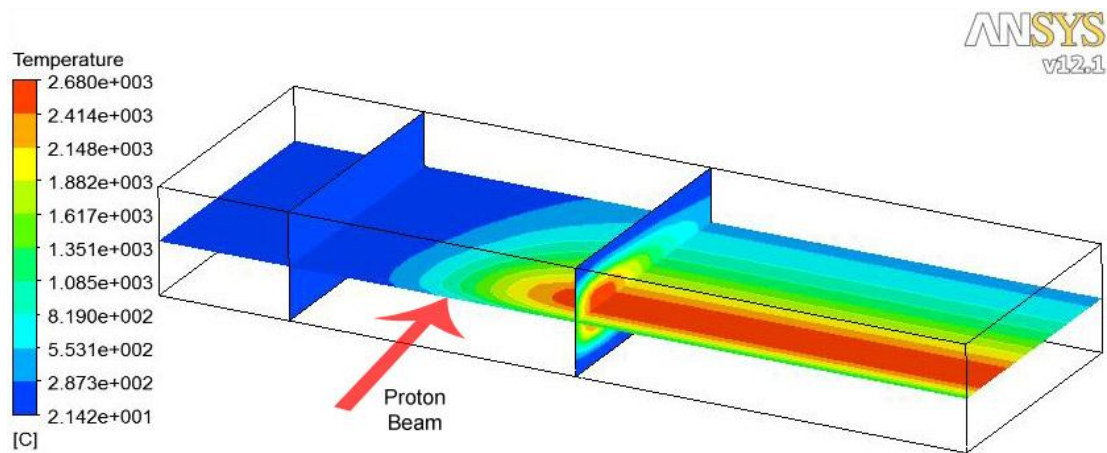


Figure 34. Contour plot, Temperature

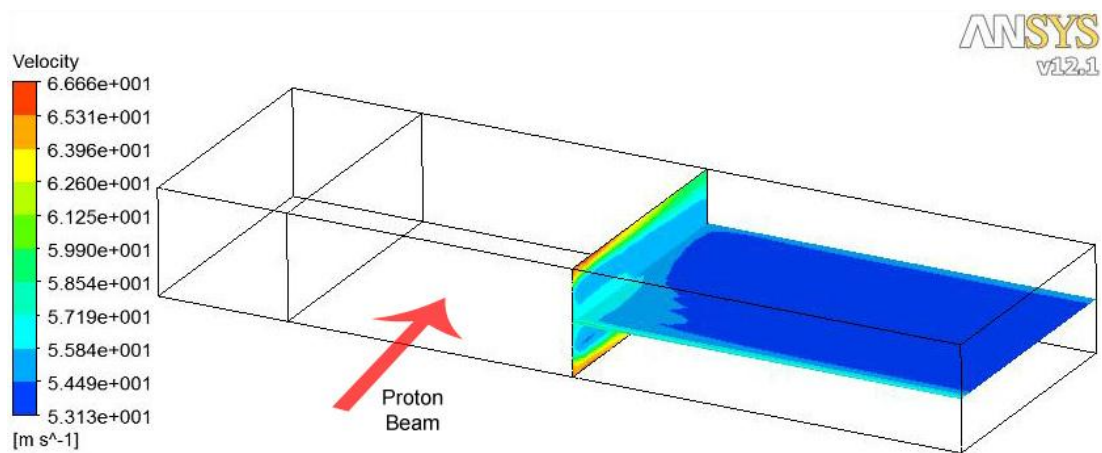


Figure 35. Contour plot, Velocity

2.2.3.1 Comparison for Zone 1

As seen in the comparison in the tables below, the temperature is a lot higher than in the analytic calculation. This is due to the mass flow escaping sideways. The gas expands due to the heat and it expands sideways. This phenomenon has not been taken into account in the analytic calculations. The tables show that the pressure drop is consistent for the CFX cases with ideal gas at different inlet pressures. The resistance coefficients have to be further developed, they should depend on the temperature and mass flow. The tables shows the maximum temperature of the helium, the pressure drop, the outlet velocity from the porous domain and the outlet velocity, all this with different maximum pressures and different porous domain options.

Properties for the different cases					
	ρ [$kg \cdot m^{-3}$]	C^{R1} [$kg \cdot m^{-3} \cdot s^{-1}$]	C^{R2} [$kg \cdot m^{-4}$]		C_p [$J \cdot kg^{-1} \cdot K^{-1}$]
			<u>Incomp</u>	<u>Ideal gas</u>	
10 bar	1.6311	1050.3 For all incompressible cases	6219.2	1569.78	5193.2 For all cases
20 bar	3.2623		12438	3097.78	
40 bar	6.5245		24877	6144.89	
60 bar	9.7868		37315	9188	

Table 12. Properties for the different analyses

	Analytic – Ideal Gas				CFX – Incompressible Gas				CFX – Ideal Gas			
	$T_{max,He}$ [°C]	ΔP [bar]	$V_{out,p}$ [m/s]	V_{out} [m/s]	$T_{max,He}$ [°C]	ΔP [bar]	$V_{out,p}$ [m/s]	V_{out} [m/s]	$T_{max,He}$ [°C]	ΔP [bar]	$V_{out,p}$ [m/s]	V_{out} [m/s]
10 bar	2194.5	3.53	195.57	N/A	2177.2	3.11	57.80	15	N/A	N/A	N/A	N/A
20 bar	1108.2	6.97	108.48	N/A	1099.7	6.20	57.85	15	2682.7	7.44	251.15	61.61
40 bar	565.1	13.83	65.42	N/A	560.9	12.35	57.81	15	907.6	7.07	135.11	40.75
60 bar	384.1	20.67	51.15	N/A	381.3	18.51	57.80	15	528.8	8.30	109.09	31.96

Table 13. Comparison of results, Table 1

	CFX – Ideal Gas, Directional Loss				CFX – As one domain			
	$T_{max,He}$ [°C]	ΔP [bar]	$V_{out,p}$ [m/s]	V_{out} [m/s]	$T_{max,He}$ [°C]	ΔP [bar]	$V_{out,p}$ [m/s]	V_{out} [m/s]
10 bar	N/A	N/A	N/A	N/A	N/A	N/A	N/A	N/A
20 bar	6517.2	7.53	253.70	58.08	5599.11	7.177	63.45	53.08
40 bar	1078.0	7.09	134.15	49.32	1039.39	6.923	34.19	30.26
60 bar	573.9	8.33	109.47	37.27	565.44	8.251	27.96	25.26

Table 14. Comparison of results, Table 2

2.2.3.2 Investigating the cause of different results

For a porous domain with isotropic loss model the mass flow should vary through the domain and side wise as well. For a directional loss model, the mass flow should be uniform through the domain and not vary side wise. A simple test is done with the two loss models to investigate the mass flow patterns within the porous domain. The mass flow is plotted on five planes evenly distributed in the porous domains.

Figure 36, Figure 37 and Figure 38 shows the mass flow plots on these planes for the 20, 40 and 60 bar cases with the isotropic loss model. The mass flow is behaving as expected, the gas expands at the hot part and flows sideways. Gas from the central hot parts expands which contributes to larger mass flow rate surrounding this hot part according to the figures. It can also be seen that the higher inlet pressure the less change in mass flow along the porous domain, it is more uniform at higher pressures. Because, the higher the pressure, the lower the compressibility of the gas.

Figure 39, Figure 40 and Figure 41 show the mass flow plots for the directional loss model. The behaviour of this is not as expected, it is instead very similar to the previous isotropic case. With the directional loss model it should be like in the analytical calculations, the flow should be uniform through the porous domain. Even with a large transverse resistance coefficient, the fluid is pushed sideways because of the large heat deposited. This could be a reason for the large temperature and pressure drop differences between the ANSYS CDX directional loss model results and the analytical calculations.

Isotropic loss model

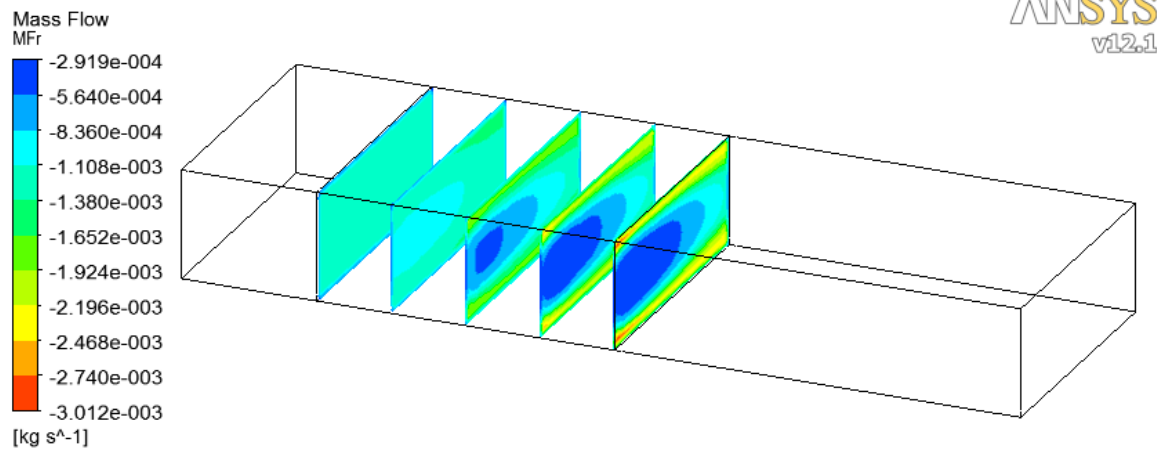


Figure 36. Mass flow contour plot of the 20 bar case. In this case the porous domain has an isotropic loss model.

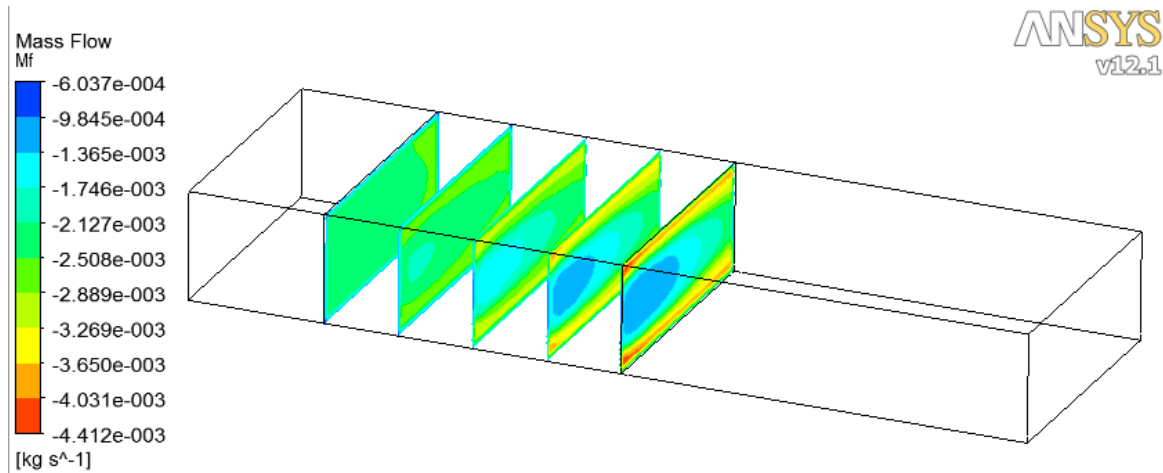


Figure 37. Mass flow contour plot of the 40 bar case. In this case the porous domain has an isotropic loss model.

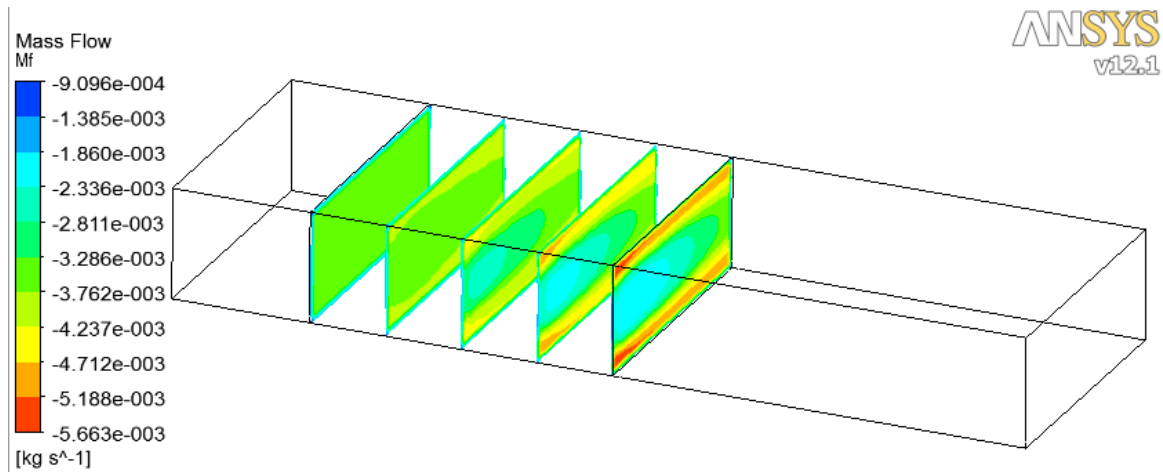


Figure 38. Mass flow contour plot of the 60 bar case. In this case the porous domain has an isotropic loss model.

Directional loss model

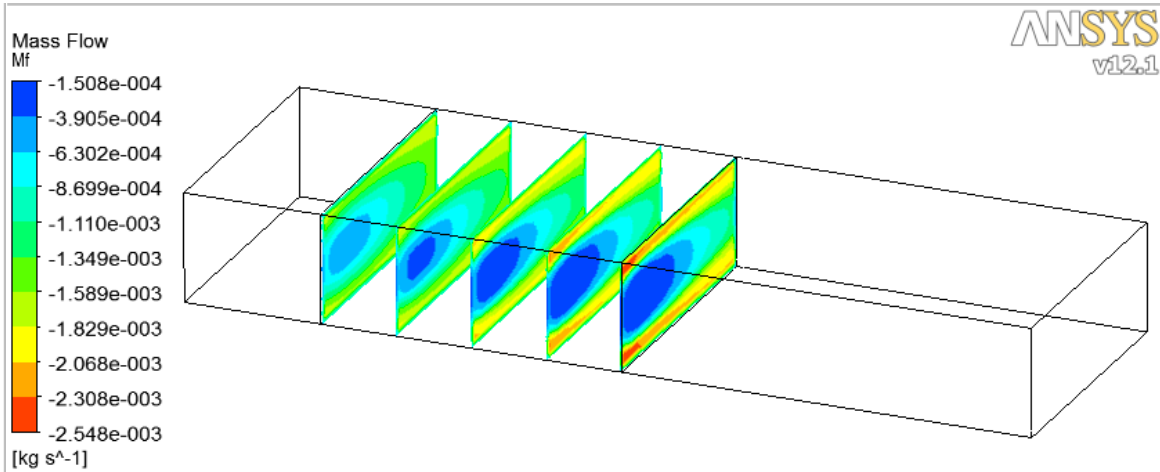


Figure 39. Mass flow contour plot of the 20 bar case. In this case the porous domain has directional loss.

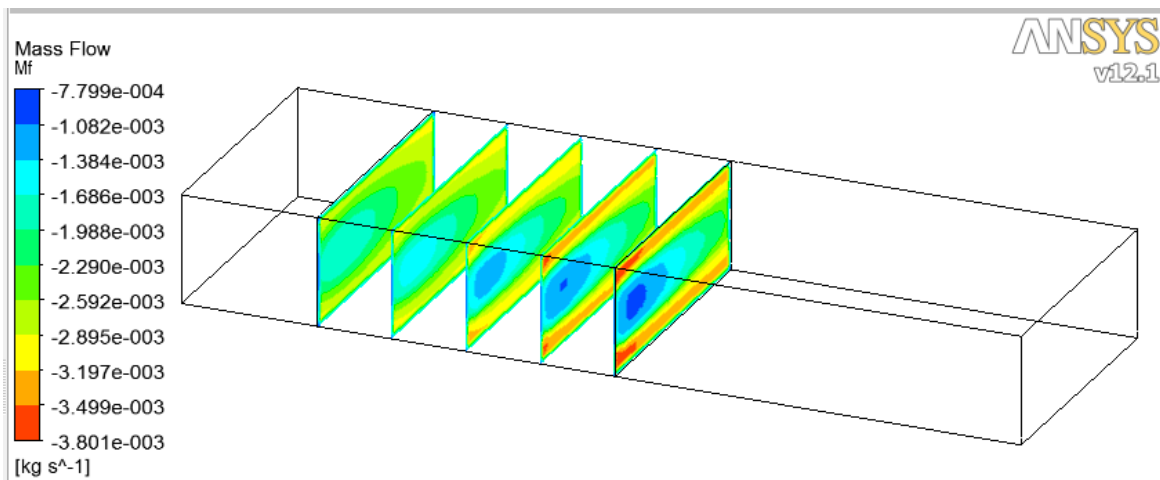


Figure 40. Mass flow contour plot of the 40 bar case. In this case the porous domain has directional loss.

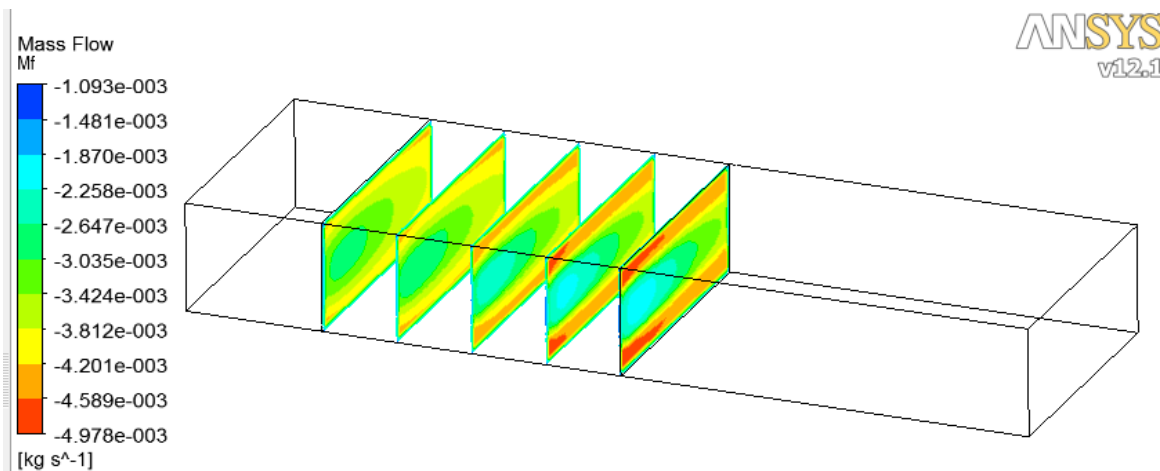


Figure 41. Mass flow contour plot of the 60 bar case. In this case the porous domain has directional loss.

To simulate a porous domain when the directional loss has an infinite transverse coefficient and to confirm that the mass flow escaping causes the large differences in the results, 9 columns were modelled at the hottest part of the target according to *Figure 42*. The centre of the columns is 4 cm in z-direction. There are imaginary walls between each column, this way the flow will be forced to be directional. There is still heat transfer between the columns. Only 2 x 2 elements are used in a column cross section. The test is done with two different column sizes to see how it affects the results, column cross sections of 0.5 x 0.5 cm and 1 x 1 cm.

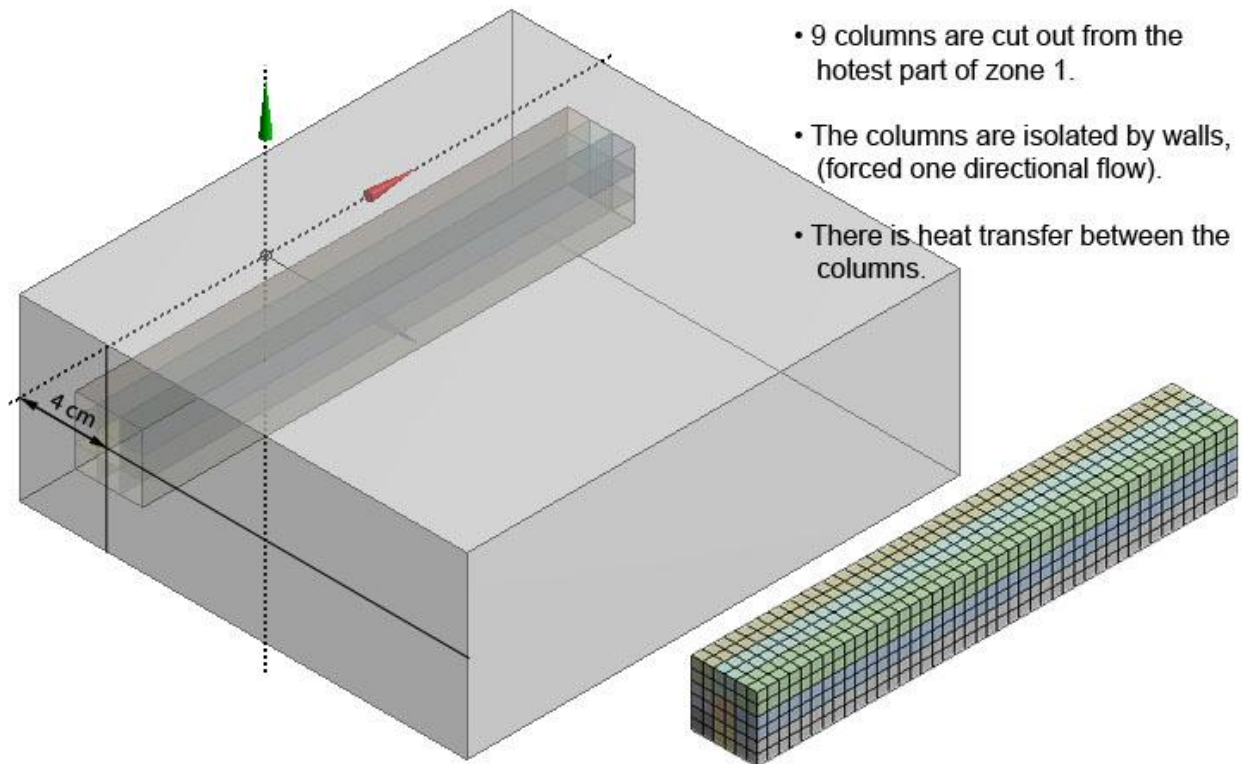


Figure 42. 9 columns of the hottest part of the target are cut out. This is located 4 cm into the target along the z-axis. The columns are isolated from each other by "imaginary" walls. This is equivalent to the analytic calculation where there is no transverse loss. There is heat transfer between the columns. 2 x 2 elements per column cross section.

Figure 43 shows the temperature along the column on a vertical and horizontal mid-plane for the 0.5 mm case. The temperature is similar to the analytic calculations. *Figure 44* shows the mass flow on 5 planes along the columns of the 0.5 cm case. It is constant through the whole column just like in the analytical calculations. The directional loss model should behave close to this. *Figure 45* and *Figure 46* show the same results as explained but for the 1 x 1 cm columns.

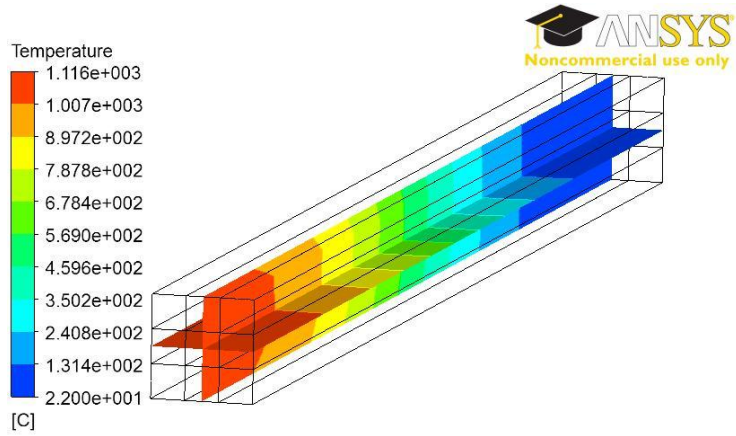


Figure 43. Temperature plot of 0.5 cm columns.

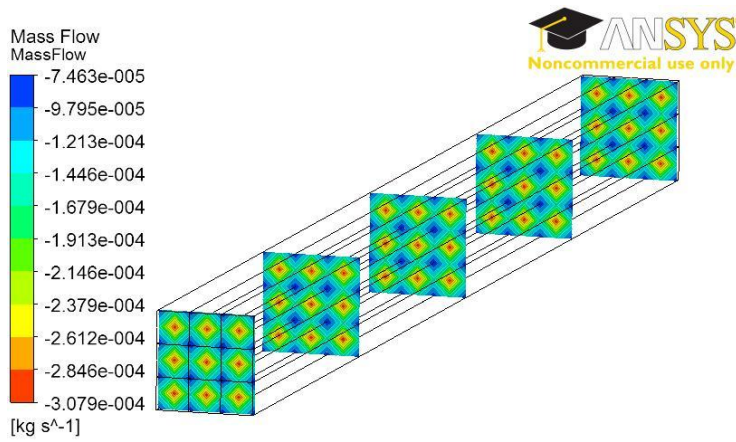


Figure 44. Mass flow plot of 0.5 cm columns. The mass flow is constant through the porous domain.

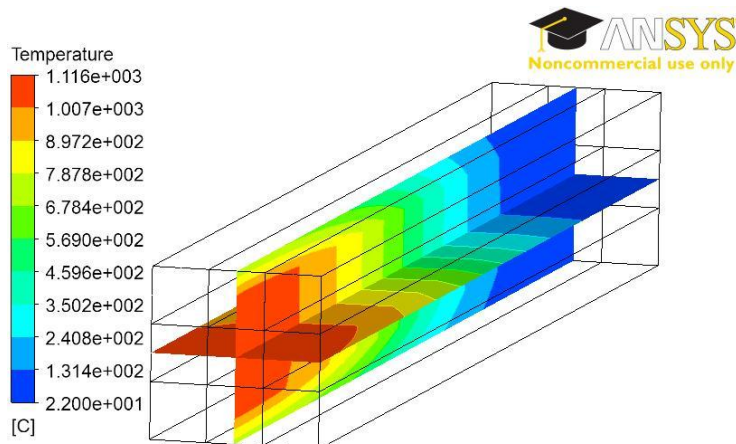


Figure 45. Temperature plot of 1 cm columns.

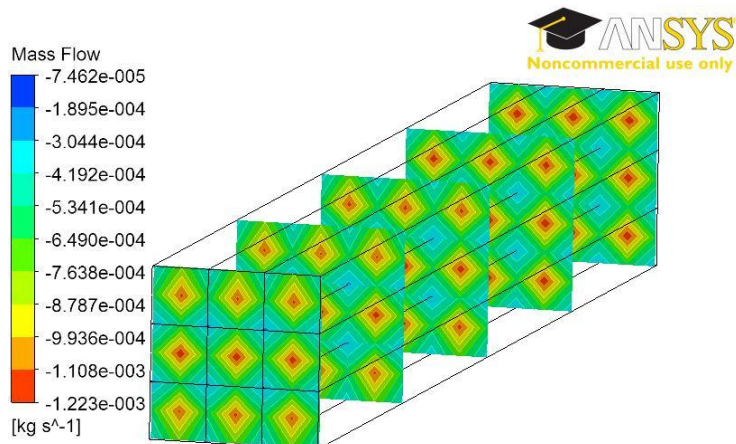


Figure 46. Mass flow contour plots of 1 cm column. The mass flow is constant through the porous domain.

2.2.4 Conclusions

Because of the large difference in temperature and pressure drop between the analytic calculations and the ANSYS CFX analyses, no other analyses with different geometries were performed. Effort was instead put on trying to find out the reason for the differences. With help of a comparison between analyses with different inlet pressures and porous settings it was concluded that the differences were caused by the mass flow loss in the target center, due to the thermal expansion of the gas. In the analytic calculations the flow is one directional, i.e. the mass flow is conserved along a column. While in ANSYS CFX the helium can flow sideways, the lack of taking this phenomenon in account in the analytical calculations causes the large differences in the results.

To demonstrate that the sidewise mass flow escaping causes the differences, a test was performed. 9 columns with imaginary walls between them were modeled. The flow is forced to be one directional in these columns. The result of this analysis was very similar to the analytic calculations. It is now obvious that the large differences of the results are caused by the different ways to handle the mass flow between ANSYS CFX and the analytic calculations.

The resistance coefficients are not correctly calculated for the compressible cases, it is important in a later step to develop new equations that take both temperature and mass flow direction in account.

3. Helium cooled rotating granular target

The target consists of tungsten cylinders packed as densely as possible, 90 %. They are packed on a circular plate with the outer diameter 150 cm and the inner diameter 50 cm according to *Figure 47*. The cylinders are 8 cm high and have a diameter of 2 cm according to *Figure 47*. The plate rotates around its axis at 30rpm. The helium enters at the bottom, of the target and exits at the top. The cooling occurs all over the target, not only at the front part where the beam hits it. The power density is considerably reduced due to the rotation and therefore the lower amount of energy received by one part of the target. This concept allows implementing a lower inlet pressure because of a very low pressure drop along the bed of rods compared to the bed of spheres. This concept has a longer target lifetime. There are many advantages with this concept compared to the stationary target with spheres.

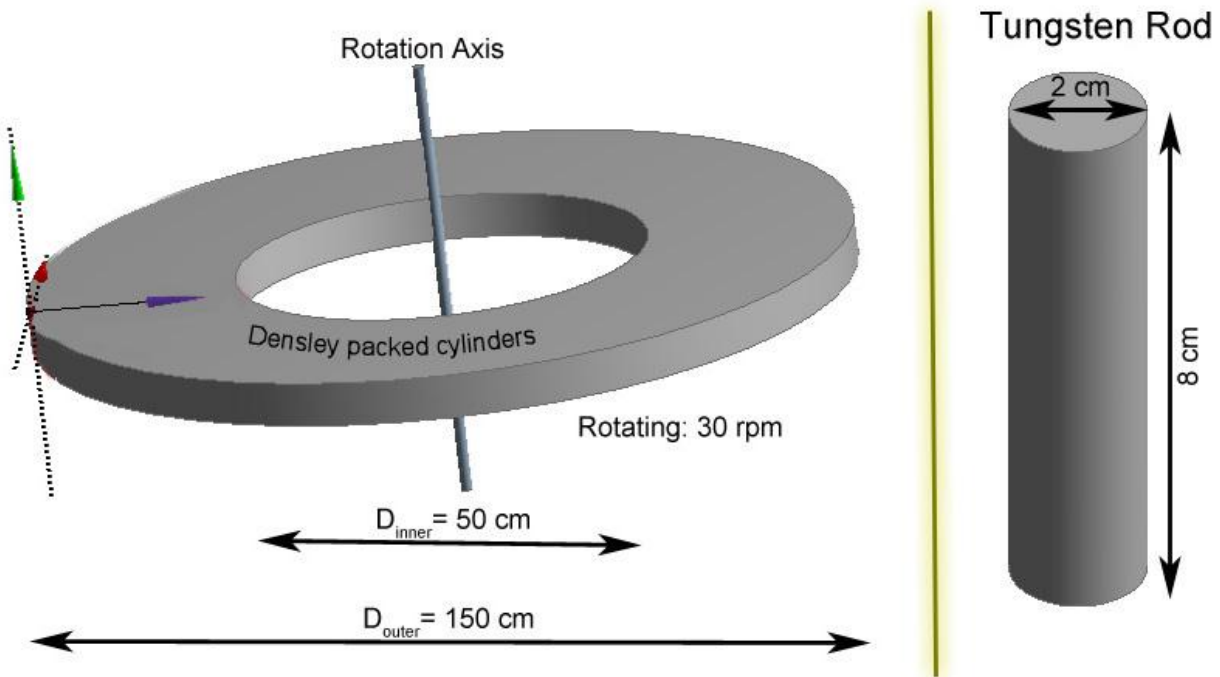


Figure 47. Problem description. A rotating target with 8 cm high cylinders with 2 cm diameter is densely packed in a circle with the outer diameter 150 cm and inner diameter 50 cm. The target rotates of 30 rpm. The beam hits the target along the z-axis (blue).

3.1 Methodology

The methodology for the simulations is the same as in the previous case and is divided into the following steps.



Figure 48. ANSYS Workbench simulation process.

3.2 Resistance coefficients

In this case the resistance coefficients are calculated with help of ANSYS CFX. This is done to be able to run analyses relatively fast on a larger part of the target with a porous domain.

The resistance coefficients are calculated with help of equation (49) taken from the theory in the appendix. The linear and quadratic resistance coefficients are defined as equation (49) below:

$$\frac{\Delta p}{\Delta y} = C_{lin} \cdot V + C_{quad} \cdot V^2 \quad (49)$$

The linear and quadratic resistance coefficients are not depending on the velocity. Therefore analyses are done with two different velocities that give two different pressure drops according to equation (50) and (51). The length Δy is set to be the same in both equations.

$$\frac{\Delta p_1}{\Delta y} = C_{lin} \cdot V_1 + C_{quad} \cdot V_1^2 \quad (50)$$

$$\frac{\Delta p_2}{\Delta y} = C_{lin} \cdot V_2 + C_{quad} \cdot V_2^2 \quad (51)$$

There are now two equations with two unknown variables, which can easily be solved. The quadratic and linear resistance coefficients are derived as equation (52) and (53) below.

$$C_{lin} = \frac{\Delta p_2 \cdot V_1^2 - \Delta p_1 \cdot V_2^2}{\Delta Y \cdot (V_1^2 \cdot V_2 - V_1 \cdot V_2^2)} \quad (52)$$

$$C_{quad} = \frac{\Delta p_1 - C_{lin} \cdot V_1 \cdot \Delta Y}{\Delta Y \cdot V_1^2} \quad (53)$$

3.3 Analysis of 1 “tube”

Because of the difficulties to model the porous domain in the previous case with the spheres, the resistance coefficient will be calculated with help of local CFD analyses. A single tube is studied at the hottest part of the target. This model will allow calculating the resistance coefficients.

3.3.1 Modeling

A triangle built from the center of three cylinders is cut out from the target according to *Figure 49*. It contains of a short inlet domain, a third of three cylinders with helium in-between them and a longer outlet domain, to prevent backflow. The center of the model is placed 4 cm into the target along the z-axis, this is the hottest and most stressed part.

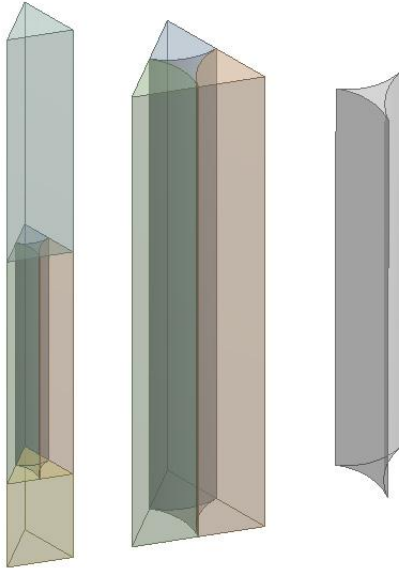


Figure 49. Model of the part cut out.

3.3.2 Meshing

The goal is to be able to study the flow pattern carefully and to collect accurate data. Therefore the helium in-between the cylinders has a very fine mesh compared to the rest of the model. The cylinders have a coarse mesh while the inlet and outlet have a medium fine mesh. Figure 50 shows three parts of the meshed model. First the whole model from a distance, here it can already be seen that the cylinders have a coarse mesh. Next, a zoomed part with two cylinders and the helium outlet domain. Finally the outlet domain is hidden so the cylinders and the helium in between can be seen from top.

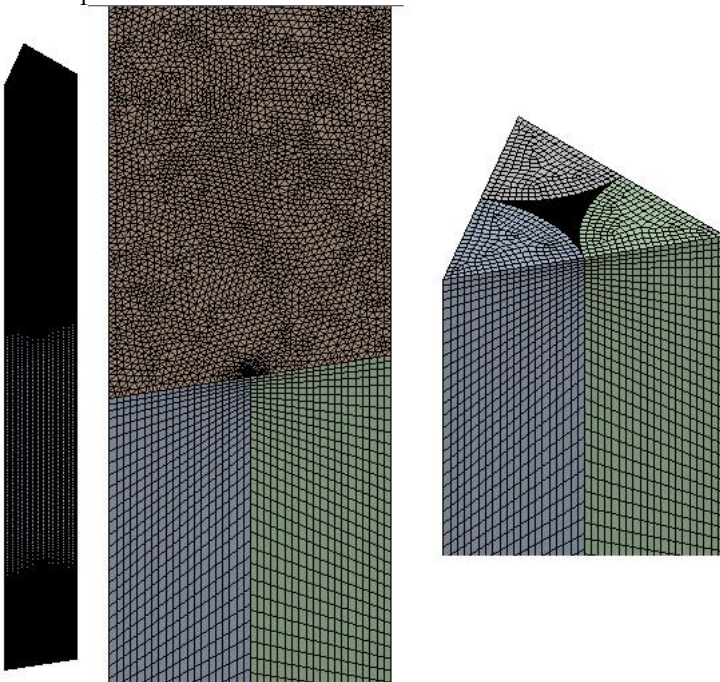


Figure 50. Mesh of the tube model. Coarse mesh on the cylinders, Medium mesh on the inlet and outlet domains, fine mesh on the helium in the middle.

To lower the number of elements, edge sizing is used on the helium and cylinders along the y-axis. It is set to 80, i.e. because the cylinders are 8 cm long, the elements are approximately 1mm long along the y-axis. This is the flow direction, and it is allowed to have longer elements. *Figure 51* shows two zoomed and cutted parts of the meshed model, one with the helium outlet domain visible and one where it is hidden. It can be seen that the elements in the helium between the cylinders are long compared to their upper area. There are significantly more elements in the helium between the cylinders than in the cylinders themselves.

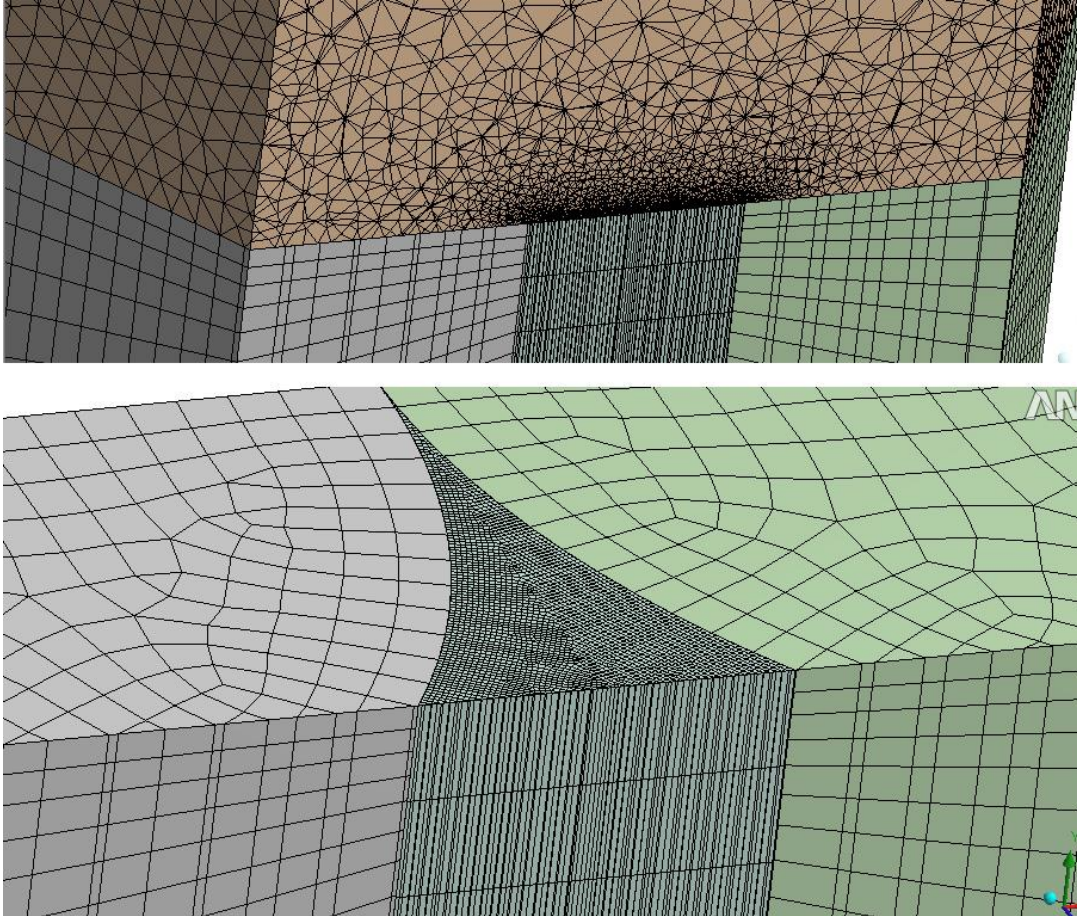


Figure 51. Mesh Zoom & cut. The helium in the middle has 1 mm long elements.

3.3.3 Pre processing

The target is rotating at 30 rpm and the proton beam is pulsed at 20Hz, a certain part of the target is only irradiated once every two seconds. I.e. the certain part is almost cooled for 2 seconds before next proton pulse. Because of this the local mass flow can be lowered, which means that the inlet pressure is lowered from 20 to 10 bar. The power density is divided by 40 compared to the static target. Two inlet velocities are considered, which means that two different analyses are performed: one with an inlet velocity set at 8 m/s and one with an inlet velocity set at 10 m/s. This is done to be able to derive the resistance coefficients according to equation (52) and (53). Both analyses have an inlet temperature of 200 °C. As outlet boundary condition, mass flow rate is used. The mass flow rate can easily be calculated, $\dot{m} = \rho(p, T) \cdot A_{In} \cdot V_{In}$. The reference pressure is set to 0 bar. The outer walls of the model are set to free slip walls. The turbulence model used is the shear stress transport model and the heat transfer option is total energy. The analysis boundary conditions are illustrated in *Figure 52* below.

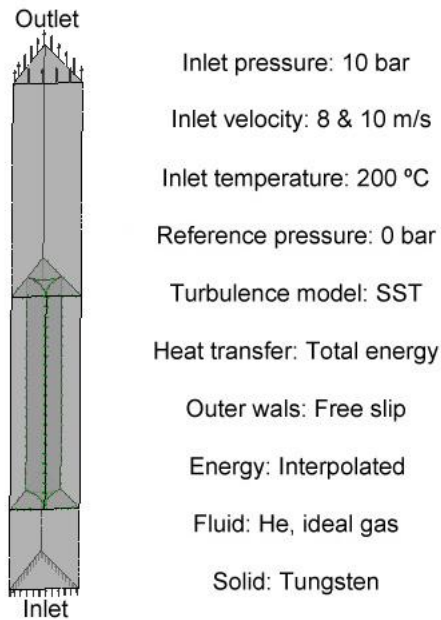


Figure 52. Boundary conditions for “1 tube”

3.3.4 Simulation

During the simulation, the RMS-residuals are monitored as well as the imbalances and two user defined monitor points. The RMS convergence criterion is set to $1e-5$. The user defined monitors are for the pressure drop and the average helium outlet temperature. The analysis runs until all of these converge. At the beginning of the simulation a physical time is used and is set to 0.1 s. This prevents divergence in the beginning of the analysis. When it has stabilized, the physical time step is increased to 1 second. This is to ensure that the flow is fully developed through the model.

3.3.5 Post-Processing

The results will be presented as contour plots on a plane in the middle of the model according to *Figure 53*. Results are also presented with equally spaces stream lines with a tubular shape starting from the inlet. Finally the data needed to calculate the resistance coefficients are saved along a line in the center of the tube, according to *Figure 54*. Data is collected at 32 points along the line, the coordinates and the pressure is saved as a table.

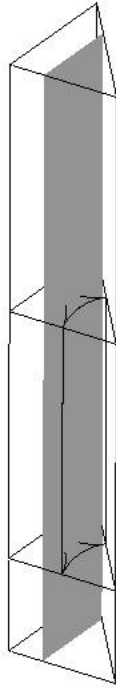


Figure 53. The contour plot plane.

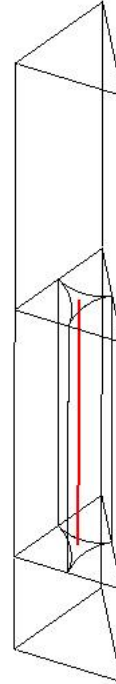


Figure 54. Line where data is collected for the resistance coefficients.

3.3.6 Results

This analysis is mainly done to study the pressure drop through the densely packed cylinders, although the velocity and temperature is presented in the results as well. *Table 15* below shows some of the results. It is a comparison between the two cases, one with the inlet velocity at 8 m/s and the other at 10 m/s. The temperatures should not be taken very seriously because it is such a small part of the model and only small parts of the cylinders are included.

	8 m/s	10 m/s
Average helium outlet temp [°C]:	250.774	240.594
Pressure drop (inlet-outlet) [bar]:	0.087	0.132
Outlet velocity [m/s]:	9.015	11.12
Max cylinder temp[°C]:	426.615	396.345

Table 15. Results of the "1 tube "

Figure 55 shows a comparison of the pressure contour plots between the two cases at the middle plane of the model. The pressure drop is higher for the faster inlet velocity. The pressure decreases significantly on a short distance right when the helium enters the densely packed cylinders. After this the pressure decreases linearly over the rest of the model. *Figure 56* shows a comparison of the helium velocity between the two cases. The maximum velocity is about 30 m/s higher for the 10 m/s inlet case.

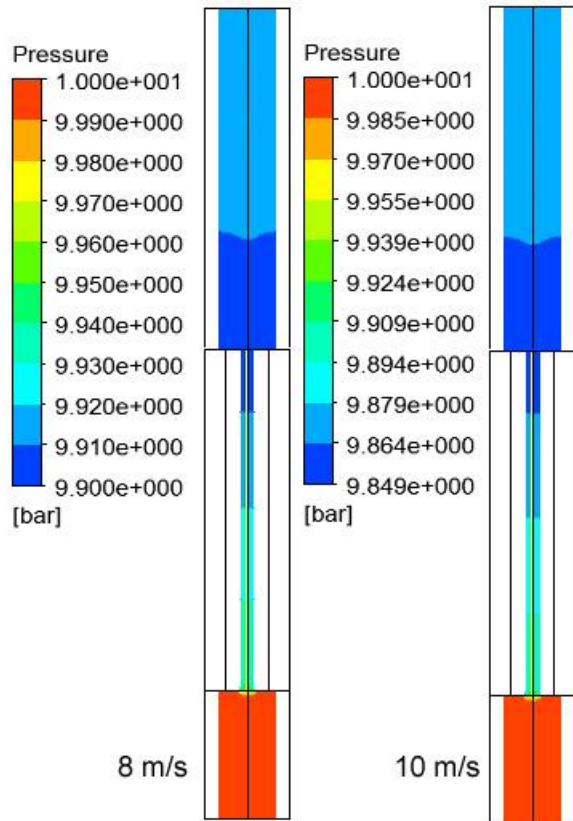


Figure 55. Contour plot of the pressure on a middle plane. A comparison between the 8m/s case and the 10m/s case.

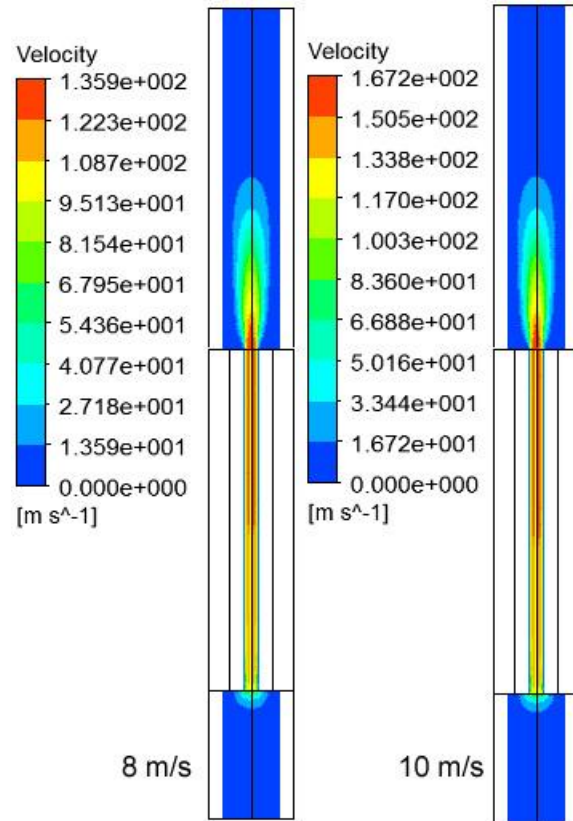


Figure 56. Contour plot of the velocity on a middle plane. A comparison between the 8m/s case and the 10m/s case.

Figure 57 shows a comparison between the helium temperatures between the two cases. The temperatures may not be accurate because of such a small model. They can be used as guidelines on how the temperature varies while increasing the inlet velocity. The 10 m/s case has a maximum temperature 30 °C cooler than the 8 m/s case.

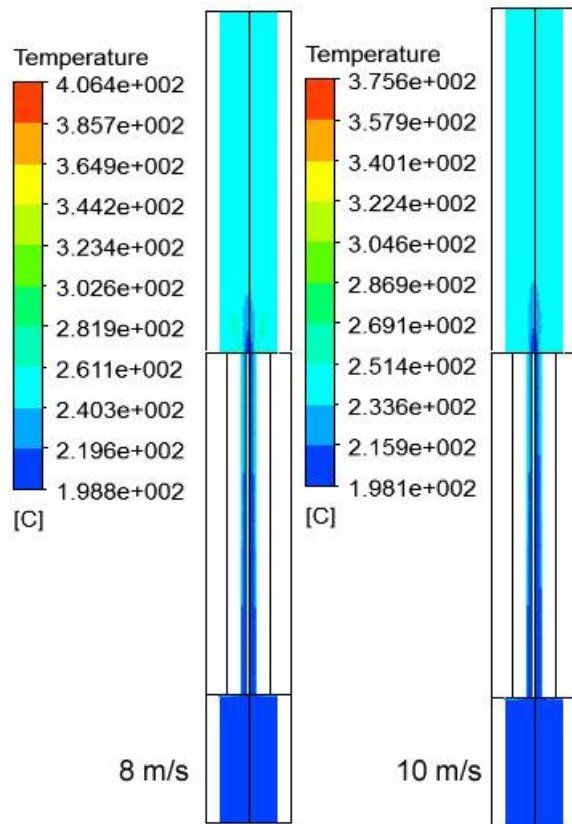


Figure 57. Contour plot of the temperature on a middle plane. A comparison between the 8m/s case and the 10m/s case.

3.3.7 Resistance coefficients

The linear and quadratic resistance coefficients have to be calculated to be able to perform the analyses on a larger scale with a porous domain acting like the cylinders. Two analyses are performed on the same model with two different inlet velocities. As mentioned earlier, data is collected at 32 equally distributed points along a line in the middle of the tube. The y coordinates and the pressure drop from both analyses are saved. The tables are then imported to ANSYS CFX as user functions, one for the linear and one for the quadratic resistance coefficient. These functions vary along the y-axis. This is interpolated into the porous volume and the pressure drop should now behave as in this analysis. Figure 58 below shows a graph over how the linear resistance coefficient behaves along the flow direction in the helium between the cylinders. In the graphs the x-axis is the target height (-4 to 4 cm), and the y-axis is the linear or the quadratic resistance coefficient.

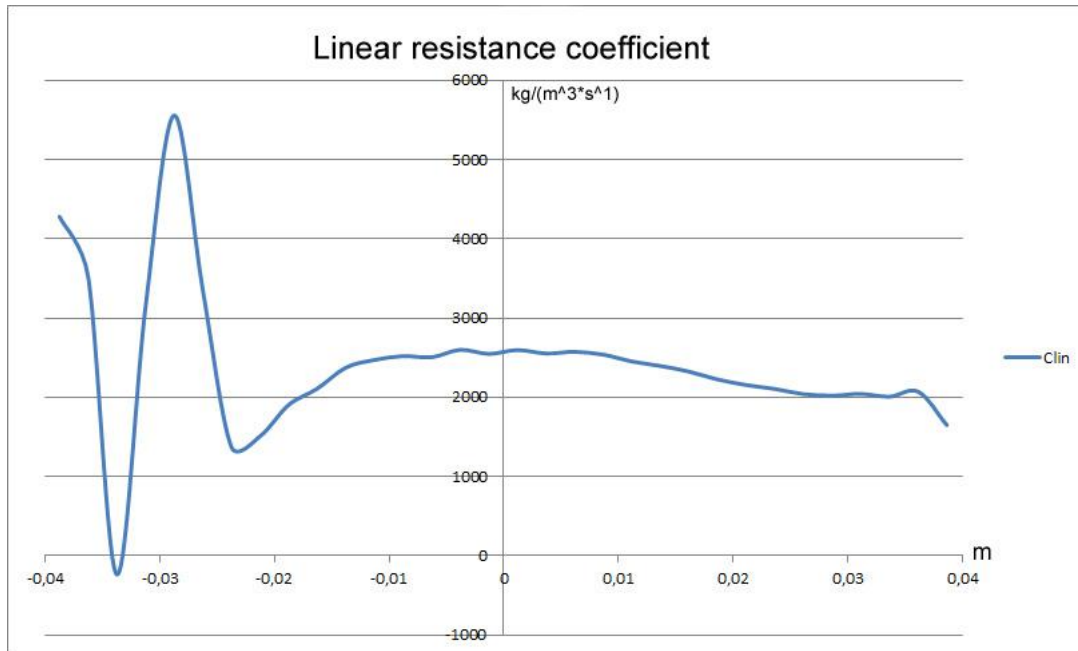


Figure 58. The linear resistance coefficients for the cylinders vs. the cylinder length. the target height, (from -4 to 4 cm).

Figure 59 shows the quadratic resistance coefficient evolution vs. the helium path between the cylinders. The quadratic resistance coefficient gets very high right when the fluid enters the cylinders, therefore the first data points have been removed to see the rest of the graph in a decent way according to Figure 60.

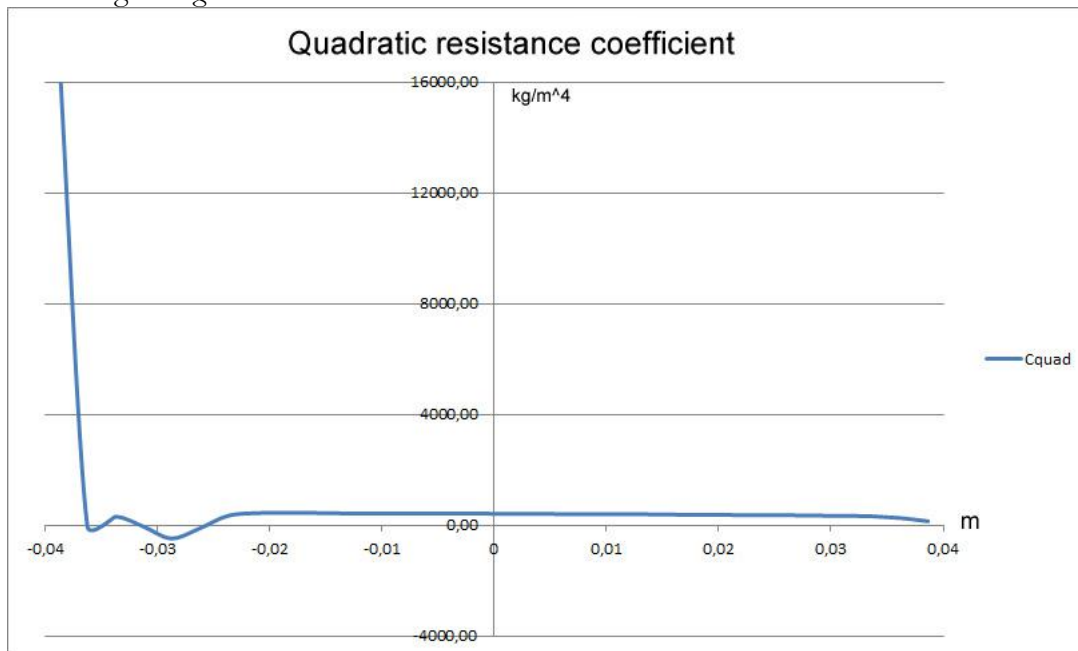


Figure 59. The quadratic resistance coefficient for the cylinders vs. the cylinder length, (the target height, from -4 to 4 cm). The y-axis is the quadratic resistance coefficient.

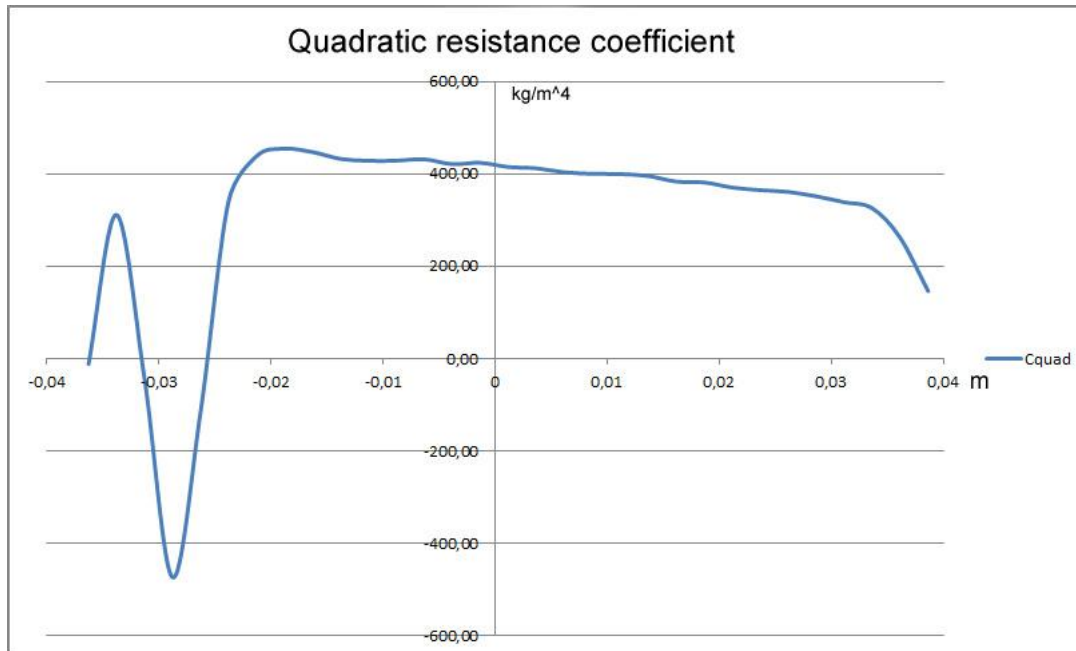


Figure 60. The quadratic resistance coefficient for the cylinders vs. the cylinder length, (the target height, from -4 to 4 cm). The y-axis is the quadratic resistance coefficient. The first points are removed to see the rest of the graph in a decent way.

3.4 Test with porous domain

In this step the resistance coefficients that were derived in the previous case are used. A part of the circular rotating target is represented only.

3.4.1 Modeling & Meshing

A part is cut out from the rotating target. This part consists of three domains: an inlet, a porous domain and an outlet domain according to Figure 61. The target is 50 cm long, 22 cm wide, the height of the inlet, porous domain and outlet is respectively 10, 8 and 20 cm. The proton beam hits the cut out part in the center of the porous domain along the z-axis. The model has a very simple mesh, it is meshed with 0.5 mm elements in all three zones. Figure 62 shows the meshed model.

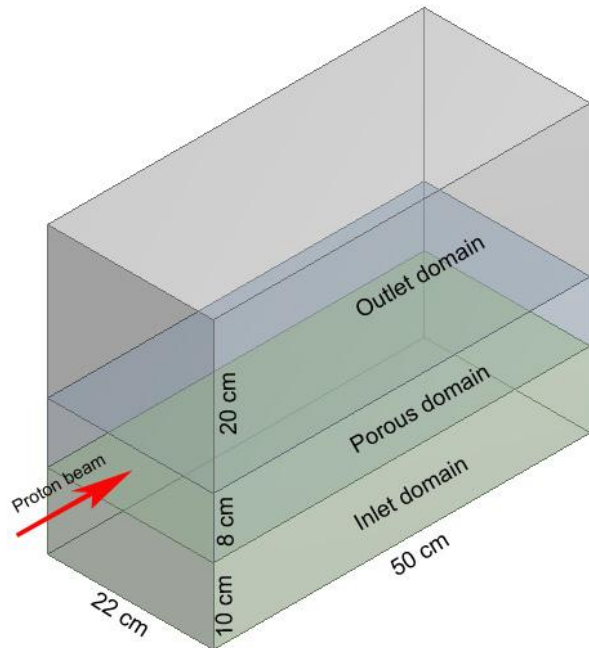


Figure 61. Model of porous domain with a part cut out of the circular rotating target. It is composed of an inlet domain, a porous domain and an outlet domain. It is 50 cm long and 22 cm wide. It has been simplified to a perfect rectangle.

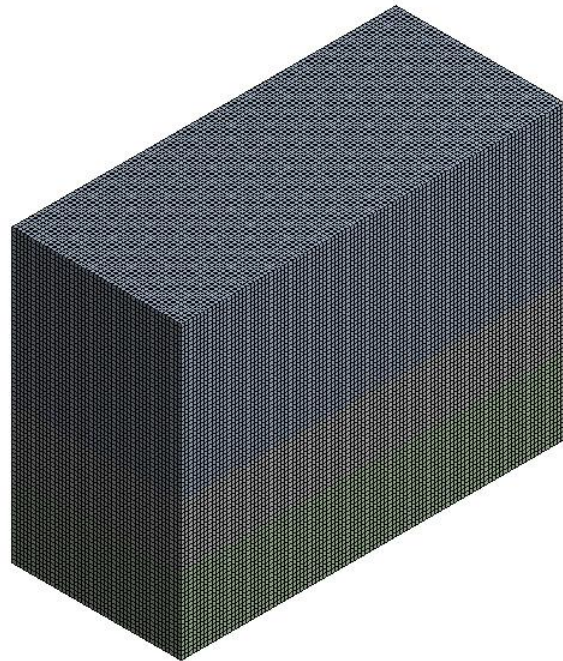


Figure 62. Meshed model of the cut out part. Very simple mesh, 5 mm body sizing on all domains.

3.4.2 Pre Processing

Once again, in the preprocessor the problem is set up with its boundary conditions. The inlet and outlet boundary conditions are chosen to be the same as in the “1 tube” analysis. The inlet pressure is 10 bar and the inlet temperature is 200°C. The outlet boundary condition is set to be mass flow rate, the value is calculated with $\dot{m} = \rho(p, T) \cdot A_{In} \cdot V_{In}$. The reference pressure is 0 bar. The energy deposition is interpolated into the volume of the porous domain. The energy deposition is implemented by the interpolation of the data given by the FLUKA [4] file. Here as well as in the previous case the energy value is divided by 40. This is because the target is rotating at 30 rpm; the beam only hits one certain part of the target once every two seconds. The resistance coefficients are defined with the tables derived from the previous case. They are imported to ANSYS CFX as user functions depending on the y-direction, the height of the porous domain. The functions with the resistance coefficient values are interpolated into the porous volume. The volume porosity of the porous domain is 0.0931. The turbulence model shear stress transport is used. As heat transfer method, total energy is used, this is described in the theory part. The outer long side walls of the three domains are set to be free slip walls. An illustration of the domains and some boundary conditions can be seen in *Figure 63* below.

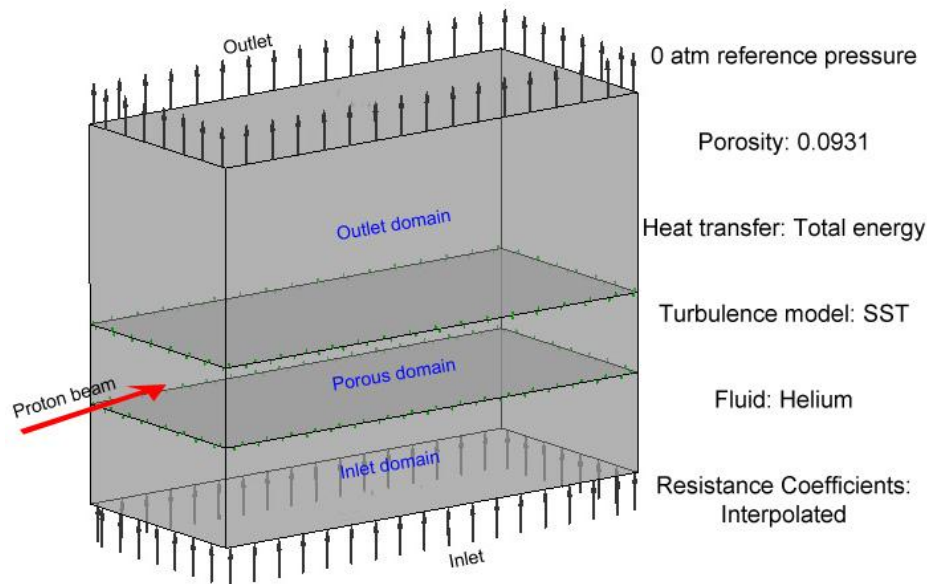


Figure 63. Boundary conditions for cut out part from the rotating target.

3.4.4 Simulation

As described before, during the simulation the RMS residuals, the imbalances and the user defined monitor points are kept under supervision. The RMS residuals are set to converge at $1e-5$. The imbalances and the user defined functions have to converge as well before the analysis is complete. The user defined monitor points are the pressure drop and the average outlet temperature. Physical times step is chosen with the value 0.1s at the start of the analysis. This is due to prevent divergence and slowly let the flow stabilize. Later the time scale is increased to 1s, in order to ensure a fully developed flow.

3.4.5 Post Processing

With help of the post processing tool the images of the results are generated. In this case the results are presented as contour plots. Five planes are created according to Figure 64, the first plane is 4 cm in the z-axis and the last plane is 4 cm in the z-axis. The three planes between them are equally distributed.

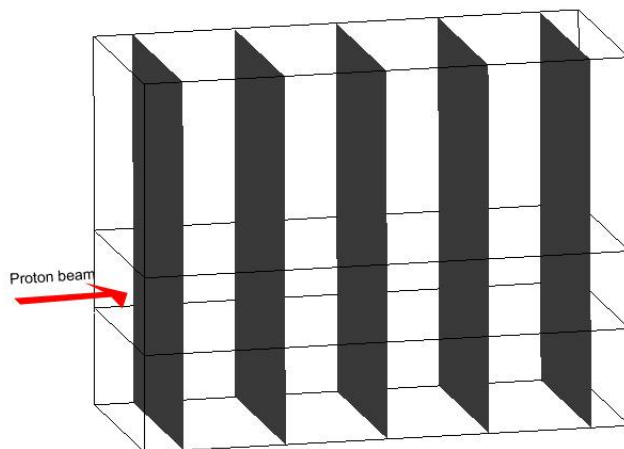


Figure 64. Planes for the contour plots. Five planes with the first 4 cm in z-axis and the last 4 cm in the z-axis. The three planes between them are equally distributed.

3.4.6 Results

The goal with this test is to study the pressure drop with the resistance coefficients derived from the previous “1 tube” case. The results present the temperatures as well. The values of this do not have to be similar to the previous case. *Table 16* below shows some of the results. Note that the average values are taken for the whole model. Due to this, the average values are lower than in the “1 tube” case.

Average helium Outlet temperature [°C]	212.176
Average Pressure drop (Inlet-Outlet) [bar]	0.0583
Max temperature [°C]:	308.92
Max velocity [m/s]:	99.196
Average outlet velocity [m/s]:	8.274

Table 16. Results of the porous domain with the resistance coefficients derived from the previous "1 tube" case.

Figure 65 shows contour plots of the pressure on 5 planes, of all three domains. One can see that the pressure drop is lower where it is hotter, this should be the other way around. The reason for this is that the data for the resistance coefficients only is collected from one line. To have accurate results all over the model, values have to be taken from more places all around the target. If this would be done a user functions depending on (x,y,z) could be interpolated into the porous volume. *Figure 66* shows contour plots of the helium temperature on 5 planes. It can clearly be seen how the temperature decreases along the z-axis.

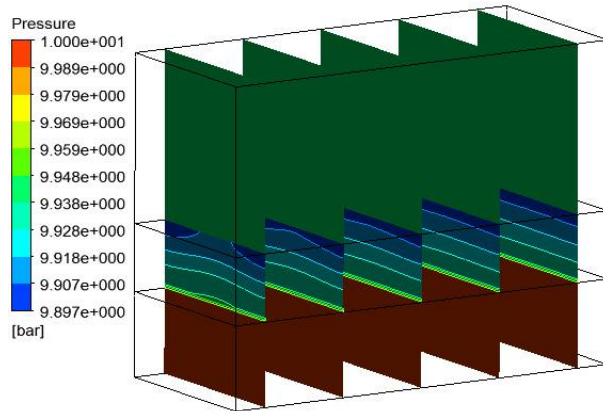


Figure 65. Contour plots of the pressure on 5 planes equally distributed along the z-axis.

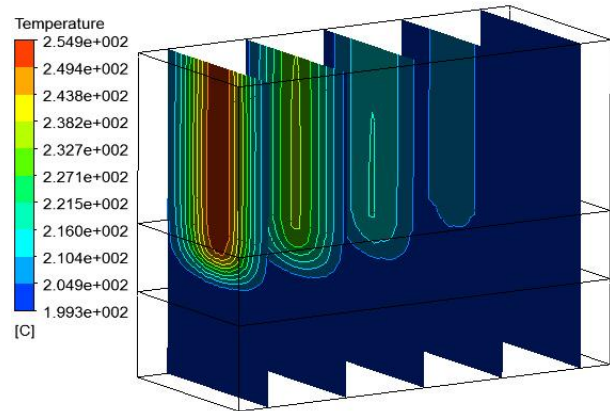


Figure 66. Contour plots of the temperature on 5 planes equally distributed along the z-axis.

Figure 67 below shows a contour plot of the pressure on the first plane. It can be seen that the pressure decreases rapidly in a short distance at the entrance of the cylinders, after this the pressure decreases almost linearly. The resistance coefficients works well at the center of the target. If the “1 tube” analysis had been performed at the sides as well and data to calculate the resistance coefficients had been saved from there, a new user function could be derived depending on (x,y,z) coordinates.

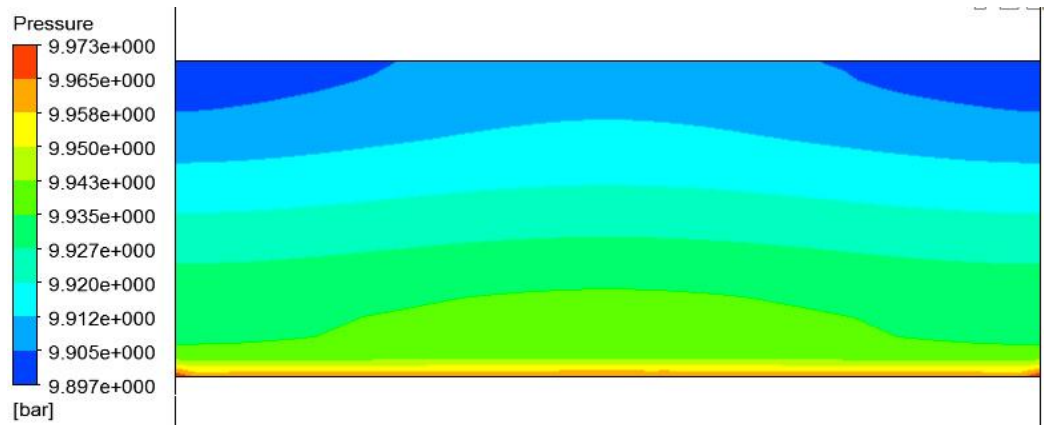


Figure 67. Contour plot of the pressure drop, only the porous domain.. This is the first contour plane located 4 cm in z-axis.

3.5 1cm of the rotating target

A small part of the rotating target along the z-axis is cut out. 1 cm is chosen to have a small and simple model as possible with fewer domains. The inlet and outlet pipes are included in the model as they should be in the real case. Such a small model is used to be able to perform an analysis relatively fast and still include the whole length of the target. Two different analyses are performed on this model and one analysis on the same model but with a flow reduction plate on the top of the cylinders.

3.5.1 Modeling

As mentioned earlier a 1 cm part of the rotating circular target is cut out. It is cut out right in front of the beam along the z-axis. It includes an inlet domain, parts of cylinders, helium between the cylinders and an outlet domain. The inlet and outlet domain are 2.5 cm high each. They are rounded with a radius of 2.5 cm at the front of the target. The model can be seen in figure Figure 68 below.

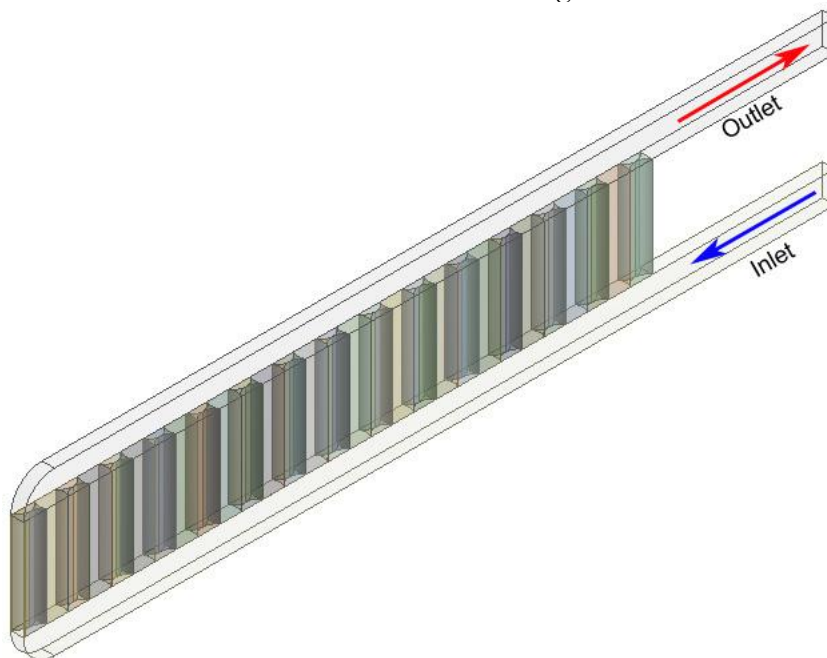


Figure 68. Iso view of the 1 cm part cut out of the rotating target. It has inlet and outlet pipe height of 2.5 cm each.

Figure 69 below shows the same model but with the outlet domain hidden and a plate on top of the cylinders that reduces the helium flow at the wanted places. The highlighted part on top of the cylinders is helium; it has a triangular shape and is cut out from a 1.5 mm metal plate placed directly on the top of the cylinders. The triangular shape prevents most of the helium flowing towards the outlet at the back of the target. This shape forces the helium to flow all the way to the front hot part of the target to get an adequate cooling all over the target.

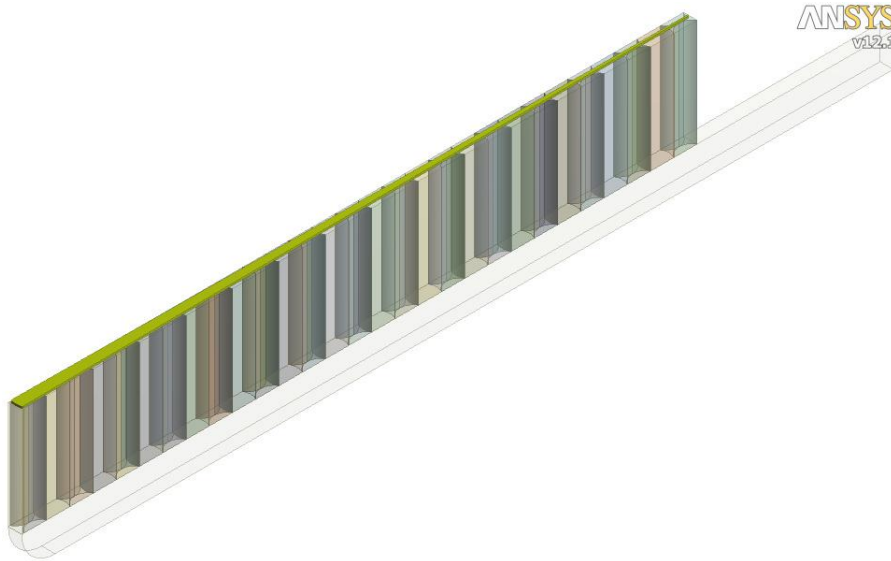


Figure 69. Iso view of the model with the outlet domain invisible and the reduction shape of the helium on top of the cylinders.

3.5.2 Meshing

The model overall is meshed with a coarse mesh. The helium between the cylinders has a finer mesh than the rest of the model. The goal is to lower the amount of elements as much as possible and still be able to get reasonable results. Edge sizing have been adapted along the flow direction on the helium between the cylinders. That means that the elements are relatively long along the flow direction. The largest elements on the inlet and outlet domain are 5mm. The mesh can be seen in Figure 70 below. Figure 71 shows the mesh from another angle and zoomed. Figure 72 shows a part of the mesh on top of the cylinders and on top of the helium between the cylinders. There are about 400 thousand elements in the model.

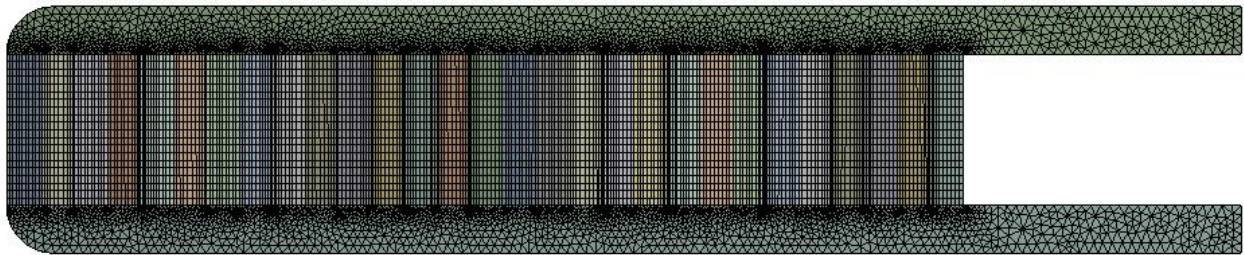


Figure 70. Meshed model from the side of the 1 cm part cut out from the rotating target.

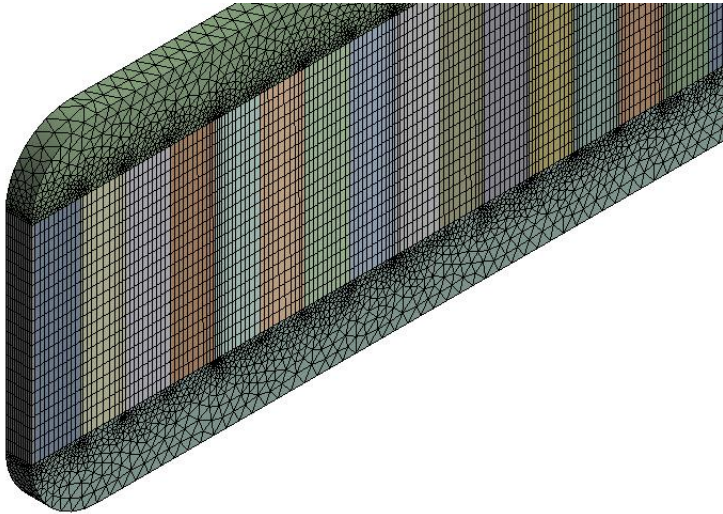


Figure 71. A zoomed iso view of the meshed 1 cm part cut out from the rotating target.



Figure 72. Mesh from top of the cylinders and helium between the cylinders.

3.5.3 Pre Processing

As in the previous cases the inlet boundary condition is set to total pressure: 10 bar and 200 °C. The outlet boundary condition is set to mass flow rate. Three different analyses are performed with the inlet velocities: 160, 100 and 40 m/s. The energy divided by 40 is interpolated into the cylinders as for the other rotating target cases. The turbulence model shear stress transport is used. The reference pressure is set to 0 bar. The sides of the helium domains are set to be free slip walls. Total energy is used as heat transfer option.

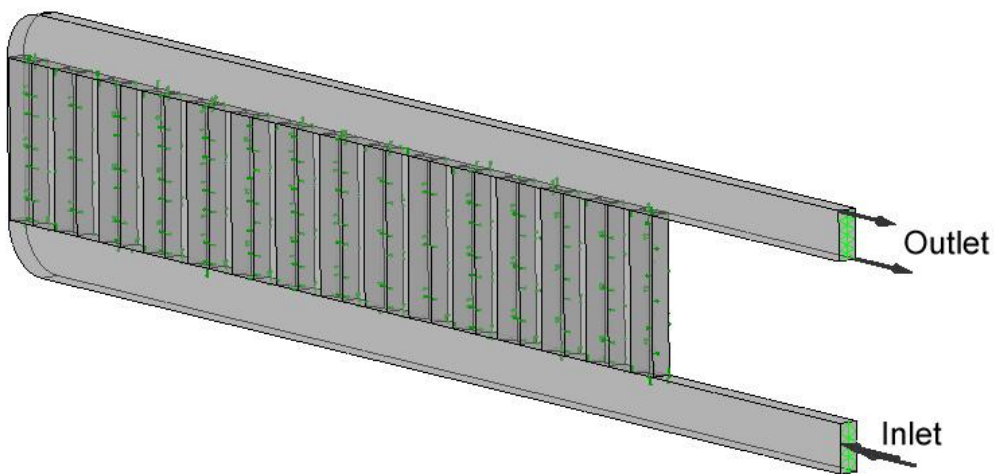


Figure 73. Illustration of the pre-processing for the 1 cm cut out case

3.5.4 Simulation

As described before, during the simulation the RMS residuals, the imbalances and the user defined monitor points are kept under supervision. The RMS residuals are set to converge at $1e-5$. The imbalances and the user defined functions have to converge as well before the analysis is complete. The user defined monitor points are the pressure drop and the average outlet temperature. Physical times step is chosen with the value 0.1s at the start of the analysis. This is due to prevent divergence and slowly let the flow stabilize. Later the time scale is increased to 1s, this is to ensure fully developed flow.

3.5.5 Post Processing

The results will be presented as contour plots of a plane in the middle of the model according to *Figure 74*

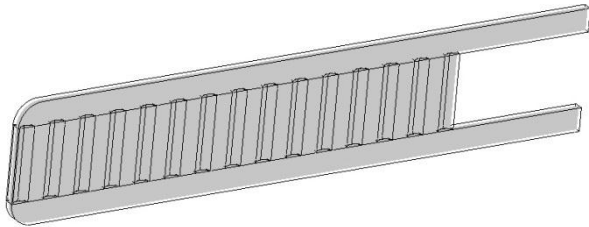


Figure 74. The contour plots are of a plane in the middle of the model.

3.5.6 Results

Three analyses are performed with different inlet velocities, one of them with a flow reduction. All of them with satisfying results. *Table 17* below shows a comparison between the three analyses with different inlet velocities, all with the same inlet area. The one with 40 m/s inlet velocity corresponds to the one with the reduction plate on top of the cylinders. The pressure drop difference is large between the analyses; although a pressure drop of 22175 Pa for the inlet velocity of 160 m/s is not large compared to the stationary target with the tungsten spheres. The temperature difference between the analyses is not large compared to the large difference in inlet velocity. The maximum allowed average helium outlet temperature is 400 °C, which they are all well below. Notice that the inlet temperature of the helium is assumed to be 200 °C, which means that the global temperature rise in the helium is only between 20-75 °C. The maximum temperature in the cylinders is higher for the 100m/s case than for the 40 m/s case. This is due mostly of the helium flowing directly towards the outlet; which means that the mass flow is lower at the front part of the target and less heat is conducted away with the helium. With the 40 m/s case most of the helium is forced to the front of the target with help of the reduction plate, therefore the mass flow is higher at the front of the target and more efficient cooling of the cylinders is achieved. The cylinder temperatures are acceptable for all cases. There is a large difference in the needed pumping power between the three cases. It shows that the velocity affect the pumping power significantly.

Inlet velocity [m/s]:	160	100	40
Pressure drop (inlet-outlet) [Pa]:	22175	8815	2116
Avg He outlet temp [°C]:	217.92	229.756	274.86
Global delta T [°C]:	19.92	29.756	74.86
Max cylinder temp [°C]:	590.781	722.647	688.928
Total pumping power [W]:	280	69.2	6.65

Table 17. Comparison between the three analyses of the 1 cm cut out part from the rotating target.

Figure 75, Figure 76 and Figure 77 below show contour plots of the temperature on a plane in the middle of the model. It shows the temperature of both the helium and the cylinders for the three cases with inlet velocities 160, 100 and 40 m/s. The temperature in the cylinders is about 130 °C hotter in the 100 m/s case than in the 160 m/s. In the case with the inlet velocity of 40 m/s, the temperature in the cylinder is lower than in the 100 m/s case, with about 35 °C. This is because of the flow reduction plate on top of the cylinders. It forces the helium to flow towards the hot front part of the target. The average helium outlet temperature is hotter in the 40 m/s case, this is because of the lower inlet velocity and the flow reduction plate. It is obvious that a lower inlet velocity leads to a higher temperature. The reduction plate makes less of the cooler helium flow towards the outlet and mix with the hot helium coming from the front of the target.

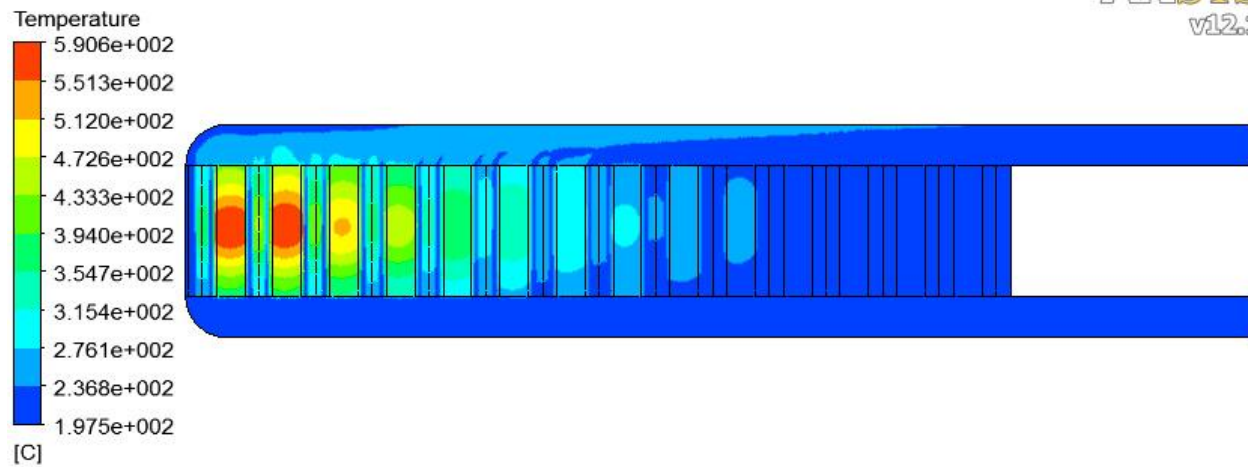


Figure 75. Contour plot on the middle plane, of the temperature in both the helium and cylinders of the 160 m/s inlet case.

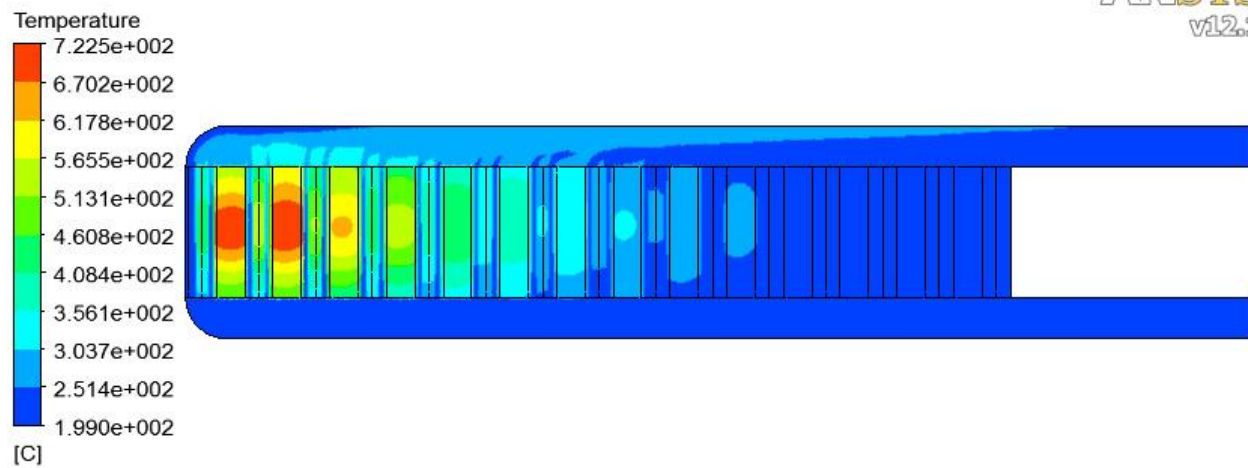


Figure 76. Contour plot on the middle plane, of the temperature in both the helium and cylinders of the 100 m/s inlet case.

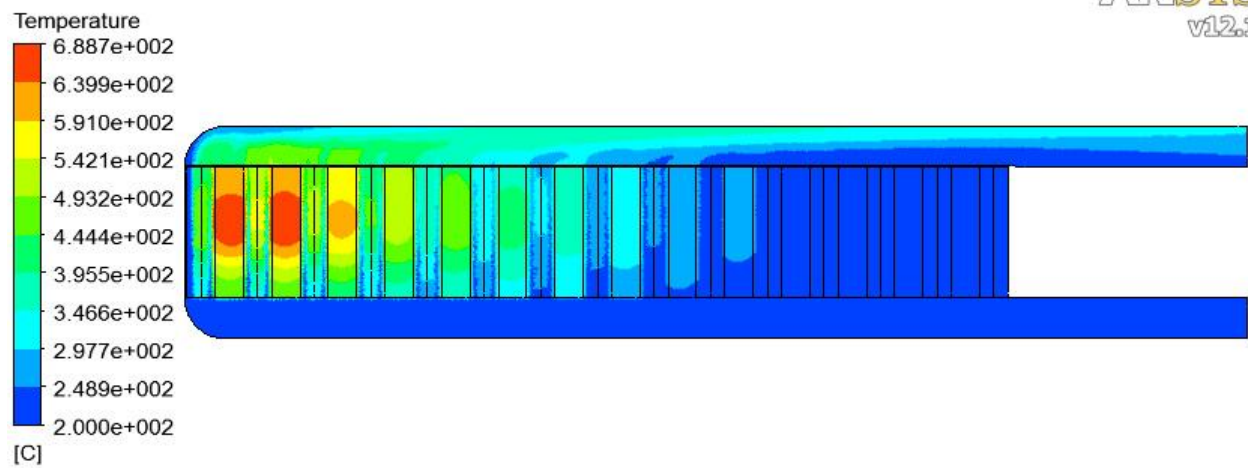


Figure 77. Contour plot on the middle plane, of the temperature in both the helium and cylinders of the 40 m/s inlet case.

Figure 78, *Figure 79* and *Figure 80* below show contour plots of the helium velocity on a plane in the middle of the model. They represent the three cases with inlet velocities 160, 100 and 40 m/s. The maximum velocity for all cases is located at the top of the outlet pipe a bit from the outlet. The difference in maximum temperature between the 160 m/s inlet and 40 m/s inlet is about 165 m/s. This is a large difference given that the temperature difference is not that large between these cases. In *Figure 78* and *Figure 79*, it can be seen that most of the helium is flowing towards the outlet already at the first tube. This is a reason why this case has lower outlet helium temperature. In *Figure 80* this does not occur because the flow reduction plate at the top of the cylinders. It forces most of the helium flowing towards the front of the target.

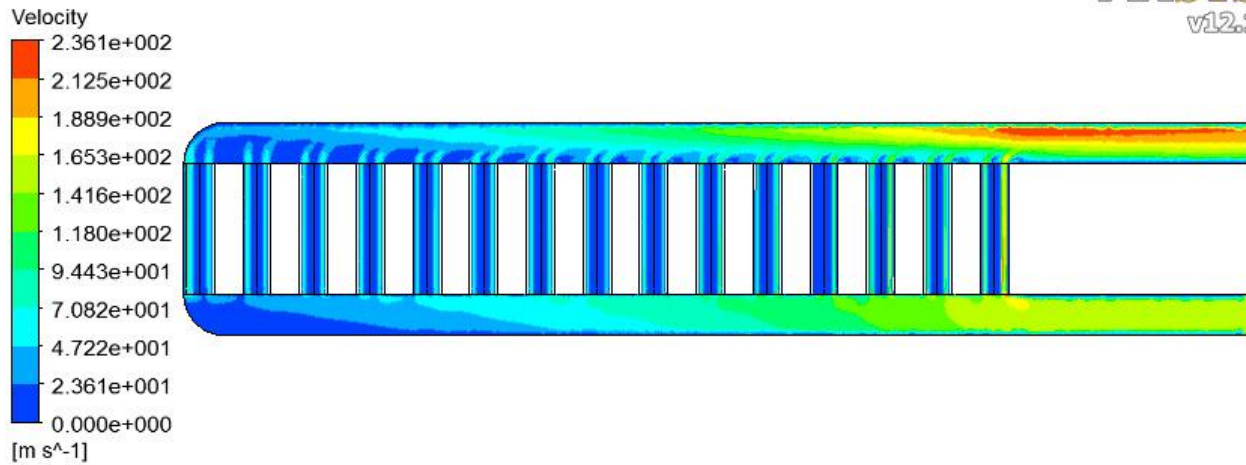


Figure 78. Contour plot on the middle plane, of the helium velocity of the 160 m/s inlet case.

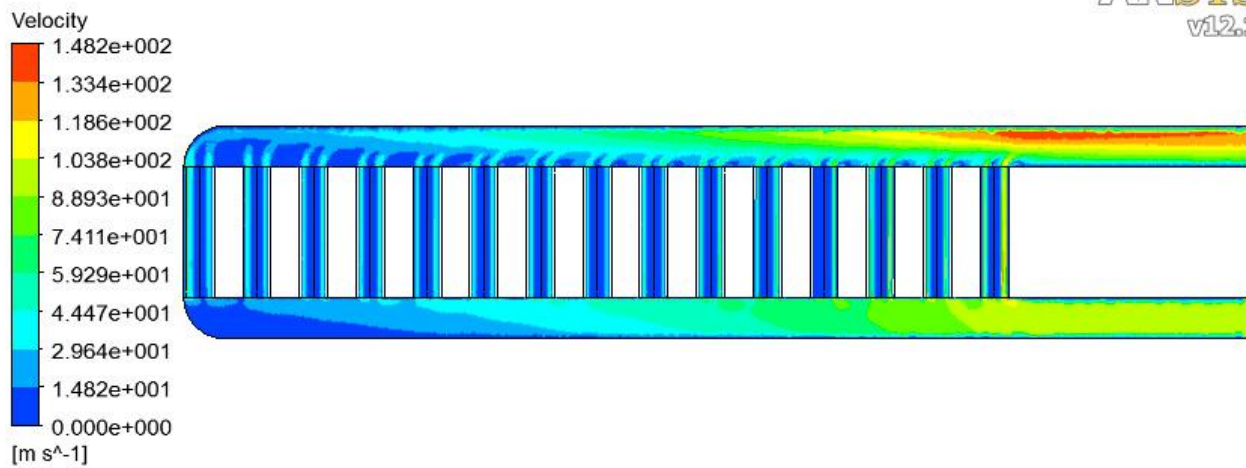


Figure 79. Contour plot on the middle plane, of the helium velocity of the 100 m/s inlet case.

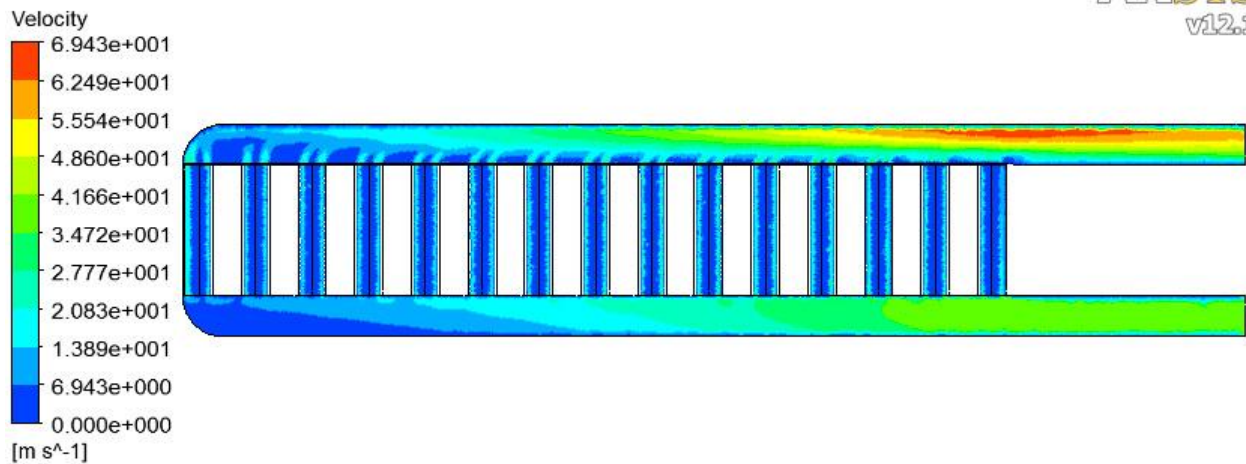


Figure 80. Contour plot on the middle plane, of the helium velocity of the 40 m/s inlet case.

Figure 81, Figure 82 and Figure 83 below show contour plots of the helium velocity in vertical direction on a plane in the middle of the model. They represent the three cases with inlet velocities 160, 100 and 40 m/s. It is important that the flow in vertical direction, i.e. the flow between the cylinders, is evenly distributed along the z- axis or having more of the helium flowing towards the hot front part of the target. The vertical flow in both the 160 m/s and 100 m/s case is highest at the back of the target, at the first couple of “tubes” and then gradually decreasing. This could be solved by having the flow entering from the other side. Another solution is the flow reduction plate that has been mentioned earlier. This reduces the flow gradually starting from the front of the target towards the back of the target with help of a triangular shape. *Figure 83* shows the results of the flow reduction case. The flow in vertical direction is now more evenly distributed along the z-axis.

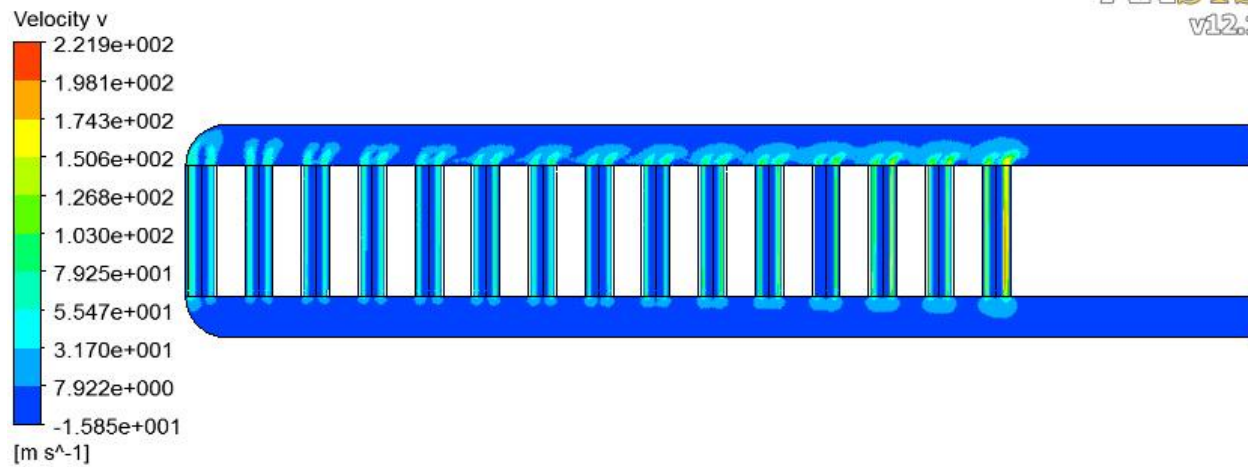


Figure 81. Contour plot on the middle plane, of the helium velocity in vertical direction, of the 160 m/s inlet case.

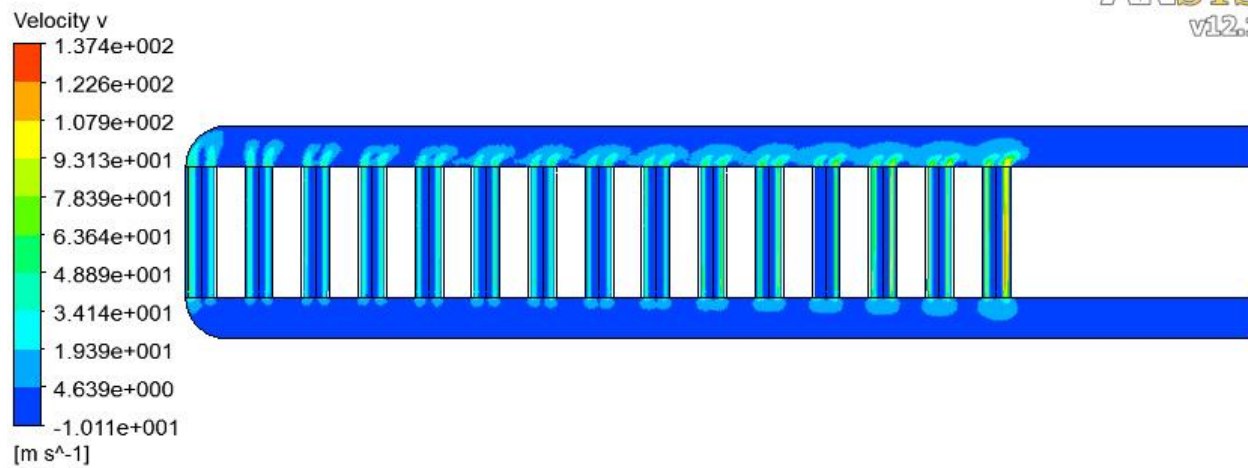


Figure 82. Contour plot on the middle plane, of the helium velocity in vertical direction, of the 100 m/s inlet case.

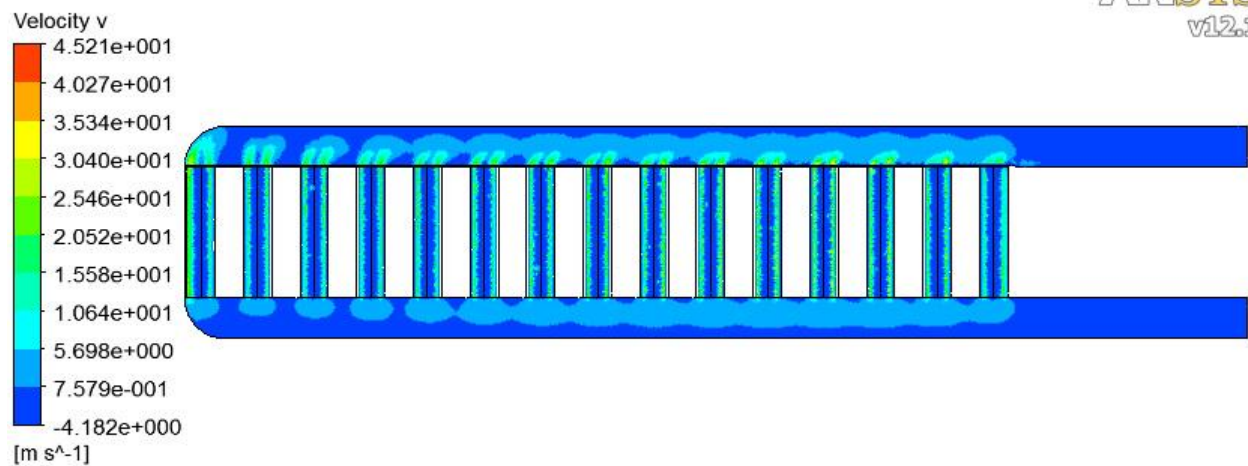


Figure 83. Contour plot on the middle plane, of the helium velocity in vertical direction, of the 40 m/s inlet case.

Figure 84, *Figure 85* and *Figure 86* below show contour plots of the pressure on a plane in the middle of the model. They represent the three cases with inlet velocities 160, 100 and 40 m/s. The contour plots show how the pressure varies in the model. It can be seen that the ones with higher inlet velocities have higher pressure drops.

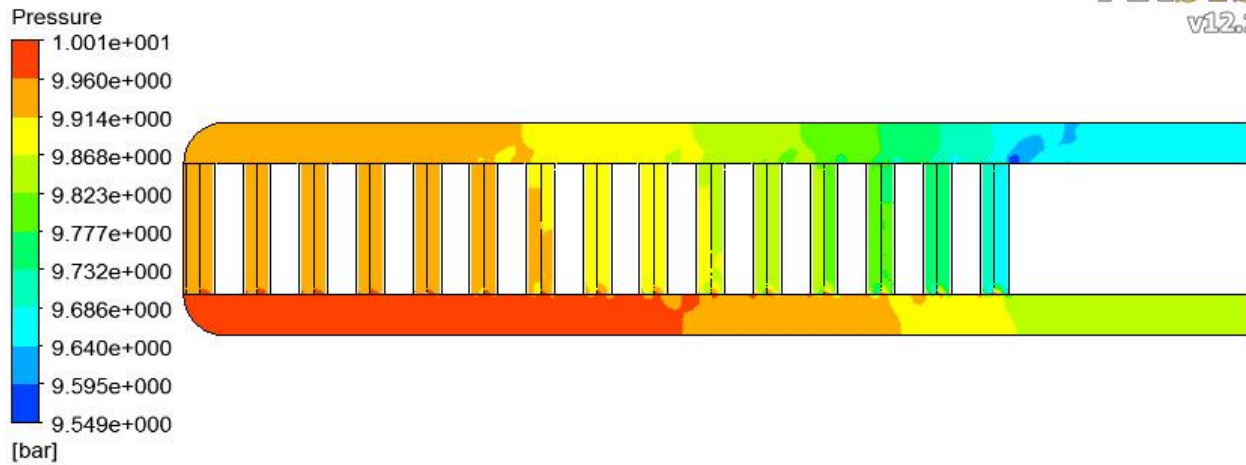


Figure 84. Contour plot on the middle plane, of the pressure, of the 160 m/s inlet case.

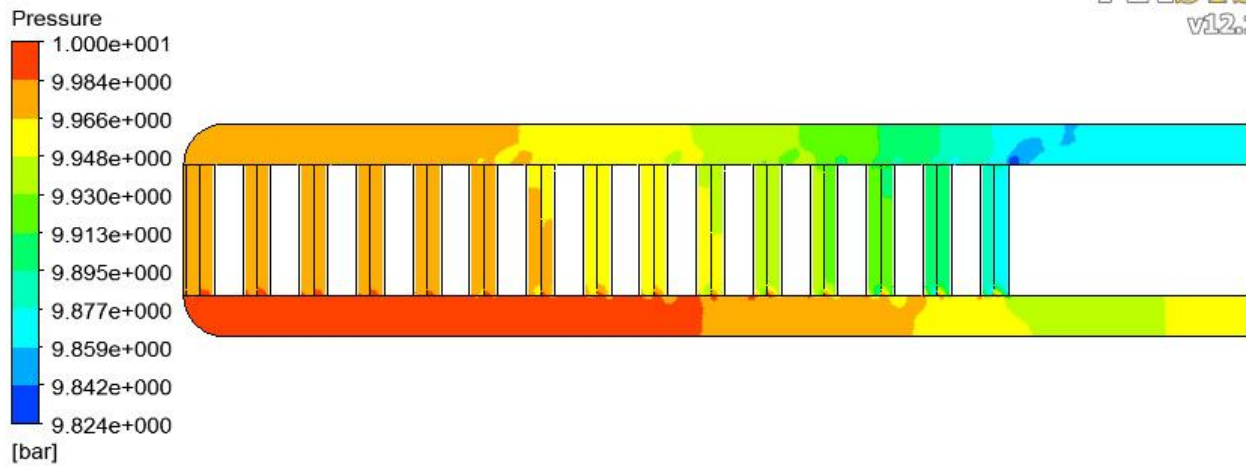


Figure 85. Contour plot on the middle plane, of the pressure, of the 100 m/s inlet case.

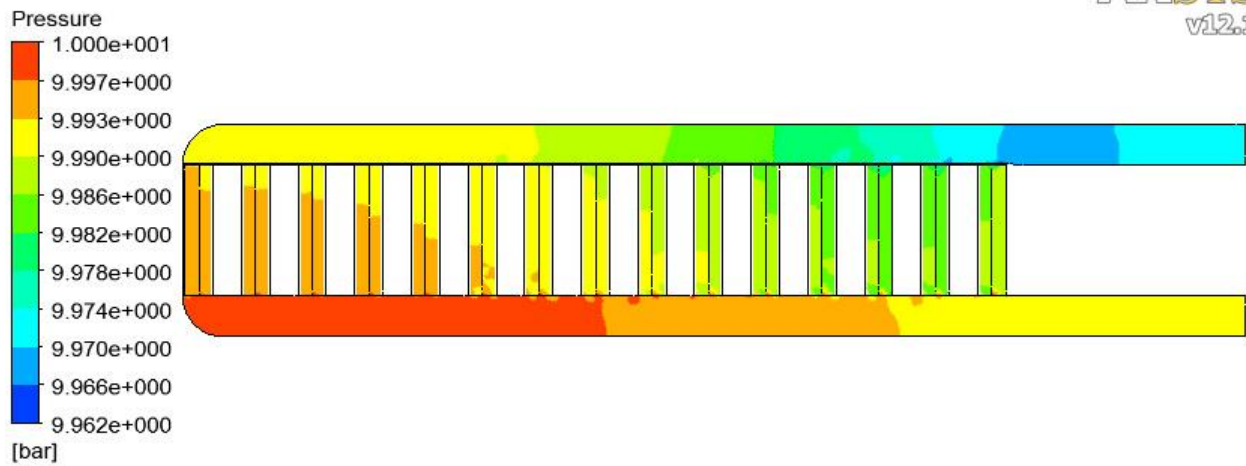


Figure 86. Contour plot on the middle plane, of the pressure, of the 40 m/s inlet case.

3.6 Conclusions

The first step in the rotating target concept was to study a small part of the target, only “1 tube” between parts of three surrounding cylinders. This was done mainly to study the flow pattern and derive resistance coefficients. Resistance coefficients had to be derived because the difficulties with the equations for the resistance coefficients in the previous concept with the tungsten sphere bed. By deriving the resistance coefficients with help of ANSYS CFX, they will only be adaptable on this specific type of solution. In this case only one tube was studied, to have accurate resistance coefficients all over the target many tubes at different places have to be studied. With help of this a user function depending on (x,y,z) of the resistance coefficient can be derived. The most desirable would be to develop equations for the resistance coefficient that were depending on the temperature, mass flow and gas expansion. In that case they could be adapted to any problem.

Next step was to try the resistance coefficients on a part of the target represented by a porous domain with an inlet and outlet domain. From the analyses with porous domains from the tungsten sphere bed concept, it is known that it is not possible to get perfect unidirectional flow with help of ANSYS CFX directional loss model. Because of this the main goal with the porous domain was to study the helium temperature and pressure variation along the y-axis on a larger part of the target. The pressure variation through the porous domain is similar to the analysis of “1 tube”, but only at the center of the porous domain. The reason for this is that the resistance coefficients derived is only made for variation in the y-axis at the front and center of the target. ANSYS should derive a new loss model that is fully unidirectional, and one should also be able to choose the size and distribution of the tubes.

Finally a larger part of the target is cut out to be studied; a 1 cm thick part of the circular rotating target is cut out to perform analyses on it. Such a thin model provides relatively low simulation time. These analyses finished with successful results regarding to the requirements. It is important to have most of the helium flowing to the front hot part of the target. A way to solve this is with some kind of flow reduction, for example like the one in this chapter. This concept is feasible regarding to variables as velocity, mass flow, temperature, maximum pressure, pressure drop and pumping power.

4. References

- [1]. Handbook of Hydraulic Resistance, 4th Edition, Chapter eight: Resistance to flow through barriers uniformly distributed over the channel cross section.
- [2]. VDI-Wärmeatlas 4. Auflage 1984
- [3]. Fulfillment of selection criteria by helium cooled granular target, 3.2.1.1 Thermal assessment of the stationary target concept. EDMS Ref: 1093880 v1.0.
- [4]. FLUKA: A Multi-particle Transport Code", A. Ferrari, P.R. Sala, A. FassÚ and J. Ranft. Geneva 2005

5. Appendix

The appendix includes ANSYS CFX theory and Mat Lab codes written for the analytical calculations.

5.1 ANSYS CFX Theory

The equations used by ANSYS CFX for calculating this type of problem are shown below. They are taken from ANSYS CFX-Solver Theory Guide.

5.1.1 Governing Equations

Transport Equations:

The continuity equation:

$$\frac{\partial \rho}{\partial t} + \nabla \cdot (\rho \mathbf{U}) = 0 \quad (54)$$

The momentum equation:

$$\frac{\partial(\rho \mathbf{U})}{\partial t} + \nabla \cdot (\rho \mathbf{U} \otimes \mathbf{U}) = -\nabla p + \nabla \cdot \boldsymbol{\tau} + \mathbb{S}_M \quad (55)$$

Where the stress tensor, $\boldsymbol{\tau}$, is related to the strain rate by:

$$\boldsymbol{\tau} = \mu \left(\nabla \mathbf{U} + (\nabla \mathbf{U})^T - \frac{2}{3} \delta \nabla \cdot \mathbf{U} \right) \quad (56)$$

The total energy equation:

$$\frac{\partial(\rho h_{tot})}{\partial t} - \frac{\partial \rho}{\partial t} + \nabla \cdot (\rho \mathbf{U} h_{tot}) = \nabla \cdot (\lambda \nabla T) + \nabla \cdot (\mathbf{U} \cdot \boldsymbol{\tau}) + \mathbf{U} \cdot \mathbb{S}_M + \mathbb{S}_E \quad (57)$$

Where h_{tot} is the total enthalpy, related to the static enthalpy $h(T, p)$ by:

$$h_{tot} = h + \frac{1}{2} \mathbf{U}^2 \quad (58)$$

The term $\nabla \cdot (\mathbf{U} \cdot \boldsymbol{\tau})$ represents the work due to viscous stresses and is called the viscous work term.

The term $\mathbf{U} \cdot \mathbb{S}_M$ represents the work due to external momentum sources and is currently neglected.

Equations of State:

The transport equations described above must be augmented with constitutive equations of state for density and for the enthalpy in order to form a closed system. In the most general case, these equations have to form:

$$\rho = \rho(p, T) \quad (59)$$

$$dh = \left. \frac{\partial h}{\partial T} \right|_p dT + \left. \frac{\partial h}{\partial p} \right|_T dp = C_p dT + \left. \frac{\partial h}{\partial p} \right|_T dp \quad (60)$$

$$C_p = C_p(p, T) \quad (61)$$

Various special cases for particular material types are described below.

Incompressible Equation of state:

This is the simplest case: density is constant and c_p can be (at most) a function of temperature.

$$\rho = \rho_{spec} \tag{62}$$

$$dh = c_p dT + \frac{dp}{\rho} \tag{63}$$

$$c_p = c_p(T) \tag{64}$$

Ideal gas Equation of state:

For an ideal gas, density is calculated from the ideal gas law and C_p can be at most a function of temperature.

$$\rho = \frac{w p_{abs}}{R_0 T} \tag{65}$$

$$dh = C_p dT \tag{66}$$

$$c_p = c_p(T) \tag{53}$$

Where w is the molecular weight, p_{abs} is the absolute pressure, and R_0 is the universal gas constant.

5.1.2 Full Porous Model

The full porous model is at once both a generalization of the Navier-Stokes equations and of Darcy’s law commonly used for flows in porous regions. It can be used to model flows where the geometry is too complex to resolve with a grid. The model retains both advection and diffusion terms and can therefore be used for flows in rod or tube bundles where such effects are important.

In deriving the continuum equations, it is assumed that “infinitesimal” control volumes and surfaces are large relative to the interstitial spacing of the porous medium, but small relative to the scales that you want to resolve. Thus, given control cells and control surfaces are assumed to contain both solid and fluid regions.

The volume porosity γ at a point is the ratio of the volume V' available to flow in an infinitesimal control cell surrounding the point, and the physical volume V of the cell. Hence:

$$V' = \gamma V \tag{67}$$

It is assumed that the vector area available to flow, \mathbb{A}' , through an infinitesimal planar control surface of vector area \mathbb{A} is given by:

$$\mathbb{A}' = \mathbb{K} \cdot \mathbb{A} \tag{68}$$

Where: $\mathbb{K} = (K^{ij})$ is a symmetric second rank tensor, called the area porosity tensor. Recall that the dot product of a symmetric rank two tensor with a vector is the vector $\mathbb{K} \cdot \mathbf{A}^i = K^{ij} A_j$. ANSYS CFX presently allows only \mathbb{K} to be isotropic; that $K^{ij} = \gamma \delta^{ij}$. The general scalar advection-diffusion equation in a porous domain becomes:

$$\frac{\partial}{\partial t}(\gamma \rho \Phi) + \nabla \cdot (\rho \mathbb{K} \cdot \mathbb{U} \Phi) - \nabla \cdot (\Gamma \mathbb{K} \cdot \nabla \Phi) = \gamma S \quad (69)$$

In addition to the usual production and dissipation terms, the source term S will contain transfer terms from the fluid to the solid parts of the porous medium.

In particular, the equations for conservation of mass and momentum are:

$$\frac{\partial}{\partial t} \gamma \rho + \nabla \cdot (\rho \mathbb{K} \cdot \mathbb{U}) = 0 \quad (70)$$

and:

$$\frac{\partial}{\partial t}(\gamma \rho \mathbb{U}) + \nabla \cdot (\rho (\mathbb{K} \cdot \mathbb{U}) \otimes \mathbb{U}) - \nabla \cdot \left(\mu_e \mathbb{K} \cdot \left(\nabla \mathbb{U} + (\nabla \mathbb{U})^T - \frac{2}{3} \delta \nabla \cdot \mathbb{U} \right) \right) = \gamma S_M - \gamma \nabla p \quad (71)$$

Where \mathbb{U} is the true velocity, μ_e is the effective viscosity – either the laminar viscosity or a turbulent quantity, and S_M is a momentum source, which could be written as $-\mathbb{R} \cdot \mathbb{U}$ (where $\mathbb{R} = (R^{ij})$ and represents the flow in the porous medium. This is in general a symmetric positive definite second rank tensor, in order to account for possible anisotropies in the resistance.

In the limit of large resistance, a large adverse pressure gradient must be set up to balance the resistance. In that limit, two terms on the right-hand side of equation (49) are both large and of opposite sign, and the convective and diffusive terms on the left-hand side are negligible. Hence, equation (49) reduces to:

$$\mathbb{U} = -\mathbb{R}^{-1} \cdot \nabla p \quad (72)$$

Hence, in the limit of large resistance, you obtain an anisotropic version of Darcy's law, with permeability proportional to the inverse of the resistance tensor. However, unlike Darcy's law, you are working with the actual fluid velocity components \mathbb{U} , which are discontinuous at discontinuity in porosity, rather than the continuous averaged superficial velocity, $\mathbb{Q} = \mathbb{K} \cdot \mathbb{U}$. Heat transfer can be modeled with an equation of similar form:

$$\frac{\partial}{\partial t}(\gamma \rho H) + \nabla \cdot (\rho \mathbb{K} \cdot \mathbb{U} H) - \nabla \cdot (\Gamma_e \mathbb{K} \cdot \nabla H) = S^H \quad (73)$$

Where Γ_e is the effective thermal diffusivity and S^H contains a heat source or sink to or from the porous medium.

5.1.3 Loss models

Isotropic loss model:

The momentum loss through an isotropic porous region can be formulated using permeability and loss coefficients as below.

$$S_{M,x} = -\frac{\mu}{K_{perm}}U_x - K_{loss}\frac{\rho}{2}|U|U_x \quad (74)$$

$$S_{M,y} = -\frac{\mu}{K_{perm}}U_y - K_{loss}\frac{\rho}{2}|U|U_y \quad (75)$$

$$S_{M,z} = -\frac{\mu}{K_{perm}}U_z - K_{loss}\frac{\rho}{2}|U|U_z \quad (76)$$

where K_{perm} is the permeability and K_{loss} is the loss coefficient. The linear component of this source represents viscous losses and the quadratic term represents inertial losses.

The source may alternatively be formulated using the linear and quadratic resistance coefficients, substituting two coefficients C_{R1} and C_{R2} as follows:

$$C_{R1} = \frac{\mu}{K_{perm}} \quad (77)$$

$$C_{R2} = K_{loss}\frac{\rho}{2} \quad (78)$$

Directional loss model:

The momentum source through an anisotropic porous region (such as a honeycomb or perforated plate) may be modeled using directional loss model. With this model, the stream wise direction (which is permitted to vary in space), must be specified. Consider a stream wise-oriented coordinate system (x', y', z') such as x' -axis is aligned with the stream wise direction and the y', z' axes lie on the transverse plane. The momentum losses in these directions are:

$$S_{M,x'} = -\frac{\mu}{K_{perm}^S}U_{x'} - K_{loss}^S\frac{\rho}{2}|U|U_{x'} \quad (79)$$

$$S_{M,y'} = -\frac{\mu}{K_{perm}^T}U_{y'} - K_{loss}^T\frac{\rho}{2}|U|U_{y'} \quad (80)$$

$$S_{M,z'} = -\frac{\mu}{K_{perm}^T}U_{z'} - K_{loss}^T\frac{\rho}{2}|U|U_{z'} \quad (81)$$

Where K_{perm}^S and K_{perm}^T are the stream wise and transverse permeabilities, and K_{loss}^S and K_{loss}^T are the stream wise and transverse loss coefficients. These quantities may also be expressed in linear and quadratic resistance coefficients.

In addition, the transverse loss may be modeled by multiplying the stream wise coefficients by some factor. If this option is used together with a stream wise permeability, the implied transverse permeability is equal to the stream wise permeability divided by this factor.

5.2 Mat lab code: “backwards” iterative method

```

clear all
clc
%%%%%%%%%%%%%%%%%%%%%%%%%%%%%%%%%%%%%%%%%%%%%%%%%%%%%%%%%%%%%%%%%%%%%%%%
%% Cooling tungsten spheres with helium %%
%% By: Jozsef Szabo, LTH                %%
%%%%%%%%%%%%%%%%%%%%%%%%%%%%%%%%%%%%%%%%%%%%%%%%%%%%%%%%%%%%%%%%%%%%%%%%

%% Helium properties
M=4.0026*10^-3;           % Molar mass [g/mol]
R=8.314;                 % Gas constant R
dyn_visc=18.6*10^-6;     % Dynamic Viscosity [Ns/m2]
cp=5.1932*10^3;         % Specific heat [J/kg * K]
khe=0.144;               % Thermal conductivity [W/m*k]

%% Tungsten Properties
dens_t=18500;            % Density of tungsten [kg/m3]
cp_t=0.135*10^3;        % Specific heat, tungsten [J/kg * K]

%% Konstant
TinC=22;                 % Inlet Temperature [Celsius]
side1=0.08;              % Side1 of the square [m]
side2=0.20;              % Side2 of the square [m]
A=side1*side2;           % Area of the square [m^2]
l0=0.22;                 % Length of sphere bed [m]
B=1.8;                   % For smooth surfaces
e=1-(pi/sqrt(18));        % Porosity
Tin=TinC+273.15;         % Inlet Temperature [K]
fil=1;                   % Shape coefficient, 1 for perfect sphere

%% Guess
w1=15;                   % Flow velocity [m/s] (Initial guess)

%% Parameters
pstatic=1.0*10^6;        % Static pressure (Pressure at outlet)
dgr=10*10^-3;            % Sphere diameter [m]
P=1.684*10^6;            % Effekt from beam [W]
Qm=5.98*10^3;            % [J/kg/pulse]
del=fil*dgr;

%% Diagram Generation
Data=zeros(1,1);        % Matrix to store data in
num=1;                   % Counter for the for-loop
for P_pump=1:5000:900*10^3
    k=1;                  % Pumping effect variation
    while k<21            % Counter for iteration

pin=(P_pump/(A*w1))+pstatic; % Pressure at the inlet

%% Calculations
dens=(M*pin)/(R*Tin);
visc=dyn_visc/dens;
Re1=(w1*del)/visc;
lambda=((360*((1-e)^2))/(e^3*Re1))+((B*(1-e))/e^3);

```

```

zeta=(lambda*10)/del;

%% Quadratic equation
C=((273*dens)/(4*(Tin^2)));
D=(P/(dens*A*cp))^2;
p=((4*Tin)+(C*D*zeta)/((P_pump/(A*w1)))+(4*C*D)/(P_pump/(A*w1)));
q=((8*C*D*Tin)/(P_pump/(A*w1))+(4*(Tin^2)));
J1=(p/2)+sqrt(((p/2)^2)-q);
J2=(p/2)-sqrt(((p/2)^2)-q);
Tex1=J1-Tin; % This is the positive one
Tex2=J2-Tin;

w1=(P/(dens*A*cp*(Tex1-Tin))); % Calculate the new inlet velocity
%Tex=(P/(A*w1*cp*dens))+Tin
k=k+1;
end

%CLin=(273*90*dens*(Tin+Tex1)*((1-e)^2)*visc)/((e^3)*(Tin^2)*(dgr^2));
%CQuad=((273*dens)/(Tin^2))*(((Tin+Tex1)*B*(1-e))/(4*(e^3)*dgr))+((Tex1-
Tin)/(Tin^2));
Tm=(Tin+Tex1)/2;
CLin=((dens*273*Tm)/(2*Tin^2))*((360*((1-e)^2)*visc)/((e^3)*(del^2)));
CQuad=((dens*273*Tm)/(2*Tin^2))*((B*(1-e))/((e^3)*del))+((2*(Tex1-
Tin))/(10*Tm));

Tout=Tex1-273.15; % Outlet temperature [Celcius]
put=pstatic;
w2=((pin*Tex1)/(put*Tin))*w1; % Outlet velocity [m/s]

% HTC calculation
fa=1+1.5*(1-e);
thermdiff=khe/(dens*cp);
pr=visc/thermdiff;
Repour=(w1*dgr)/(visc*e);
Nulam=0.644*sqrt(Repour)*((pr)^(1/3));
Nuturb=(0.037*(Repour^0.8)*pr)/(1+(2.443*(Repour^-0.1)*((pr^(2/3))-1)));
Nueinz=2+sqrt(Nulam^2+Nuturb^2);
Nu=fa*Nueinz;
alfa_t=(Nu*khe)/dgr;

%% Sphere heat calculations
radius_sphere=dgr/2;
volume_sphere=(4*pi*(radius_sphere^3))/3; % Sphere volume [m3]
surface_sphere=4*pi*radius_sphere^2; % Sphere surface [m2]
m_sphere=dens_t*volume_sphere; % Mass of 1 sphere [kg]
t0=(m_sphere*cp_t)/(alfa_t*surface_sphere);
deltaT_pulse=Qm/cp_t;
tp=50*10^-3;
T2=Tout-TinC;
T1=(deltaT_pulse*exp(-(tp/t0)))/(1-exp(-(tp/t0)));
T0=20+(0.5*T2)+T1+deltaT_pulse; % Temperature of hottest sphere [Celsius]

Data(num,1)=P_pump;
Data(num,2)=Tout*(-1); % Set as negative to handle easier in excel
Data(num,3)=T0;

```



```

Data(num,4)=pin;
Data(num,5)=w1;
Data(num,6)=w2;
Data(num,7)=alfa_t;
Data(num,8)=dens;
Data(num,9)=CLin;
Data(num,10)=CQuad;

```

```

num=num+1;
end

```

5.3 Mat lab code: handling the FLUKA file

```

function [edep]=NewFLUKAprogram(Length,Heigth,Width,Cellside)

```

```

%% Import Data from fluka file
[Data]=fluka;
%[Data]=hdensfluka11;
%[Data]=ldensfluka11;

```

```

%% Information about the geometry and the cells (Edited by user) [cm]
%Length=Z-Direction
%Heigth=Y-DFirection
%Width=X-Direction
%Cellside=side of a cubic cell

```

```

nrcells=(Length*Heigth*Width)/Cellside^3;
centercell=Cellside/2;

```

```

%% Create a cell,insert vectors with the values of each cell in W/cell volume

```

```

AllColumns=cell((Length*Heigth)/Cellside^2,1);
count=0;
columncount=0;
for zStart=centercell:Cellside:(Length-centercell)
    for yStart=(-Heigth/2)+centercell:Cellside:(Heigth/2)-centercell
        xcount=Width/Cellside;
        for xStart=(-Width/2)+centercell:Cellside:(Width/2)-centercell
            count=count+1;
            column(xcount)=Data(count,4)*(2*10^6)*Cellside^3;
            xcount=xcount-1;
        end
        columncount=columncount+1;
        AllColumns{columncount,1}=column;
    end
end
end

```

```

%% Arrange the vectors with the values in a cell: Heigth*Length

```

```

count=0;
ArrangedHeigthLength=cell(Heigth,Length);
for i=1:1:Length/Cellside
    for j=1:1:Heigth/Cellside
        count=count+1;
        ArrangedHeigthLength{Heigth/Cellside+1-j,i}=AllColumns{count};
    end
end

```

```
end
```

```
%% Renaming to more appropriate Name  
edep=ArrangedHeigthLength;
```

5.4 Mat lab code: straight forward method

```
clear all  
clc  
%%%%%%%%%%%%%%%%%%%%%%%%%%%%%%%%%%%%%%%%%%%%%%%%%%%%%%%%%%%%%%%%%%%%%%%%  
%% Cooling tungsten spheres with helium %%  
%% By: Jozsef Szabo, LTH %%  
%%%%%%%%%%%%%%%%%%%%%%%%%%%%%%%%%%%%%%%%%%%%%%%%%%%%%%%%%%%%%%%%%%%%%%%%  
  
%% Entering The Geometry [cm]  
Length=60;  
Heigth=8;  
Width=22;  
Cellside=0.5;  
  
%% Run flukaprogram to get wanted data  
[edep]=NewFLUKAprogram(Length,Heigth,Width,Cellside);  
  
%% Helium properties  
M=4.0026*10^-3; % Molar mass [g/mol]  
R=8.314; % Gas constant R  
dyn_visc=18.6*10^-6; % Dynamic Viscosity [Ns/m2]  
cp=5.1932*10^3; % Specific heat [J/kg * K]  
khe=0.144; % Thermal condutivity [W/m*k]  
  
%% Tungsten Properties  
dens_t=18500;%[HighDens] % Density of tungsten [kg/m3]  
%dens_t=14000;%[LowDens]  
cp_t=0.135*10^3; % Specific heat, tungsten [J/kg * K]  
  
%% Geometry  
l0=Cellside*10^-2;  
A=(Cellside*10^-2)^2; % Inlet area of a column  
dgr=10*10^-3; % Diameter in [m] och spheres  
  
%% Constant  
e=1-(pi/sqrt(18));  
B_line=1.8;  
fil=1;  
del=fil*dgr;  
radius_sphere=dgr/2;  
volume_sphere=(4*pi*(radius_sphere^3))/3; % Sphere volume [m3]  
surface_sphere=4*pi*radius_sphere^2; % Sphere surface [m2]  
m_sphere=dens_t*volume_sphere; % Mass of 1 sphere [kg]  
tp=50*10^-3;  
  
HeTemp=cell(Heigth/Cellside,Length/Cellside);  
Pressure=cell(Heigth/Cellside,Length/Cellside);  
SphereTemp=cell(Heigth/Cellside,Length/Cellside);
```

```

PumpingPower=cell (Heigth/Cellside,Length/Cellside);
PressureDrop=cell (Heigth/Cellside,Length/Cellside);
Velocity=cell (Heigth/Cellside,Length/Cellside);
mPrick=cell (Heigth/Cellside,Length/Cellside);
Density=cell (Heigth/Cellside,Length/Cellside);
HTC=cell (Heigth/Cellside,Length/Cellside);
OutVel=cell (Heigth/Cellside,Length/Cellside);
for i=1:1:Length/Cellside
    for j=1:1:Heigth/Cellside
        % Input Parameters
        w1=15.0; % Flow v elocity in [m/s]
        TinC=22; % Inlet temo in celcius
        Tin=TinC+273.15; % Temperture in i kelvin
        pin=2.0*10^6;

        for k=1:1:Width/Cellside
            dens=(M*pin)/(R*Tin);
            %dens=3.26;
            visc=dyn_visc/dens;
            mprick=dens*w1*(A);
            P=edep{j,i}(k);
            Tex=(P/(mprick*cp))+Tin;
            Tout=Tex-273.15;

            Rel=(w1*del)/visc;
            lambda=((360*((1-e)^2))/(e^3*Rel))+((B_line*(1-e))/e^3);
            zeta=(lambda*l0)/del;
            Tm=(Tin+Tex)/2;
            delta_zeta_t=2*((Tex-Tin)/Tm);
            zeta_t=zeta+delta_zeta_t;
            wlm=w1*(Tm/Tin);
            dens_m=dens*(273/Tm);
            deltaP=((dens_m*(wlm^2))/2)*zeta_t;

            CLin{j,i}(k)=(180*((1-e)^2)*dens*visc)/((e^3)*(del^2));
            %CLin{j,i}(k)=(273*90*(Tin+Tex)*((1-
e)^2)*visc)/((e^3)*(Tin^2)*(del^2));
            CQuad{j,i}(k)=(B_line*(1-e)*dens)/(2*(e^3)*del);
            %CQuad{j,i}(k)=((273*dens)/(Tin^2))*(((Tm*B_line*(1-
e))/(2*(e^3)*del))+((Tex-Tin)/(Tin^2)));

            put=pin-deltaP;
            P_pump=((mprick/dens)*(deltaP));
            w2=((pin*Tex)/(put*Tin))*w1;

            fa=1+1.5*(1-e);
            thermdiff=khe/(dens*cp);
            pr=visc/thermdiff;
            Repour=(w2*dgr)/(visc*e); % Shoult it be w2?
            Nulam=0.644*sqrt(Repour)*((pr)^(1/3));
            Nuturb=(0.037*(Repour^0.8)*pr)/(1+(2.443*(Repour^-0.1)*(pr^(2/3)-
1)));

            Nueinz=2+sqrt(Nulam^2+Nuturb^2);
            Nu=fa*Nueinz;
            alfa_t=(Nu*khe)/dgr;

```

```

Qm=edep{j,i}(k)*(1/(((Cellside*10^-2)^3*dens_t)*10^3)*20))*10^3;
deltaT_pulse=Qm/cp_t;
t0=(m_sphere*cp_t)/(alfa_t*surface_sphere);
%T2=Tout-TinC;
T1=(deltaT_pulse*exp(-(tp/t0))/(1-exp(-(tp/t0))));
%T0=20+(0.5*T2)+T1+deltaT_pulse;
T0=((Tout+TinC)/2)+T1+deltaT_pulse;

w1=w2;
Tin=Tex;
TinC=Tin-273.15;
pin=put;

HeTemp{j,i}(k)=Tout;
Pressure{j,i}(k)=put;
SphereTemp{j,i}(k)=T0;
PumpingPower{j,i}(k)=P_pump;
PressureDrop{j,i}(k)=(deltaP);
Velocity{j,i}(k)=w2;
mPrick{j,i}(k)=mprick;
Density{j,i}(k)=dens;
HTC{j,i}(k)=alfa_t;
OutVel{j,i}(k)=w2;
end
end
end

%Matrixes of different outlet variables.
for i=1:1:Length/Cellside
    for j=1:1:Heigth/Cellside
        HeOutTemp(j,i)=HeTemp{j,i}(Width/Cellside);
        PressureOut(j,i)=Pressure{j,i}(Width/Cellside);
        SphereTempOut(j,i)=SphereTemp{j,i}(Width/Cellside);
        VelocityOut(j,i)=Velocity{j,i}(Width/Cellside);
        mPrickOut(j,i)=mPrick{j,i}(Width/Cellside);
        DensityOut(j,i)=Density{j,i}(Width/Cellside);
        HTCOut(j,i)=HTC{j,i}(Width/Cellside);
    end
end

%% For XZ-Plane Plot
Plane=6;
for i=1:1:Length/Cellside
    for j=1:1:Width/Cellside
        XZ_Plane(j,i)=HTC{Plane,i}(j);
        %XZ_Plane(j,i)=HeTemp{Plane,i}(j);
    end
end

%% Sum and avreage of different things for different zones.
count=1;
for z=0:Length/Cellside/3:Length/Cellside-1
    high=1*10^-9;

```

```

highqm=1*10^-9;
highphet=1*10^-9;
sumPumpingPower=0;
sumPressureDrop=0;
sumPressureOut=0;
sumPower=0;
sumHeOutTemp=0;
sumSphereTemp=0;
sumCLin=0;
sumCQuad=0;
for i=1+z:1:Length/Cellside/3+z
    for j=1:1:Heigth/Cellside
        sumPressureOut=sumPressureOut+PressureOut(j,i);
        sumHeOutTemp=sumHeOutTemp+HeOutTemp(j,i);
        for k=1:1:Width/Cellside
            this=SphereTemp{j,i}(k);
            if this>high
                high=this;
            end
            %thisqm=edep{j,i}(k);
            thisqm=edep{j,i}(k)*(1/(((Cellside*10^-
2)^3*dens_t)*10^3)*20)*10^3;
            if thisqm>highqm
                highqm=thisqm;
            end
            thisphet=HeTemp{j,i}(k);
            if thisphet>highphet
                highphet=thisphet;
            end
            sumPumpingPower=sumPumpingPower+PumpingPower{j,i}(k);
            sumPressureDrop=sumPressureDrop+PressureDrop{j,i}(k);
            sumPower=sumPower+edep{j,i}(k);
            sumCLin=sumCLin+CLin{j,i}(k);
            sumCQuad=sumCQuad+CQuad{j,i}(k);
        end
    end
end
LargestQmZoneX(count)=highqm;
HottestSphereZoneX(count)=high;
HePeakTempZoneX(count)=highphet;
TotalPumpingPowerZoneX(count)=sumPumpingPower;

AvgPressureDropZoneX(count)=sumPressureDrop/(((Length/Cellside)/3)*(Heigth/Cel
lside));

AvgPressureOutZoneX(count)=sumPressureOut/(Length/Cellside/3*Heigth/Cellside);
PowerZoneX(count)=sumPower;
AvgHeOutTempZoneX(count)=sumHeOutTemp/(Length/Cellside/3*Heigth/Cellside);
AvgCLin(count)=sumCLin/(Length/Cellside/3*Heigth/Cellside*Width/Cellside);

AvgCQuad(count)=sumCQuad/(Length/Cellside/3*Heigth/Cellside*Width/Cellside);
count=count+1;
end

%% Creating a Data file with important parameters for zones
ZoneInfo(1,:)=AvgHeOutTempZoneX;

```

```
ZoneInfo(2,:) = HottestSphereZoneX;  
ZoneInfo(3,:) = TotalPumpingPowerZoneX;  
ZoneInfo(4,:) = AvgPressureOutZoneX;  
ZoneInfo(5,:) = AvgPressureDropZoneX;  
ZoneInfo(6,:) = PowerZoneX;  
ZoneInfo(7,:) = LargestQmZoneX;  
ZoneInfo(8,:) = AvgCLin;  
ZoneInfo(9,:) = AvgCQuad;
```